School of Civil and Mechanical Engineering

Development of green blended binder consisting of high-volume slag and fly ash with nano CSH seed accelerator

Kumuditha Sathyajith Senadheera Imihami Mudiyanselage

This thesis is presented for the Degree of
Master of Philosophy
of
Curtin University

July 2024

DECLARATION

To the best of my knowledge and belief this thesis contains no material previously published by any other person except where due acknowledgment has been made.

This thesis contains no material which has been accepted for the award of any other degree or diploma in any university.

Signature: …….

Date: ……...

ACKNOWLEDGEMENT OF COUNTRY

We acknowledge that Curtin University works across hundreds of traditional lands and custodial groups in Australia, and with First Nations people around the globe. We wish to pay our deepest respects to their ancestors and members of their communities, past, present, and to their emerging leaders. Our passion and commitment to work with all Australians and peoples from across the world, including our First Nations peoples are at the core of the work we do, reflective of our institutions' values and commitment to our role as leaders in the Reconciliation space in Australia.

Dedicated

To my beloved father and mother, who have always been there for me through both success and failure.

And to my loving wife, whose unwavering support and motivation have propelled me to achieve great things in life.

And my father-in-law and mother-in-law for the continuous support

And to Professor Faiz Shaikh who believed in me and provided the opportunity to pursue my Master of Philosophy in Civil Engineering.

ACKNOWLEDGEMENT

I wish to express my sincere gratitude to Professor Faiz Shaikh, of School of Civil and Mechanical Engineering, Curtin University, for his invaluable supervision, guidance, and unwavering support throughout the completion of my Master of Philosophy thesis over the past two years.

I am also thankful to Professor Prabir Sarker, my co-supervisor, and Associate Professor Faisal Anwar, the thesis panel chairperson, for their constructive feedback and advice, which significantly contributed to refining my research program. Special thanks are due to Associate Professor Ranjan Sarukkalige, Director of Graduate Research at Curtin's Civil & Mechanical Engineering department, for his insightful direction and support during my studies.

I extend my appreciation to Dr. Arifur Rahman for his technical guidance, essential to the successful completion of my thesis. Additionally, I acknowledge Dr. Anwar Hosan for his expertise in conducting SEM/EDS analysis and his support throughout the research.

I am grateful to Master Builders Solutions and Mr. Luke Curran for their sponsorship through the provision of Master X-Seed 1500 for my research. My thanks also go to Mr. Darren Isaac, Technical Operations Coordinator, and the technical team comprising Mr. Leon Forgus, Mr. Bill Swerlowycz, Dr. Rajab Abousnina, and Ms. Alicia Farrelly of Curtin's Civil Engineering Laboratory for their invaluable assistance during the testing phase.

I appreciate the support from Dr. Manjin Kim and Ms. Kate Putman at the XRD facility, as well as Ms. Elaine Miller at the Microcopy and Microanalysis facility of the John de Laeter Centre for their assistance with XRD and SEM testing. I am grateful to Dr. Shagraf and Dr. Samsun from Curtin Water Laboratory for facilitating TGA/DSC testing.

Special thanks are due to Mr. Sean Conheady, my Manager at SRG Global, for his encouragement and support throughout my research journey.

I would like to express my deepest gratitude to my wife, Minoli Nishshankaarachchi, for her unwavering support, patience, and motivation during the past two years. I also extend heartfelt thanks to my parents, Mr. Saman Senadheera and Mrs. Suneetha

Dasanayaka, my brothers Hasitha and Sachintha, and my in-laws Mr. Wasantha Nishshankaarachchi and Mrs. Ramya Rasnyaka, as well as my sister-in-law Milangi, for their constant encouragement and support.

I am thankful to Dr. Kamal Jayasinghe, Mrs. Rupa Jayasinghe, and the brothers Piyumal and Ransumal for their immense support. Also, I would like to thank Mr. Bharatha Kurukulasooriya, Mrs. Prasadi Weeratunge, and their family for their assistance and support during my studies.

Finally, I extend my gratitude to all my friends, colleagues, and fellow researchers at Curtin University for their kindness and support throughout my academic journey.

ABSTRACT

This thesis presents the effectiveness of using nano calcium silicate hydrate (NCSH) seed accelerator as an admixture to compensate early age strength development in cement binder containing high volume fly ash (HVFA) and high-volume slag (HVS) towards development of sustainable binder. Three types of sustainable binders are considered with addition of 2.5%,5% and 7.5% NCSH seed accelerator. In first binder, HVS at 70, 80 and 90% as partial replacement of Ordinary Portland Cement (OPC) is considered. The second binder contains class F, HVFA at 70, 80 and 90%, while in the third binder both slag and fly ash are used at 70, 80 and 90% as partial replacement of cement and slag: fly ash ratio was kept 50:50. The binder pastes were tested for initial flow after mixing and compressive strengths at 3, 7 and 28 days. Optimum binders were selected by comparing the strength development results and eight mixes were selected for further microstructural analysis. Isothermal calorimetry test was done for the selected samples to understand the hydration heat of the mixes. Scanning electron microscopy (SEM) was used to understand the microstructure of the paste. X-ray diffraction (XRD) was done for 7-day and 28-day dried samples to evaluate the Calcium Silicate Hydrate (CSH) gel formation and the Calcium Hydroxide (CH) in the mix. Thermogravimetric Analysis (TGA) was conducted for 28-day paste samples to evaluate the CH content in the mix. The HVS mixes showed better results with the increase of compressive strength when NCSH seed is used as an accelerator. The mix with 80% slag replacement with 7.5% NCSH seed accelerator achieved 88% and 99% of the strength of control OPC mix in 3 days and 28 days, respectively. Also, it increased the 28-day compressive strength by 195% and 44% in 3 and 7 days respectively when compared to the strength of the same mix without NCSH seed accelerator. This is also confirmed by SEM images of the mix, XRD data and TGA data. Two concrete samples were casted for the control OPC mix and the mix with 80% slag replacement with 7.5% NCSH seed accelerator to evaluate the fresh concrete, mechanical and durability properties such as water permeability, volume of permeable voids (VPV) and rapid chloride permeability Test (RCPT). Better results were achieved with the resulted binder in all three aspects confirming NCSH seeds an effective admixture in terms of developing sustainable concrete by reducing the CO_2 emissions and improving concrete performance.

Keywords: NCSH seed accelerator, fly ash, slag, cement binder

TABLE OF CONTENTS

LIST OF ACRONYMS

AS	Australian Standards
ASR	Alkali silica reaction
ASTM	American Society of Testing Materials
BFS	Blast Furnace Slag
BSE	Backscattered Electron
C_3A	Tricalcium Aluminate
C_3S	Tricalcium Silicate
CAH	Calcium Aluminate Hydrate
CASH	Calcium Alumino Silicate Hydrate
CH	Calcium Hydroxide
CO_2	Carbon Dioxide
CSH	Calcium Silicate Hydrate
DSC	Differential scanning calorimetry
EDS	Energy-dispersive X-ray Spectroscopy
FA	Fly Ash
GGBFS	Ground Granulated Blast Furnace Slag
GPa	Giga Pascal
HVFA	High Volume Fly Ash

HVS	High Volume Slag
HVS-FA	High Volume Slag Fly Ash
ITZ	Interfacial Transition Zone
MPa	Mega Pascal
NA	Nano Alumina
NC	Nano Calcium Carbonate
NCSH	nano Calcium Silicate Hydrate
NS	Nano Silica
OPC	Ordinary Portland Cement
RCPT	Rapid Chloride Permeable Test
SCC	Self-compacting Concrete
SCM	Supplementary Cementitious Materials
SD	Standard Deviation
SEM	Scanning Electron Microscope
SF	Silica Fume
SSD	Saturated Surface Dry
TGA	Thermogravimetric Analysis
VPV	Volume of Permeable Voids
XRD	X-ray Diffraction

LIST OF FIGURES

LIST OF TABLES

CHAPTER 1: INTRODUCTION

1.1. Background

Concrete is the second most utilized material in the world after water. Cement is the key constituent of concrete that when mixed with water makes the binder in concrete. Cement production is a highly energy intensive process. Global production of cement caters around 7-8% of total anthropogenic CO_2 emissions in the world (Mugahed et al. ,2002)., CO_2 is emitted mainly from the kilns used to produce the clinker from limestone through fuel in the kiln, as well as from power used to operate the cement manufacturing plants (Worrell et al., 2001). Since the cement demand is increasing day by day with large infrastructure projects coming up in the world, the cement manufacturers are taking steps to reduce the CO_2 emission in cement production. Changing the clinker minerology to reduce the calcination temperature and the clinker factor in the cement, usage of alternative fuels to reduce the adverse environmental impact are highly considered. Also, using SCM to produce blended cement is an inexpensive way of reducing the carbon footprint of the cement is widely used by cement manufacturers over the world. For this, research is carried out to evaluate the feasibility of using industrial waste materials and mine waste residue as partial replacement in OPC. Fly ash, ground granulated blast furnace slag (GGBFS), metakaolin & rice husk ash is widely used as SCM to produce concrete.

But there are several drawbacks of using SCM as partial replacement of cement in concrete such as low early strength development, increased setting time leading to higher construction costs in terms of other factors like labour, formwork, and the cycle time mainly in vertical constructions (Snellings et al., 2023). To account for this low strength development, accelerators are used to improve the early strength in the concrete and accelerate the hydration reaction.

In the construction industry, replacement of OPC with SCM like fly ash and slag up to 30-40% of cement is widely used and, in some instances, they are researched up to 60% use of these SCM (Shukla et al., 2023, Hussain et al., 2020). But the use of fly ash and slag in higher volume replacement of OPC is rarely used in the industry due to the lack of confidence with the end users.

To overcome these challenges using activators or accelerators for concrete with SCM is highly interested in the concrete industry. Various nano materials and salt-based admixtures are used to enhance the early age strength and reduce the setting time of the concrete with using SCM. Seeded calcium silicate nano particles in concrete is a novel method to increase the early age strength development in concrete specially in the precast industry. Therefore, the feasibility of using the seeded calcium silicate hydrate nanoparticles (NCSH) with high volume fly ash and high-volume slag in concrete is evaluated in this study.

1.2. Research Significance

Fly ash and steel slag are major industrial waste materials in the world as well as in Australia. Around 300-360 Mt/year of slag is produced worldwide and ~300Mt is utilised as SCM, also around 700-1100 Mt/year of coal fly ash is produced worldwide and 330–400Mt is used as SCM (Juenger et al. 2019) Therefore, utilising these waste materials into sustainable construction materials is highly regarded. At present fly ash and slag are used as SCM in concrete or in blended cement up to 30% and 60%, respectively as partial replacement of OPC. (Shukla et al. 2023, Hussain et al., 2020) Higher level of replacement is not widely used in the industry due to less research in using fly ash and slag in higher volumes to produce blended cements. Therefore, this research focuses on the usage of fly ash and slag in higher volumes as partial replacement of OPC to produce a green binder incorporating NCSH seed accelerator. Though research is carried out to find out the feasibility of using different activators in high volume fly ash and slag based green cements, the use of NCSH seed accelerator with HVFA and HVS based green binder up to 90% replacement of OPC is not well researched. Therefore, there is a potential research gap to evaluate the feasibility of using NCSH seed accelerator in HVFA and HVBFS based green binder for concrete.

1.3. Aim and Objectives

The aim of this research is to evaluate the effectiveness of NCSH seed accelerator in enhancing the early age compressive strength of HVFA and HVS binder and develop low carbon binder consisting of low volume OPC and HVFA or HVS. To achieve the above aim the specific objectives of this research are as follows:

1. Evaluate the effect of various NCSH seed contents on early age compressive strength of HVFA, HVS and high-volume slag-fly ash (HVS-FA) blended binders.
2. Establish optimum blended binder mixes and investigate the microstructural development of these selected blended binders.
3. Study the mechanical and durability properties of concrete containing the best performing blended binder containing NCSH seeds and benchmark its performance with control OPC concrete.

1.4. Scope of Work

Material Characterisation is done through the material test results from recently published data available in Hosan et al. (2020) from the same laboratory. X-ray fluorescence (XRF), XRD and particle size distribution of the source materials was studied in the first phase.

Mix proportions were considered based on the replacement percentages of OPC with the fly ash, slag and fly ash and slag blending at 50:50 ratio. 70%, 80% & 90% replacement levels of OPC were considered for these mixes and control mix with 100% OPC was used as the reference for the Strength Activity Index (SAI) calculations.

NCSH Seed accelerator percentages were selected as 2.5%, 5% & 7.5% for each replacement level and mix without NCSH was also cast as a control mix in each replacement level.

Flow of each mix was measured with the flow table test and 50 x 50 x 50 mm cubes were cast. Minimum of 9 specimens were cast for each mix for 3d, 7d & 28d compressive strength testing.

Nine mixes were selected based on their early strength development with the addition of NCSH seed accelerator and specimens were retained and dried in the oven at 60 $^{\circ}$C for 48hr in 7 day & 28 days for the SEM, EDS, XRD and TGA, Differential Scanning Calorimetry (DSC). Isothermal Calorimetry was conducted for the selected mixes to study their heat of hydration.

Polished surface samples were prepared from the dried samples for SEM and EDS analysis and micronized powder samples were prepared for XRD and TGA testing.

Two concrete mixes were cast for the control mix with OPC and the mix with the best performing binder from the previously selected eight samples and workability, mechanical properties and durability properties were evaluated. Slump test is performed to measure the workability of fresh mixes, compressive strength, split tensile strength and elastic modulus tests are performed as part of mechanical properties and water permeability, VPV, and RCPT are performed as part of durability properties.

1.5. Outline of the Thesis

Chapter 1 - Introduction of the research is presented in this chapter along with the background, significance, and aim & objective of the research.

Chapter 2 - A comprehensive literature review is presented in this chapter comprised of the previous research work carried out with the supplementary cementitious materials, usage of NCSH Seeds for the concrete, Cement industry and the challenges faced in cement manufacturing, need of sustainable solutions for cement production was studied in this review.

Chapter 3 - Detailed research methodology is presented in this chapter. Materials used in the research; technical data of materials experimental methods considered in the research are presented in this chapter.

Chapter 4 - This chapter presents the experimental results and a discussion of the test results. Flow, Compressive strength, Isothermal Calorimetry, XRD, TGA and SEM/EDS data are discussed.

Chapter 5 – Conclusions of the research and the recommendations for further research work is presented in this chapter.

CHAPTER 2 – LITERATURE REVIEW

2.1. Introduction

This chapter provides an overview of the past research work conducted on HVFA and HVS binders and the usage of nano materials to enhance the early age mechanical properties and durability properties of concrete.

Using nano materials in minor dosages with cementitious materials is an extensively researched area due to the capability of nano materials to enhance the early age mechanical properties and durability properties of concrete by accelerating the hydration reaction due to the huge specific surface area and fineness of the nano material creating more nucleation sites to create more hydration products such as CSH gel in the matrix. Extensive research has been conducted to understand the effects of using nano materials such as nano silica (NS), nano calcium carbonate (NC) nano alumina (NA) with OPC.

2.2. HVFA and HVS concretes and binders containing nano materials.

Using nano materials in smaller replacement levels with other supplementary cementitious materials (SCM) has been used in the cement and concrete industry to enhance the mechanical and durability properties of the concrete with SCM, mainly the low early strength development of concrete with SCM is occurred due to the slow pozzolanic reaction in the binder. This phenomenon is often attributed to the sluggish pozzolanic reactions that occur within the binder matrix. By leveraging the unique properties of nanomaterials, particularly their high specific surface area, researchers have found that these materials can effectively accelerate the hydration reactions associated with SCMs. This acceleration not only improves early strength but also contributes to the overall durability of the concrete.

Research conducted by Land and Stephan (2012) delved into the influence of NS on the hydration processes of OPC. Their study focused on how varying particle sizes and specific surface areas of NS provide critical nucleation sites for the formation of CSH gel. The researchers synthesized NS particles of different sizes and incorporated them into concrete mixes. The results demonstrated a clear correlation between the specific surface area of NS and the acceleration of cement hydration, suggesting that finer

particles can significantly enhance the early strength of concrete by facilitating quicker and more effective hydration. Addition of NS accelerated the consumption of tricalcium silicate (C_3S) and the development of homogenous groups of CSH composition that are created on the silica surface which increased the hydration heat and early strength as a result. Zhang et al. (2012) further expanded on these findings by examining the effects of NS on HVS concrete. In their experiments, they utilized NS at contents ranging from 0.5% to 2%, in conjunction with a 50% partial replacement of cement with fly ash, while maintaining a constant water-to-cement ratio of 0.45 across all mixes. The study concluded that the inclusion of NS led to notable increases in compressive strength at all test ages, reaching up to 91 days. Importantly, the researchers also explored different mixing methods, concluding that ultrasonication produced superior results for dispersing NS compared to conventional mechanical mixing methods. The incorporation of NS increased the production of CSH gel through the pozzolanic reaction. The additional CSH reduced the amount of CH in the matrix, a less desirable by-product that contributes to the porosity and weakens the structure. By covering the CH to CSH, the strength of the cement matrix is significantly enhanced.

The research by Shaikh et al. (2014) focused on understanding the impact of NS on the compressive strength of HVFA mortars and concretes. In this study, the researchers replaced cement with fly ash at levels ranging from 40% to 70% and conducted tests to measure compressive strength at 7 and 28 days. The findings revealed a 5% and 7% increase in strength at 7 days for the 40% and 70% replacement mixes, respectively. Notably, strength improvements were more pronounced in mixes with replacement levels above 50% at the 28-day mark. This suggests that incorporating NS can mitigate some of the early strength deficiencies typically associated with high levels of fly ash replacement, which they attributed to the increased nucleation and hydration rate. Also, they pointed that the NS has a physical filling effect that reduces the overall porosity of the matrix. The high specific surface of NS allows it to fill voids at the nano level, improving the packing density and contributing to a denser microstructure, which results in higher compressive strength. In a related study, Shaikh & Hosan (2019) investigated the combined use of HVFA, HVS, and NS in concrete formulations. Their findings indicated that concrete mixes containing 70-80% SCMs not only maintained compressive strengths comparable to control mixes but also

significantly reduced the carbon footprint of the paste by 66-76%. The study emphasized that NS played a crucial role in enhancing the compressive strength of the mixtures, thereby contributing to sustainable construction practices without compromising performance.

Liu et al. (2019) conducted research that specifically addressed the effects of NS on the early strength and microstructure of steam cured HVFA cement systems. By utilizing a 50% fly ash replacement and varying NS content from 1% to 4%, the study found that the inclusion of NS significantly boosted the strength of steam cured HVFA mortar after just 9 hours. This effect was particularly pronounced at higher NS concentrations, demonstrating that NS not only accelerates hydration but also influences the microstructural development of the cement matrix. Their study confirmed that NS act as a nucleation site, which increases the rate of hydration. The results in faster formation of hydration products, improving the strength of the paste and reducing the setting times.

Roychand et al. (2015) researched the feasibility of using fly ash in high volume NS, and hydrated lime with a set accelerator replacing 70% of Portland Cement. They concluded that using NS alone in cement mix increases the compressive strength, while using with hydrated lime and set accelerator does not show any impact in the strength development. Roychand et al. (2017) presented the effect of using 80% replacement of OPC with fly ash with 5-7.5% NS, 2.5-5% NC and 2.5-5% of NA. The 7 results showed that using NS significantly improved the compressive strength by totally consuming available portlandite and significantly increasing the CSH gel in 28 days. The compressive strength improvement increased with the higher NS content in 7 days this improvement was not subtle due to the formation of silica rich hydrogarnet and dropping the formation of CSH. Addition of NC did not show any improvement of the pozzolanic reaction in the 7 days, but with the increase of NC content slight compressive strength increase was observed, but in 28 days the compressive strength increase was evident. On the other hand, the addition of NA increased the compressive strength only with using lower dosage. Roychand et al. (2017) further highlighted that the higher dosage shows a reduction of the compressive strength due to the formation of aluminium hydroxide ($Al(OH)_3$) gel resulting low formations of CSH/calcium aluminosilicate hydrate (CASH) gel in the matrix. The incorporation of nano materials

extends beyond mechanical properties to enhance the durability characteristics of concrete.

Shaikh & Supit (2014) studied the mechanical and durability properties of HVFA concrete with 40% and 60% cement replacement using NC particles. Their findings indicated that NC not only improved early and long-term compressive strength but also resulted in better durability characteristics. Improvements included reduced permeability, lower porosity, and higher resistance to water sorptivity, as well as diminished chloride permeability. These enhancements were attributed to the reaction of high-silicate and aluminate fly ash with the NC particles, effectively increased the CH consumption in the matrix leading to the production of additional hydration products in the HVFA concrete system.

Xu et al. (2017) examined the early-age hydration and mechanical properties of HVFA and HVS concrete at varying curing temperatures. They discovered that the hydration process for fly ash mixes is more sensitive to temperature fluctuations compared to slag mixes. Their results indicated that both HVFA and HVS contributed to accelerated hydration during the initial induction period ($t < 3$ hours) due to dilution and filler effects; however, this acceleration diminished with increasing fly ash content (55% and 70% replacements).Hannesson et al. (2011) explored the influence of HVFA and HVS on the compressive strength of self-consolidating concrete. They noted that the early-age compressive strength was generally lower than that of control mixes, a finding attributed to the reduced pozzolanic activity associated with high-volume replacements. The setting times for low-level replacement mixes remained relatively stable, but significant changes were observed after exceeding 60% replacements.

The study by Velandia et al. (2016) evaluated the use of activated HVFA systems with various activators such as Sodium Sulphate (Na_2SO_4), lime, and quicklime. This research focused on the chemical activation of four distinct fly ashes in blends with Portland cement, assessing their effects on hydration and compressive strength. The results highlighted that the amorphous content of fly ash was a critical factor in determining compressive strength development when activators were not used. An increase in amorphous content corresponded with improved strength; however, instances of decreased compressive strength were observed when both particle size

and loss on ignition (LOI) content were reduced, likely due to insufficient amorphous content in the finer fractions of some fly ashes.

Shaikh and Hosan (2019) investigated the effects of NA on high-volume slag and fly ash combined concrete, utilizing partial replacement levels of 70%, 80%, and 90% with NA content ranging from 1% to 4%. Their findings indicated that the addition of NA contributed to a 2-16% increase in compressive strength and significantly reduced capillary pores within the concrete matrix. The ultrasonication method employed for dispersing NA in water further enhanced its effectiveness in achieving desired performance outcomes.

The incorporation of nanomaterials, particularly NS, NC, and NA, into concrete mixtures represents a promising avenue for enhancing both mechanical and durability properties. Through various studies, it is evident that these materials can effectively address the challenges associated with high-volume replacements of traditional cement with supplementary cementitious materials. By accelerating hydration reactions and improving microstructural characteristics, nanomaterials not only contribute to higher early strength but also bolster the overall durability of concrete, making it suitable for a wide range of applications in modern construction. As research continues to evolve, the potential for these advanced materials to contribute to sustainable and high-performance concrete solutions remains significant.

2.3. Concrete containing nano Calcium Silicate Hydrate (NCSH) Seed Accelerator

Nano Calcium Silicate Hydrate (NCSH) seeding is a novel technology utilised to accelerate cement hydration. Cement is mixed with NCSH particles to stimulate the formation of CSH nuclei during initiation of cement hydration, which accelerates the CSH formation in the cement hydration process. Presence of NCSH can lead to a denser microstructure in the cement paste. This is primarily due to the increased rate of CSH formation, which fills the voids and contributes to the overall strength of the material. The smaller particle size of NCSH enables a larger surface area for interaction with the cement particles, further enhancing the hydration kinetics. (Land & Stephan., 2015).

Figure 2.1 shows the role of NCSH nucleation seeding on the hydration of OPC. The green arrows highlight the movement of the CSH growth away from the dissolving clinker particle volumes (inner CSH) towards the capillary porosity regions (outer CSH) caused by the nucleation seeding (NCSH). The red arrows note the concentration gradients in ionic species which are exacerbated by NCSH nucleation seeding (Cuesta et al., 2023).

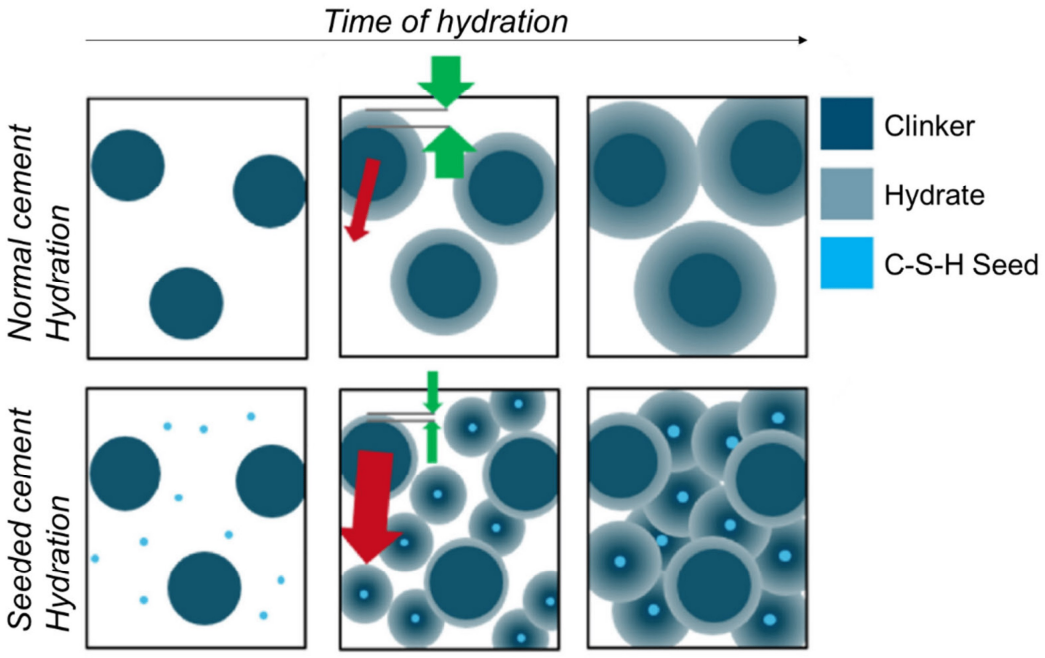

Figure 2.1: Schematic representation of the role of NCSH nucleation seeding on the hydration of PC (Adopted from Cuesta et al., 2023)

Wang et al. (2019) carried out research to prepare NCSH seeds by means of mechanical method and they evaluated the effect of NCSH in early hydration of cement by the isothermal calorimetry. They concluded that the mechanochemical synthesis of NCSH seeds is a simple and effective way to synthesize NCSH seeds which will accelerate the cement hydration. The influence of the C/S ratio on the morphology of NCSH seeds were concluded with the SEM images and calcium rich particles shows a formation like a cauliflower and silicon rich particles tend to form a chain like shape. NCSH seeds had an average particle size of approximately 4 µm made with primary NCSH particles which having an average particle size of 40-50nm concluding that dispersants could improve to reach to the particle surface for nucleation and improve performance of NCSH seeds. Currently, pozzolanic method, sol-gel method, and precipitation method are three main methods for the preparation

of NCSH seeds in the literature. Wang et al. (2019) used the mechanochemical method, which is a branch of pozzolanic reaction based on the chemical reaction shown in equation (1) to produce NCSH seed accelerator.

$$xCa(OH)2 + ySiO2 + zH2O \rightarrow xCaO.ySiO2.(x+y)H2O \quad - \quad \text{Eq (1)}$$

Alzaza et al. (2022) studied the impact of using NCSH seeds with binders consisting of OPC and GGBFS cured at 0°C to demonstrate the strength development and the reaction kinetics of cement with supplementary cementitious materials in low ambient temperature in cold weather regions which undergo freeze thaw actions. They concluded that the NCSH seeds has recovered the reduction of strength occurring due to addition of GGBFS is the binder, and this is more evident in low GGBFS contents like 30% replacement. Better frost resistance was gained in the seeded binder containing 30% GGBFS than in the pure PC binder. Alzaza et al. (2022) further studied the 30% GGBFS replacement at (-10°C) and they mentioned that they were able to achieve 96% of the compressive strength of control cement paste cured at room temperature in 28 days also with similar durability parameters. Alzaza et al. (2022) studied the mechanical and durability properties of cement mortar consisting of NCSH seed accelerator along with GGBFS as fine aggregate replacement and concluded that the replacement of natural sand with 50% GGBFS fine aggregate in mortar will enhance frost resistance with a very slight reduction in compressive strength. In industrial areas and sewage pipes, in which acidic attacks are expected, natural sand can be fully substituted with GBFS aggregate to reduce the effect on the degradation of cement concrete by the acid attack since the acid resistance was directly proportional to the percentage of GGBFS aggregate in the mix according to his study.

Szostak & Golewski (2020) assessed the improvement in cement strength by addition of Siliceous fly ash and NCSH Seeds. They tested the strength of the resulting specimens at 8h, 12h, 1d, 3d, 7d, 14d and 28d after casting. Also, hydration heat tests were carried out within first 24 hours of the casting. Observations concluded that NCSH seeds contributed to the development of the strength significantly in first hours of curing and a clear influence was noted in the first 24 hours. With the time the effect of added nano admixture decreased. Hydration heat test showed that much larger amount of heat was dissipated in the case of the nano admixture modified cement matrix.

Golewski & Szostak (2021) studied the feasibility of using NCSH seed accelerator and fly ash to be used in precast industry and asserted that the early strength development is accelerated in the binder. Since nano admixture reacts with fly ash faster it enters to an accelerated pozzolanic reaction with cement paste. Therefore, this intensified reactivity causes the self-healing process to recover early age internal cracks. Gu et al. (2022) researched the applicability of NCSH seeds originated with GGBFS and Carbide slag with Portland Cement. They noted that addition of 4% NCSH seeds in OPC paste, increased the early strength by 131.4% at 12h and final setting time has been reduced by 46.3%. NCSH seeds has accelerated the hydration and further expedite the hydrates formation in OPC.

Zhou et al (2023) studied the early-age properties of using of NCSH modified HVFA concrete and environmental impact of the same. They examined the use of fly ash replacement of 60% and 70% with NCSH percentages of 0.5%, 1% and 1.5%. The results showed that the mixes with 1% NCSH with 60% fly ash and 1.5% NCSH with 70% fly ash showed the maximum strength and shortest setting time. The mix with 1% NCSH having the highest strength among fly ash 60% mixes, achieved 94.11% of the strength of control OPC mix at the age of 14 days. The mix with 1.5% NCSH with the highest strength among 70% fly ash mixes achieved 88.93% of the strength of OPC concrete at the 14th day. The compressive strength result of this study is shown in Figure 2.2. They concluded that the addition of NCSH crystals accelerated the hydration of Tricalcium Aluminate (C_3A) and Tricalcium Silicate (C_3S) to form more CSH gel and ettringite which accounts for the concrete strength and has densified the overall microstructure of the paste matrix. Calcium Hydroxide (CH) content is also reduced at the age of 28 days due to its reaction with fly ash.

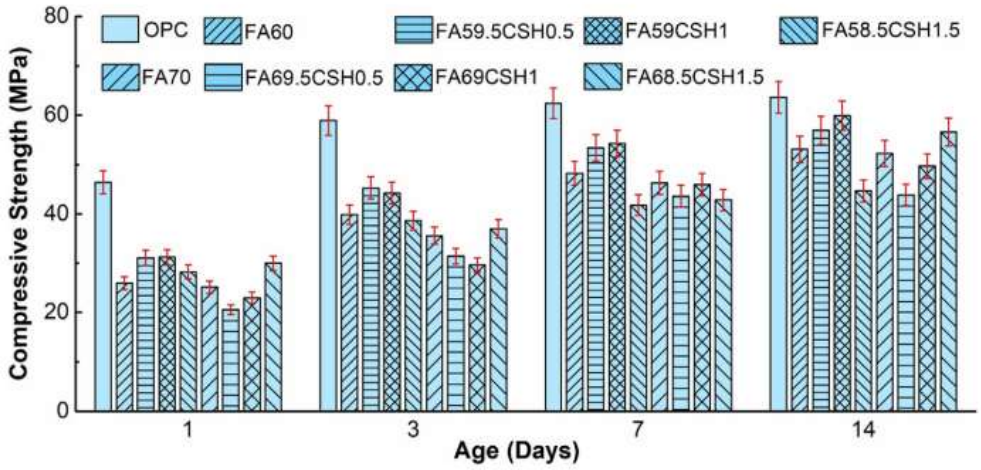

Figure 2.2: Compressive Strength development of fly ash concrete with NCSH seeds adopted from Zhou et al. (2021)

Summary and research gap:

Various researchers have used different nano materials to improve the mechanical and durability properties of HVFA and HVS concrete. NS, NC, and NA was studied in most of the studies with high volume fly ash and slag. 50-90% partial replacement of fly ash, slag and fly ash and slag combinations were studied in most of the research that has been done with nano materials. These nano materials also show various issues in terms of using in the concrete mixes such as they require special dispersion methods like ultrasonication for better mixing in the concrete mix which is an extra processing before using in the concrete. Also, some nano materials like nano alumina and nano calcium carbonate have shown adverse impact on compressive strength when they are used in higher contents. NCSH seed accelerator was used widely with OPC in the previous studied and with fly ash up to 70% was studied previously. The studies showed that the commercially available NCSH seed accelerators can be used with the concrete without using special mixing methods like ultrasonication and improved results were shown with OPC and with low volume of SCM replacement levels. There was less research conducted on utilizing fly ash and slag in high volume replacement levels and combination of fly ash and slag with NCSH seed accelerator. Therefore, possible research gap of utilizing slag, fly ash and slag and fly ash combined binders in higher replacement levels of 70-90% with NCSH seed accelerator was identified, and this research was conceptualised based on this research gap.

CHAPTER 3 – METHODOLOGY

3.1. Introduction

The experimental procedure was carried out in three phases. In first phase, flow characteristics of binder pastes and compressive strength at 3, 7 and 28 days (3d, 7d and 28d) was tested with varying replacement levels of slag, fly ash and slag-fly ash blend. In second phase based on the early age compressive strength development, eight mixes were selected for further microstructural analysis namely heat of hydration, XRD, TGA and SEM/EDS. In the third phase two concrete mixes were cast one for control OPC and the best performing binder among eight mixes exhibited highest early age strength development.

3.2. Materials

The materials used in this research were all locally sourced material available in the Curtin University's civil engineering laboratory. Only the NCSH seed accelerator was sourced from Master builder solutions. The chemical and physical properties of the materials were adopted from a recent research paper of Hosan et al. (2020) using the same sources of materials in the laboratory.

Table 3.1: Chemical and physical properties of cement, slag and fly ash adopted from Hosan et al. (2020)

		Cement	Slag	Fly Ash
Chemical Composition	CaO	64.39		
	SiO_2	21.1		
	Al_2O_3	5.24		
	Fe_2O_3	3.10		
	MgO	1.10		
	MnO	-		
	K_2O	0.57		
	Na_2O	0.23		
	P_2O_5	-		
	TiO_2	-		
	SO_3	2.52		
	LOI	1.22		
Physical Properties	Particle Size	25-40% ≤ 7µm	40% of 10 µm	50% of 10 µm
	Surface area(m^2/g)	-	-	-
	Specific gravity	2.7 to 3.2	2.6	-

3.2.1. Cement

Cement used in this research is locally sourced OPC complying with AS3972, manufactured by Cockburn cement with the specific gravity 2.7-3.2 and 25% to 40% of particles ≤ 7μm size. The physical properties and chemical composition of OPC is shown in Table 3.1.

3.2.2. Fly Ash

Fly ash used in this research complied with AS 3582.2 – "Supplementary Cementitious Materials – Part 1: Fly Ash. Fly ash used in this research was sourced from Eraring power station of NSW and classed as class F fly ash. Table 3.1 shows physical and chemical composition of the fly ash.

3.3.3. Ground Granulated Blast Furnace Slag (GGBFS)

"Slag" is the primary waste product in metal industry which is the refine from ore in a blast furnaces. There is slag in iron, copper, and other metals. But iron slag is the most widely used material as SCM in concrete. This iron slag when milled in a cement mill is referred as "Ground Granulated Blast Furnace Slag-GGBFS". GGBFS supplied by BGC cement Australia is used in this research. The physical and chemical composition is shown in the Table 3.1.

3.3.4. NCSH Seed accelerator

A commercially available Master X-Seed 1500 was used in this research which is a product of Master Builders solutions. Master X-Seed 1500 complies with AS1478.1-2000 Type SAc Special Purpose Accelerating. It consists of synthetically produced nanoparticles suspended in a liquid and boosts the hardening properties of the concrete mix. A CryoSEM of Master X-Seed active crystals growing in between the cement particles is shown in Figure 3.1, the image shows the accumulation of the crystal seeds improving the CSH gel formation in between the cement particles. The physical properties of Master X-Seed 1500 are summarised in Table 3.2 and the appearance of NCSH seed accelerator in room temperature is shown in figure 3.2. The strength development of a fluid concrete with cement content of 380kg/m^3 of CEM1 52.5R is shown in Figure 3.3. The figure shows the mix with Master X-seed shows an accelerated early strength gain with respect to the traditional accelerators.

Table 3.2: Properties of Master X-Seed 1500

Appearance	White liquid
Specific gravity @ 20°C	1.14 ± 0.02 g/cm3
pH @ 20 °C	10 - 11
Solid Content	22%

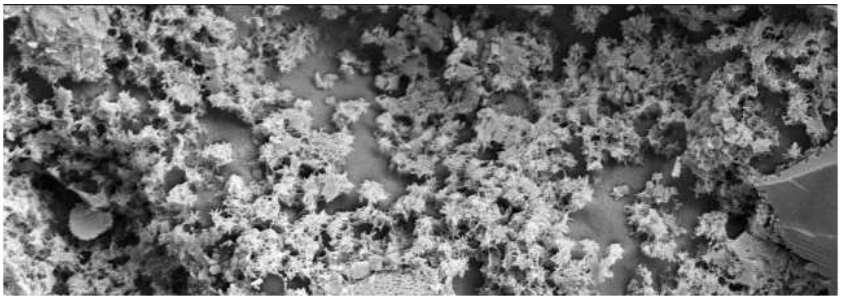

Figure 3.1: CryoSEM of Master X-Seed adopted from BASF (2015)

Figure 3.2: Appearance of Master X-seed 1500 in room temperature.

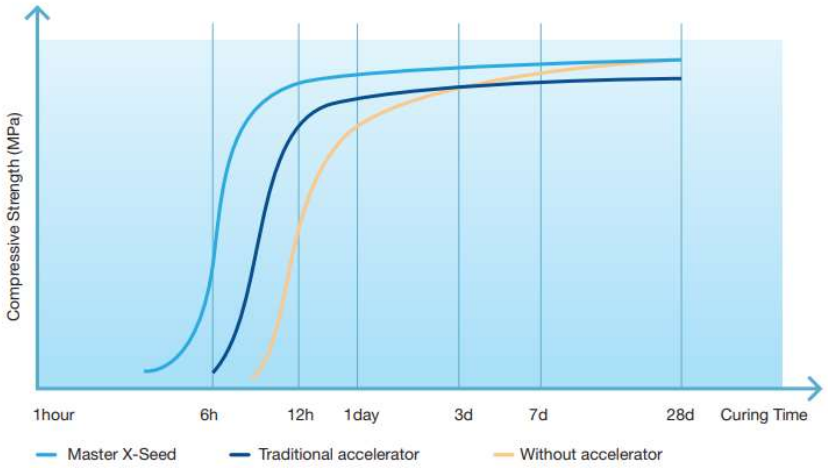

Figure 3.3: Strength development of Master X-Seed -Accelerator effect (fluid concrete with 380kg/m^3 CEM1 52.5R adopted from BASF (2015)

3.3 Experimental plan and mix proportions.

All the mixes were designed with total binder content of 2500g and a constant water/binder ratio of 0.35 was used in all the mixes. Water content of the NCSH seeds were considered when calculating total water in the mix and the weight of water of NSCH was reduced from the required water content. Target flow of the control mix was 200-220mm. Table 3.3 shows all the mixes considered in the research.

Table 3.3: Mix proportions of blended binder pastes.

	Mix Design	Cement(g)	Fly Ash(g)	Slag(g)	Water(g)	NCSH (g)
1	100C	2500	-	-	875	-
2	C100CSH2.5	2500	-	-	820	62.5
3	C100CSH5	2500	-	-	767	125
4	C30S70	750	-	1750	875	-
5	C30S70CSH2.5	750	-	1750	820	62.5
6	C30S70CSH5	750	-	1750	767	125
7	C30S70CSH7.5	750	-	1750	711	187.5
8	C20S80	500	-	2000	875	-
9	C20S80CSH2.5	500	-	2000	820	62.5
10	C20S80CSH5	500	-	2000	767	125
11	C20S80CSH7.5	500	-	2000	711	187.5
12	C10S90	250	-	2250	875	-
13	C10S90CSH2.5	250	-	2250	820	62.5
14	C10S90CSH5	250	-	2250	767	125
15	C10S90CSH7.5	250	-	2250	711	187.5
16	C30FA70	750	1750	-	875	-
17	C30FA70CSH2.5	750	1750	-	820	62.5
18	C30FA70CSH5	750	1750	-	767	125
19	C30FA70CSH7.5	750	1750	-	711	-
20	C20FA80	500	2000	-	875	-
21	C20FA80CSH2.5	500	2000	-	820	62.5
22	C20FA80CSH5	500	2000	-	767	125
23	C20FA80CSH7.5	500	2000	-	711	187.5
24	C10FA90	250	2250	-	875	-
25	C10FA90CSH2.5	250	2250	-	820	62.5
26	C10FA90CSH5	250	2250	-	767	125
27	C10FA90CSH7.5	250	2250	-	711	187.5
28	C30FS70	750	875	875	875	-
29	C30FS70CSH2.5	750	875	875	820	62.5
30	C30FS70CSH5	750	875	875	767	125
32	C20FS80	500	1000	1000	875	-
33	C20FS80CSH2.5	500	1000	1000	820	62.5
36	C10FS90	250	1125	1125	875	
37	C10FS90CSH2.5	250	1125	1125	820	62.5

Mix designs were named according to the weight percentage of OPC, SCM and the weight percentage of NCSH. For example, C30S70CSH7.5 means a mix containing 30% OPC, 70% Slag and 7.5% NCSH seed accelerator. 3 different NCSH percentages were selected to check establish a relationship between the percentage of NCSH and the performance of resulting mix designs. The replacement levels of the OPC are 70%, 80% and 90% by the total weight of the mix in the mix designs.

3.4. Specimen casting and curing

Samples were weighted according to the required ratios and Hobart mixer was used to mix the weighted materials to prepare specimens for testing. Initially the cement and SCM are dry mixed for 3 minutes and then NCSH seed accelerator mixed with water is added into the mix. The materials are mixed for another 3 minutes and then the flow table test is conducted on the mix. The mix is then poured in to 50mm cube moulds, casted in 2 layers and vibrated using the vibrating table to remove the entrapped air voids. Nine cubes in each mix were cast to test the compressive strength of the binder in 3d, 7d and 28d. Samples were demoulded after 24h and water cured in room temperature and tested for compressive strength at above test ages.

3.5. Test Methods for Paste Samples

3.5.1. Flow Test

Flow table test was carried out according to the ASTMC230 to measure the flow of the binder paste to determine the consistency of the paste. Total water content of all the mixes were kept constant in the mixes to evaluate the effect on the flow of the mixes with the replacing of cement with slag, fly ash and slag + fly ash mixes and the addition of NCSH seed accelerator.

Figure 3.3: Flow table apparatus.

3.5.1. Compressive Strength of Binder Pastes

Compressive strength of the binder paste samples were tested in 3d, 7d and 28d for the wet cured 50mm x 50mm x 50mm cubes in accordance with ASTM C109 in Shimadzu 300kN testing machine using a loading rate of 0.33MPa/s as shown in the Figure 3.4.

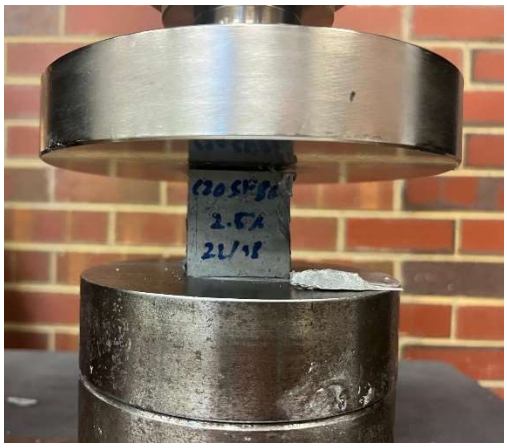

Figure 3.4: Paste sample compressive strength.

3.5.2. Isothermal Calorimetry of Binder Paste

Isothermal Calorimetry test of selected nine mixes was carried out with TAM Air 8 Channel Isothermal Calorimeter shown in Figure 3.5. Sample of 6g from freshly mixed binder was placed inside the 20mL Ampoule and the ampoules are placed in the calorimeter and the readings were collected for 92hrs.

Figure 3.5: TAM Air 8 Channel Isothermal Calorimeter.

3.5.3. Scanning Electron Microscopy (SEM)/ Energy Dispersive X-Ray Spectroscopy (EDS)

Microstructural analysis of the selected paste samples was carried out with the MIRA3 TESCAN SEM equipment as shown in Figure 3.6. 10mmx10mmx2mm size small part is cut from the 7d and 28d wet cured dry specimens using a mechanical cutter and were oven dried to remove the moisture. The samples were then mounted in epoxy resin, polished and 20 nm thick carbon coating was applied to reduce the charging of particles during the scanning process.

Figure 3.6: MIRA3 TESCAN SEM equipment

3.5.4. Thermogravimetric Analysis (TGA)

Thermogravimetric analysis was conducted on oven dried samples using NETZSCH STA 449 F5 Jupiter equipment shown in Figure 3.7. Thermogravimetric analysis (TGA) and Differential scanning calorimetry (DSC) was carried out in a controlled Nitrogen(N_2) gas atmosphere with a heating rate of 10°C/ min from 25°C -1000°C. An Alumina crystal (AL_2O_3) crucible was used to hold the samples. Simultaneous Thermogravimetry Analysis (STA) machine was preheated for minimum of 4h before the test. NETZSCH software is opened, and a new test method is specified including the temperature range and the heating rate. The empty crucible is then tared in the machine, and it is taken out and samples were filled up to 3/4 of the volume of crucible. The filled crucible is then place inside the machine and the test is started. With the given temperature range the test was carried out for 90mins and the same time was

taken to cool down to the initial temperature. The results were extracted from the Proteus TGA analyser software and then exported to Excel for further analysis of the data.

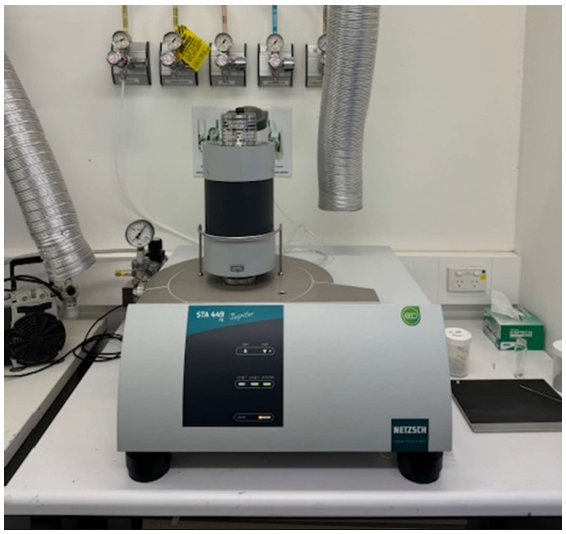

Figure 3.7: NETZSCH STA 449 F5 Jupiter equipment

3.5.5. X-Ray Diffraction (XRD)

Binder pastes samples which were retained from 7d and 28d compressive strength test were oven dried at 60ºC in oven. Those samples were then grinded with the ring mill and 3g of ring milled samples were further micronized with the micronizing mill. Then those samples were packed with the backloading specimen packer and XRD testing was carried out with Bruker D8 Cu Ka from 2 Theta angle 10^0 to 90^0 as shown in Figure 3.8. Test results were then analysed with the DIFFRAC software for qualitative phase ID. PDF database was used to identify the peaks of the resulting XRD spectrums.

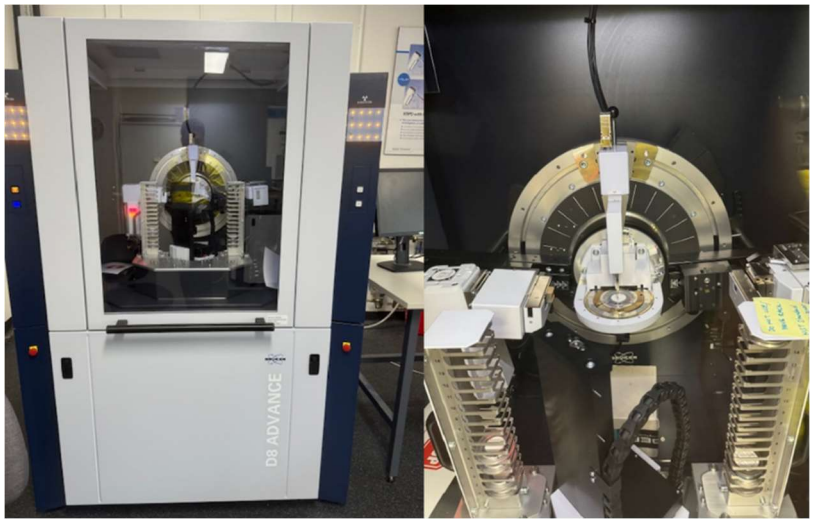

Figure 3.8: Bruker D8 ADVANCE XRD Machine

3.6. Concrete Tests

The optimum paste mix which was selected based on the early strength development and maximum cement replacement level is used to cast concrete specimens and a control concrete mix containing 100% OPC is also cast for comparison. Concrete casting was done using a 70L pan mixer. Initially, the coarse and fine aggregates were prepared for saturated surface Dry (SSD) condition and the raw materials (OPC and slag) were weighed and put into the pan mixer. The NCSH seed accelerator was mixed with 50% of water and kept separately. Dry mixing is carried out for 5 minutes and then the water with the NCSH seed is added to the mix and then the rest of the water is added to the mix after 2 minutes. Mixing is carried out for another 2 minutes and then a slump test is conducted immediately. Steel cylinder moulds were cast in three layers and compacted on a vibrating table. 100mm diameter and 200mm high cylinders were used for compressive strength, modulus of elasticity and for durability tests, while 150mm diameter by 300mm high cylinders were cast for split tensile strength testing. Samples were demoulded after 24 hours of casting and then placed in water curing tanks at room temperature for 28 days before carrying out the mechanical and durability property tests. The mix design used for casting the concrete is shown in Table 3.4

Table 3.4: Concrete mix details - kg/m3

Parameter	**Unit**	**C100**	**C20S80CSH7.5**
Cement	kg	400	80
Slag	kg	0	320
20mm Aggregate	kg	828	828
10mm Aggregate	kg	356	356
Sand	kg	684	684
Water	L	168	141
Master X Seed 1500	L	0	30
w/b ratio		0.42	0.42

3.6.1. Workability

Slump of the concrete mixes was measured as per ASTM C143. A standard slump cone was placed on the tray on levelled ground and the cone was filled with fresh concrete in three layers, each layer was compacted with 25 blows with the rod and then the excess concrete was levelled off with the rod. The cone is slowly pulled up and the rod is placed on the inverted cone and the height of the mix to the rod is measured using a measuring tape as shown in Figure 3.9.

Figure 3.9: Slump of control mix

3.6.2. Compressive Strength

The compressive strength of all concrete cylinders was tested using a multifunctional control console machine (MCC8) according to ASTM C39 standards using a loading rate of 0.33 MPa/sec after 28-day water curing at room temperature. For each mix minimum of 3 samples were tested and the average compressive strength was calculated and reported in this thesis. The test setup is shown in Figure 3.10 below.

Figure 3.10: Compressive strength test setup

3.6.3. Indirect Tensile Strength

Indirect tensile strength test was carried out by using MCC8 test apparatus with the loading rate of 0.067 MPa/sec. The cylinder was placed horizontally on the test apparatus as shown in Figure 3.11 and subjected to a diametric compressive force along its length as per ASTM C 496/C 496M. The failure of the cylinder occurred on the vertical axis of the face of the cylinder as shown in Figure 3.11.

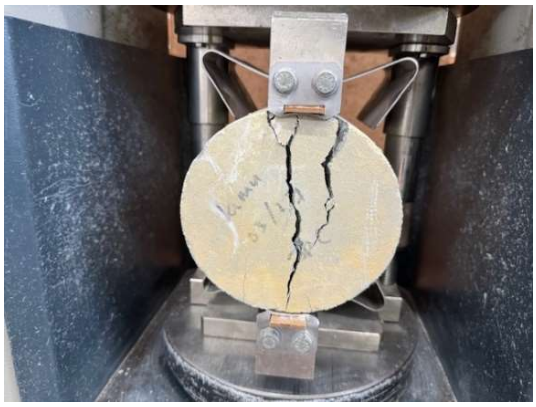

Figure 3.11: Indirect tensile strength test setup

3.6.4. Modulus of Elasticity

The modulus of elasticity is also tested as per ASTM C469 using the MCC8 testing machine with the strain gauges attached to the concrete cylinder. Firstly, the cylinder surfaces were polished with the sample polishing machine to create an even surface. Then the strain gauges were fixed to the cylinder as per Figure 3.11 and then a test load of 40% of the ultimate compressive strength was applied at least three cycles of loading and off-loading on the specimen to test the modulus of elasticity. A computerised data logger was connected to the strain measuring gauges to collect the data and analysed to find out the elastic modulus of each specimen.

Figure 3.12: Modulus of elasticity test preparation

3.6.5. Volume of Permeable Voids

Volume of Permeable voids was tested as per ASTM C 642 – 06. Initially 50mm thick discs from 28-day water cured samples were cut from the 100mm diameter cylinder and the samples were dried in an oven at a temperature of 100 to 110 ° until a constant dry mass is achieved. The mass is recorded as the oven-dry mass and then the samples are soaked in room temperature water for 48hrs, and the weight is recorded as the saturated mass after immersion. Then the sample is boiled in a covered tap water bath for 5h and then the saturated mass after boiling is recorded. Finally, the immersed apparent mass is calculated by submerging the sample in water. The permeable void percentage is calculated according to the formula given in the standard.

3.6.6. Rapid Chloride Permeability Test

Rapid chloride permeability test is conducted as per the ASTM C1202 standard. 50mm thick samples were cut from 100mm diameter cylindrical moulds and then an epoxy coating was applied on the curved surface to avoid leaking from the sides. The samples were then dried for 3 hours in a vacuum desiccator and then fill the desiccator with de-aerated water to cover the samples while the pump was running and left the vacuum pump to run for an additional hour. The vacuum pump was turned off and then left the samples inside the desiccator for at least 18 hours. The specimens were left from water and then install the sample to the RCPT cells as shown in Figure 3.12 and fill the two cells with 3.0% NaCl and 0.3N NaOH solutions to the respective cell. The cables were fixed accordingly, and the test was started and left to run for 6 hours.

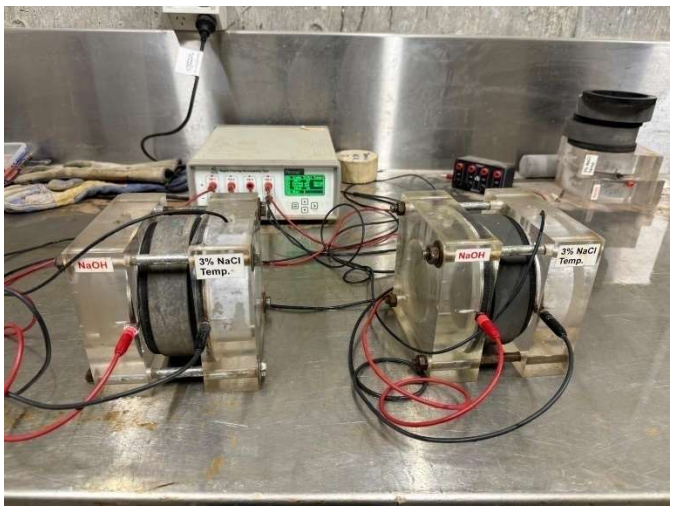

Figure 3.13: RCPT Test Apparatus

3.6.7. Water Permeability Test

The water penetration depth test was conducted according to BS EN 12390–8 standard. Three cylinders of each mix with a diameter 100mm and height of 200mm were placed in the water penetration depth measurement apparatus as shown in Figure 3.13 and a constant pressure was applied maintaining 500 ± 50 kPa for 72 h. After removal, the cylinders were split into two pieces and marked and measured the water penetration depth.

Figure 3.14: Water penetration test apparatus

CHAPTER 4: RESULTS AND DISCUSSION

4.1. Introduction

This chapter presents the results of the experimental programme carried out as per the methodology in chapter 3. The results are presented in 3 parts. In first part the flow and compressive strength of all the mixes conducted in the research is presented and evaluated. In second part, the selected eight mixes which exhibited higher early age compressive strength out of the 37 mixes for further investigation is presented. Isothermal calorimetry, SEM/EDS and TGA data are presented for those mixes. In the third part the mechanical and durability properties of the resulted optimum high volume slag concrete and the control concrete mixes are presented and evaluated. For concrete mixes, slump, 7d and 28d compressive strength, split tensile test, modulus of elasticity, water penetration, volume of permeable voids, rapid chloride permeability test results are presented.

4.2. Flow test

The flow results of all mixes are shown in Figure 4.1. The flow test measures the workability of the binder paste mix, which is an important factor in determining its suitability for various construction applications. The flow diameter was measured in two perpendicular directions and the average was reported below.

The initial flow diameter of the control mix was designed for 200+/-10 and the effect of the addition of SCM and NCSH seed accelerator was studied while maintaining the total water content of the mix a constant.

From the results, it is observed that the flow decreased slightly when slag replacement levels are increased in the mix, compared to the control mix. This decrease in flow can be attributed to the angular shape of slag particles and the increased viscosity of the mix due to the finer particles of slag.

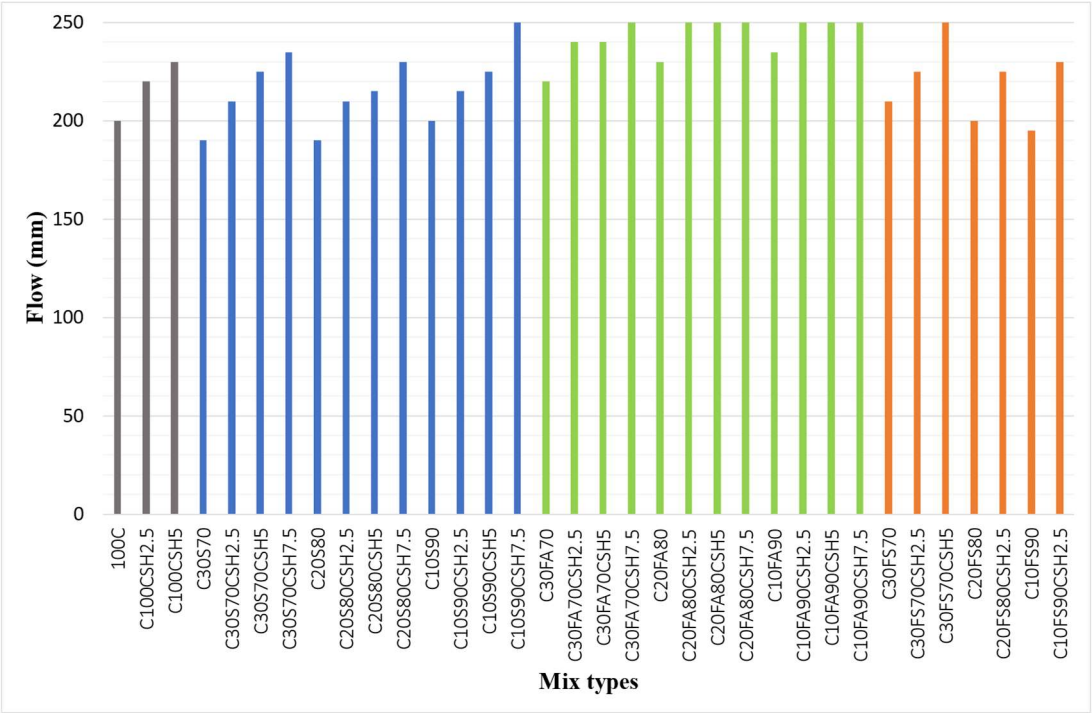

Figure 4.1: Flow test results of each mix

However, with the addition of the NCSH seed accelerator, there was a notable improvement in the flow. The flow increased gradually with the addition of 2.5%, 5%, and 7.5% of the NCSH seed accelerator. This improvement can be attributed to the water-reducing capability of the Master X-Seed 1500, which accounts for a 15-20% reduction in water content. Since the total water content of all the mixes was kept constant, this water-reducing capability resulted in improved workability and flow of the binder paste.

On the other hand, when fly ash was used as a replacement material, the flow increased compared to the control mix. This can be explained by the spherical shape and the smooth surface texture of fly ash particles, which improve the flow characteristics of the mix. With the addition of the NCSH seed accelerator, the flow increased even further, and the mix began to exhibit bleeding at 5% and 7.5% NCSH addition. This suggests that the addition of NCSH seeds significantly enhances the flow properties, but excessive amounts may lead to segregation and bleeding.

In the slag + fly ash mixes with the increase of the replacement levels, the flow increased but this increase was less than the mixes with fly ash replacement but higher than the slag replaced mixes. This is because of the spherical shape of the fly ash

particles are being dominant in the mix for the flow characteristics but with the presence of angular slag particles it shows a bit less workability than the fly ash mixes. These fly ash + slag replaced mixes also show an increase of workability with the addition of NCSH seed accelerator and with the increase of NCSH seeds, resulted in higher bleeding of the mix but, those mixes also showed a better cohesion. Also, some mixes which showed bleeding had higher strength, but the standard deviation of the results were very high.

In summary, the addition of NCSH seeds has a beneficial effect on the flow characteristics of the concrete mixes. It enhances workability, especially when combined with slag or fly ash replacements. However, it is essential to optimize the dosage of the NCSH seed accelerator to prevent issues like bleeding, which can affect the quality and durability of the concrete.

4.3. Compressive Strength

The compressive strength of the paste samples was measured using a Shimadzu 300kN universal testing machine. The compressive strength tests were conducted at three different ages: 3 days, 7 days, and 28 days, to assess the early and long-term strength development of the concrete mixes. For each test, 50mm cube samples were cast and subjected to water curing to ensure proper hydration and strength gain.

The strength activity index (SAI) was calculated using the strength results obtained from these tests. This index provides a comparative measure of the strength performance of the different concrete mixes relative to the control mix.

The results are presented with the standard deviation of the compressive strength values for each mix at each test age, shown as error bars in the compressive strength result graph. These error bars indicate the variability and consistency of the strength measurements, providing insights into the reliability of the results.

The effect of the NCSH seed accelerator was evaluated in different scenarios, including high-volume slag paste, high-volume fly ash pastes, and a combination of high-volume fly ash and slag pastes. The performance of each mix was analysed to understand the influence of the NCSH seed accelerator on the compressive strength development.

4.3.1. Effect of NCSH seed accelerator with HVS mixes

The compressive strength development of HVS binder pastes with NCSH seed accelerator demonstrates significant variability depending on the replacement levels and the percentage of accelerator used. Figure 4.2 based on table A1-A16 of appendix, presents the compressive strength values of various mixes, highlighting the impact of different NCSH seed accelerator percentages on strength development. The addition of NCSH seed accelerators enhances the compressive strength across all mixes. For instance, a mix with 80% slag and 7.5% NCSH seed accelerator exhibits significant early strength gains, particularly at 3 days. This mix achieves the highest early age strength increase, emphasizing the effectiveness of NCSH seed accelerator in accelerating early strength development. Also, the isothermal calorimetry data proves this with the increased initial heat dissipation of the sample. The primary mechanism involves their ability to serve as nucleation sites for the formation of additional CSH gel, which is the main strength-giving phase in cement. When nano CSH seeds are introduced into the cement mix, they provide a larger surface area for hydration reactions to occur. The presence of these seeds accelerates the hydration of cement particles, leading to more rapid formation of CSH. This process is particularly effective at early ages, where the initial hydration reactions are critical for strength development.

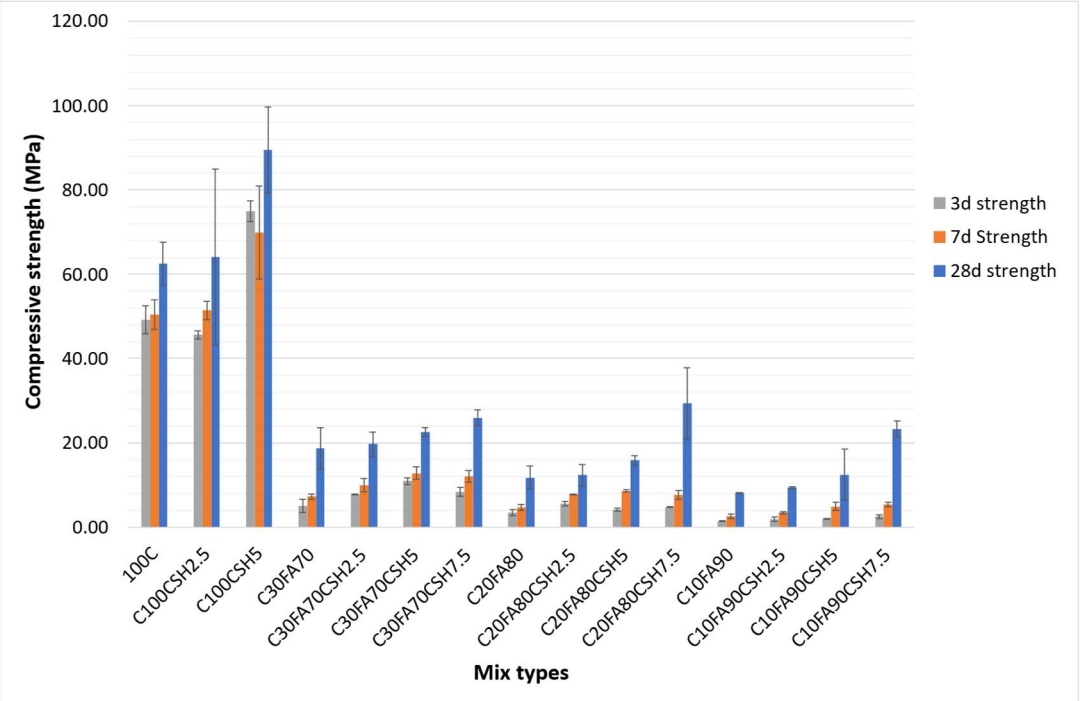

Figure 4.2: Compressive strength of slag mixes with control mix.

Figure 4.3 illustrates the SAI for various slag mixes at 3, 7, and 28 days. Notably, a 70% replacement of slag with OPC leads to a considerable reduction in compressive strength, especially in the early days: 68% at 3 days, 42% at 7 days, and 33% at 28 days. This trend is more evident with higher replacement levels of 80% and 90% slag, indicating that increasing slag content further reduces early and late age compressive strengths.

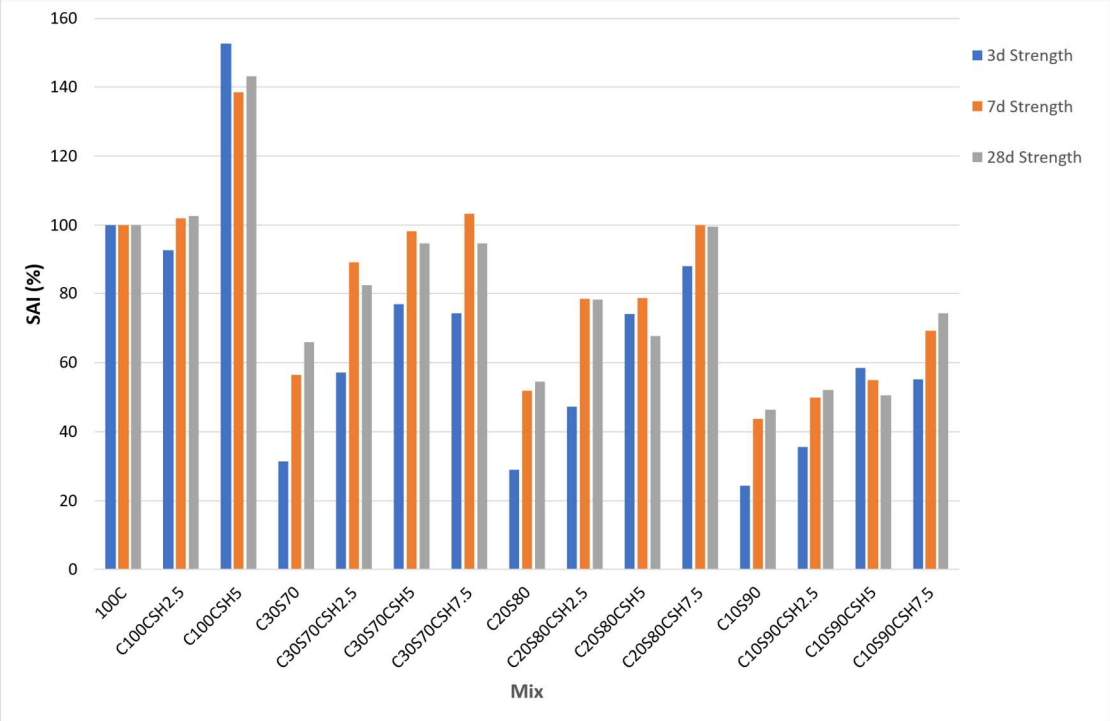

Figure 4.3: SAI of slag mixes

Figure 4.4 breaks down the compressive strength development for 70%, 80%, and 90% slag mixes with varying percentages of NCSH seed accelerator with respect to same replacement levels without NCSH seed accelerator. With 70% slag, the addition of 2.5%, 5%, and 7.5% NCSH seed accelerators increases the 3-day strength by 82%, 145%, and 167%, respectively. Similar trends are observed at 7 and 28 days, although the percentage gains decrease slightly over time. This pattern highlights the critical role of NCSH seed accelerator in enhancing both early ages and 28 days strengths of high-volume slag binder pastes.

In summary, the inclusion of NCSH seed accelerator significantly boosts the compressive strength of slag mixes, with the most substantial improvements observed in early (3 days) strength development. Higher percentages of NCSH seed accelerator consistently yield greater strength increases, particularly at early ages (3 and 7 days).

These findings emphasize the potential of NCSH seed accelerator in optimizing the performance of high-volume slag binder pastes, making them viable alternatives to conventional OPC mixes for various construction applications.

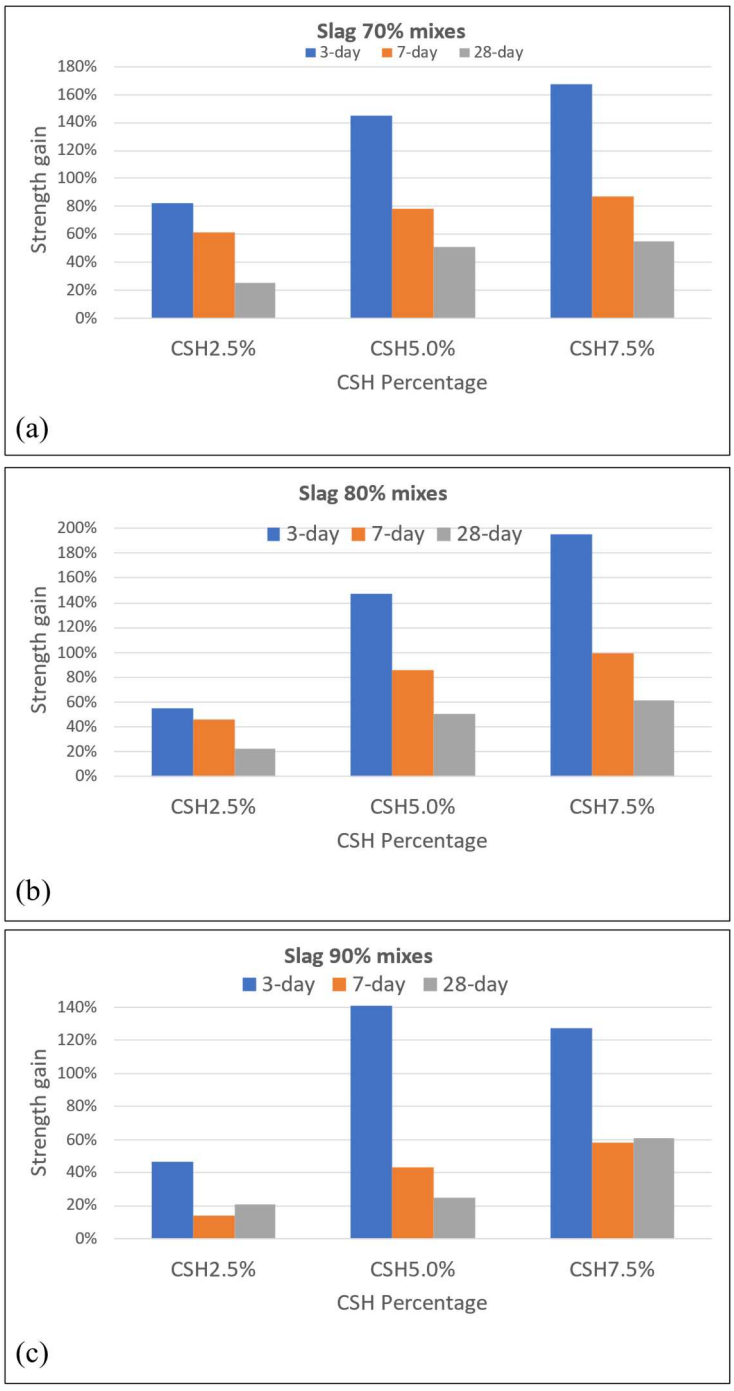

Figure 4.4: Compressive strength gain of HVS pastes with varying NCSH seed accelerator content with respect to the HVS pastes without NCSH.

4.3.2. Effect of NCSH seed accelerator with HVFA mixes

The compressive strength development of high-volume fly ash mixes with and without NCSH seed accelerator shows diverse trends. Figure 4.5 based on table A17- A27 of appendix presents the compressive strength at 3 days, 7 days, and 28 days for different mix types. The data indicates that adding fly ash reduces the compressive strength significantly, particularly in the early stages. For instance, at a 70% fly ash replacement level, the 3-day, 7-day, and 28-day strengths decrease by 89.8%, 85.5%, and 70%, respectively, compared to the control mix with 100% OPC. The addition of NCSH seed accelerator, however, improves both early age and 28 days strengths, this was less prominent than in slag mixes. The error bars in Figure 4.5 indicate variability in the data, likely due to the high flow and bleeding of the mixes.

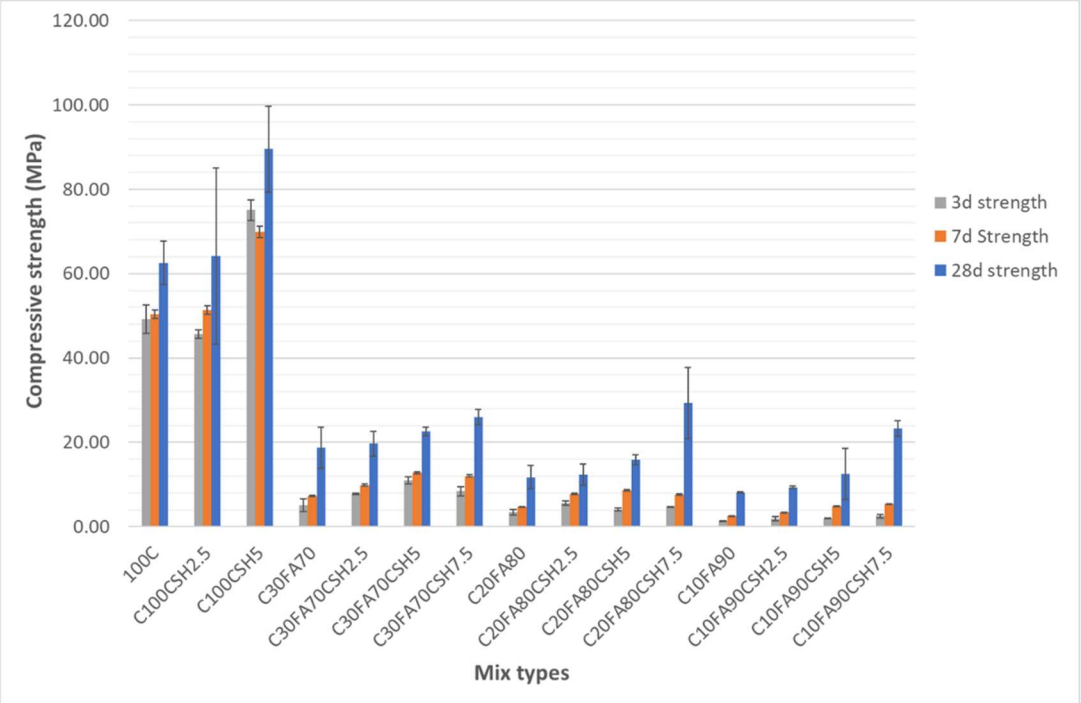

Figure 4.5: Compressive strength of Fly ash mixes with control mix.

Figure 4.6 displays the SAI for various fly ash mixes, showing that fly ash addition reduces the 28-day strength by 65%, 77%, and 93% at 70%, 80%, and 90% replacement levels, respectively. The slight increase in early strength with NCSH seed accelerator suggests an initial enhancement in the pozzolanic reaction of fly ash. However, the strength gains are more significant at 28 days, which might be related to the slower pozzolanic reaction of fly ash.

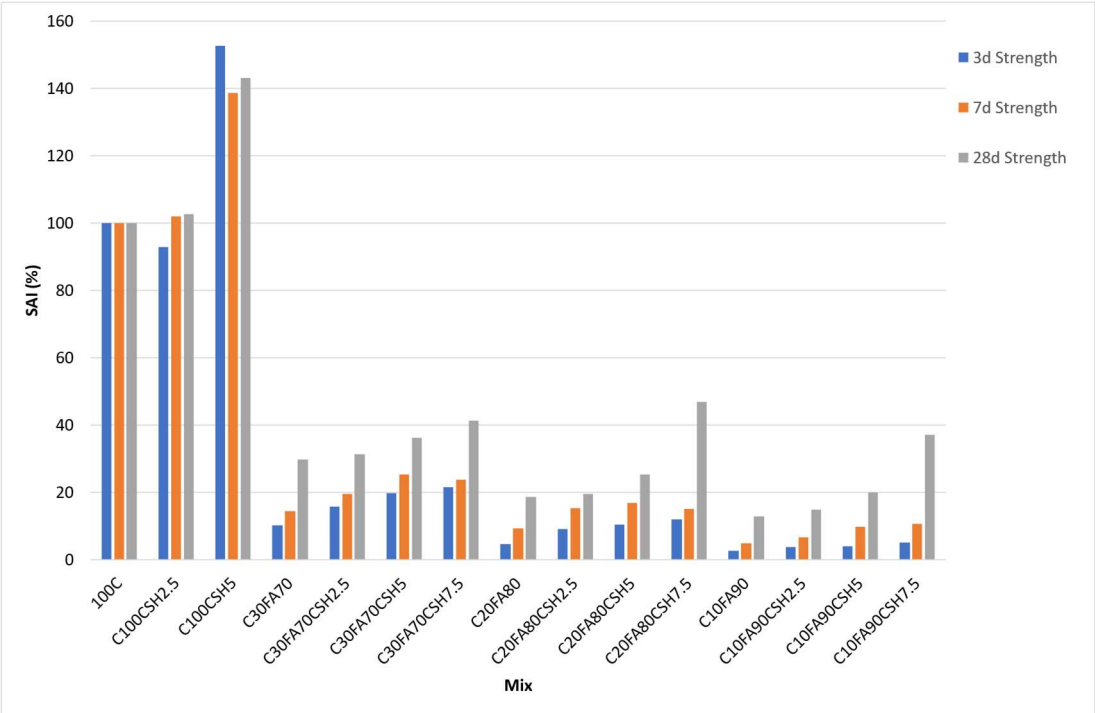

Figure 4.6: SAI of fly ash mixes

Figure 4.7 shows the percentage strength development for each replacement level with varying NCSH seed accelerator contents with respect to same replacement levels without NCSH seed accelerator. At a 70% fly ash replacement level, adding 2.5% NCSH seeds increases the 3-day, 7-day, and 28-day strengths by 54%, 36%, and 5%, respectively. With 5% NCSH seeds, the increase is more noticeable at 95%, 71%, and 21%, respectively. The 7.5% NCSH seed accelerator results in even higher gains, with 111%, 66%, and 38% increases in 3-day, 7-day, and 28-day strengths, respectively. These trends emphasize the effectiveness of NCSH seed accelerator in enhancing the compressive strength of fly ash mixes, especially in the early stages.

In summary, while the addition of NCSH seed accelerator enhances the compressive strength of HVFA mixes, the pattern of strength development is less consistent than slag mixes. The highest strength gains are observed at higher NCSH seed accelerator contents, particularly at early ages (3 and 7 days). However, the overall improvement is less visible, indicating that the pozzolanic reaction of fly ash is slower and less reactive than that of slag. The lower effectiveness of NCSH seeds in fly ash-based mixes compared to slag-based mixes can be attributed to the differing pozzolanic reactivity of these materials. Fly ash, primarily composed of silica, alumina, and iron oxide, exhibits slower and less reactive pozzolanic behavior than slag, which has

higher glass content and a more uniform composition that enhances its reactivity in alkaline environments (Bai et al., 2017; Zhang et al., 2020). When NCSH seeds are added, they effectively accelerate hydration in slag-based mixes, leading to rapid formation of additional CSH gel and improved mechanical properties (Yao et al., 2021). However, in fly ash-based mixes, the slower pozzolanic reactions limit the interaction with the nano seeds, resulting in less effective hydration and lower strength. SEM and calorimetry results can further illustrate these differences by highlighting the denser microstructure and greater heat evolution in slag-based systems compared to the fragmented structure in fly ash mixes (Chia et al., 2020). Thus, the inherent characteristics of fly ash significantly hinder the performance of nano CSH seeds, underscoring the need for optimization in their use with fly ash. These findings suggest that optimizing the amount of NCSH seed accelerator can significantly enhance the performance of high-volume fly ash binder pastes, making them more viable for construction applications.

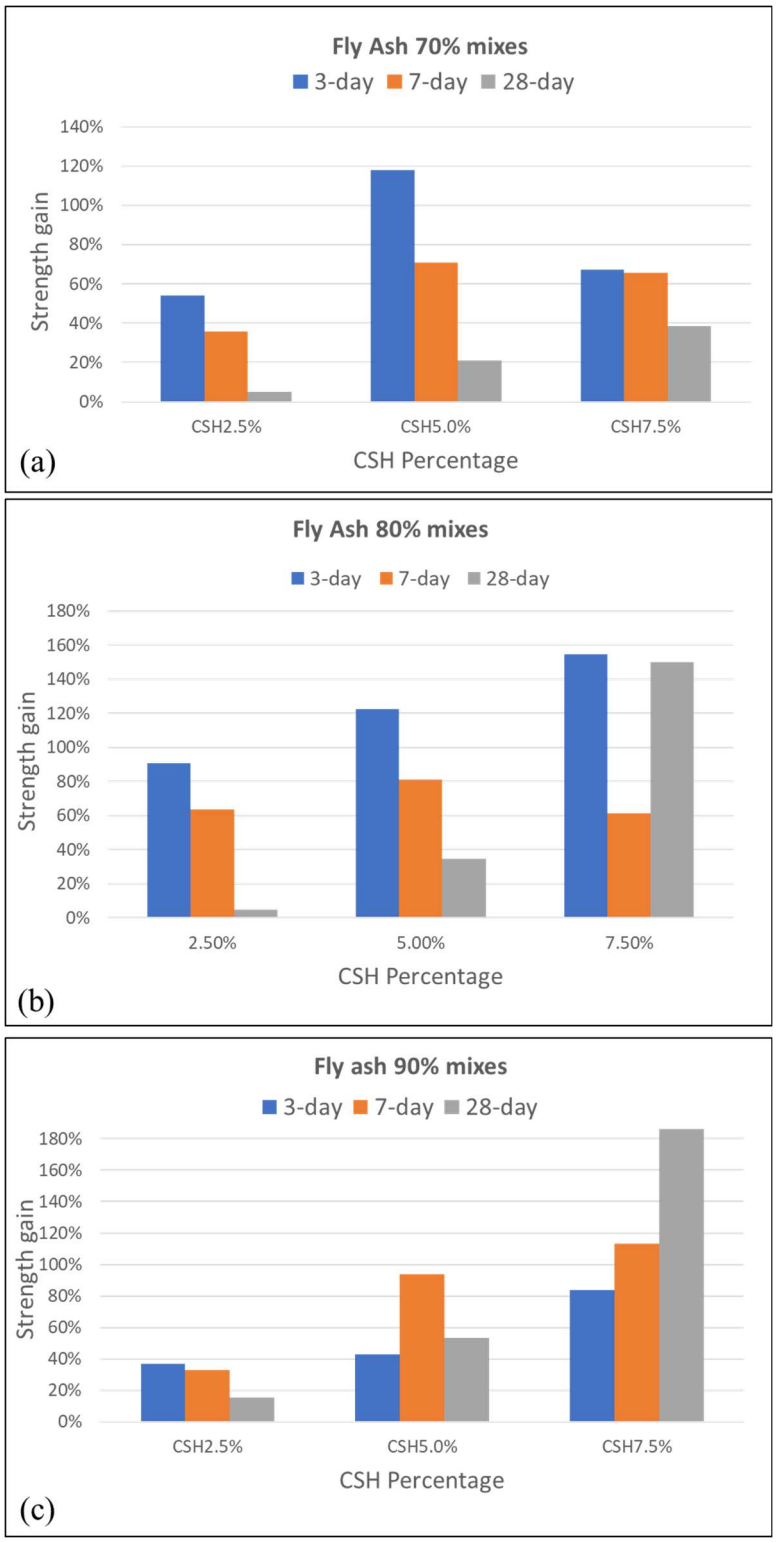

Figure 4.7: Compressive strength gain of HVFA pastes with varying NCSH seed accelerator content with respect to the HVFA pastes without NCSH.

4.3.3. Effect of NCSH seed accelerator on HVS-FA mixes

The compressive strength of high-volume fly ash mixes combined with slag, and NCSH seed accelerator reveals key understandings into the performance of these materials, as demonstrated in Figures 4.8, 4.9, and 4.10. Figure 4.8 based on table A28-A34 of appendix, shows that the inclusion of fly ash and slag significantly reduces the 28-day compressive strength by 57%, 71%, and 70% for 70%, 80%, and 90% replacement levels, respectively. This reduction emphasizes the slower pozzolanic reaction rates of fly ash compared to pure OPC mixes. However, the addition of a 2.5% NCSH seed accelerator to these mixes significantly enhances the compressive strength, with the 80% replacement mix showing a notable 114% increase in 28-day strength, highlighting the accelerator's efficacy in improving late-age strength. The less strength in 5% NCSH may be due to the bleeding and segregation effect of the paste.

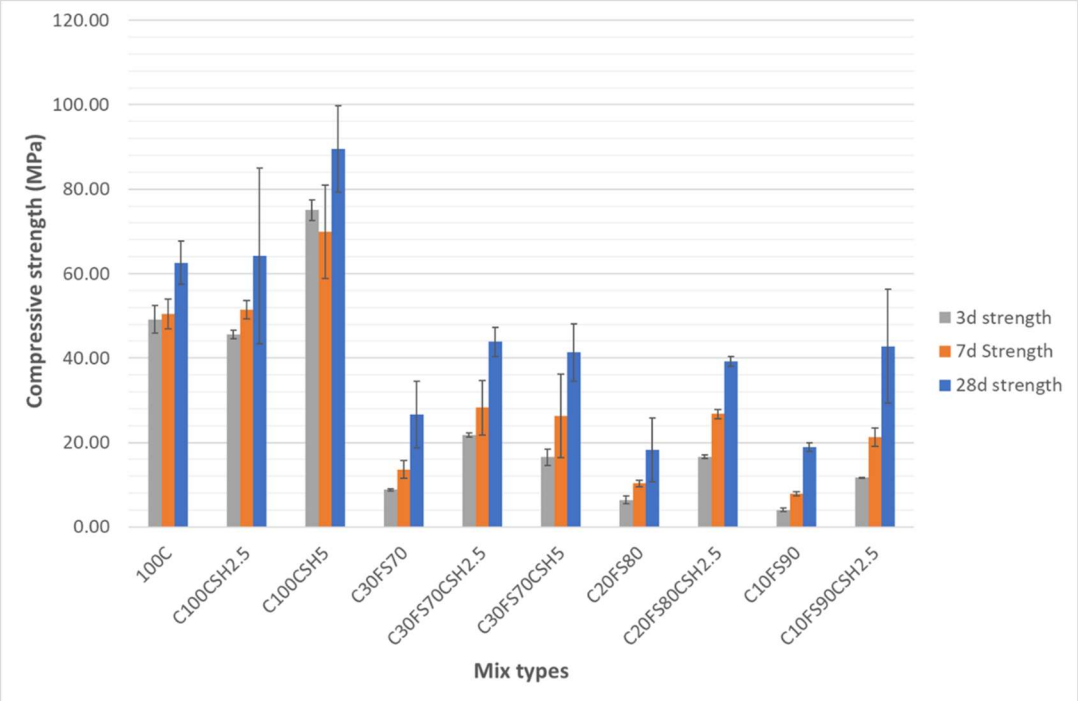

Figure 4.8: Compressive strength of slag+ fly ash mixes with control mix.

When considering the combined effects of slag and fly ash replacements, Figure 4.9 shows the SAI, reflecting how strength development varies with different NCSH seed accelerator contents. For a mix with 35% slag and 35% fly ash (70% total replacement), the strength reduction is significant: 82%, 73%, and 57.4% at 3, 7, and 28 days, respectively, compared to the 100% OPC control mix. The addition of 2.5%

NCSH seeds remarkably increases strength by 147%, 108%, and 64% at these respective time points, while 5% NCSH seeds result in 87%, 94%, and 55% increases.

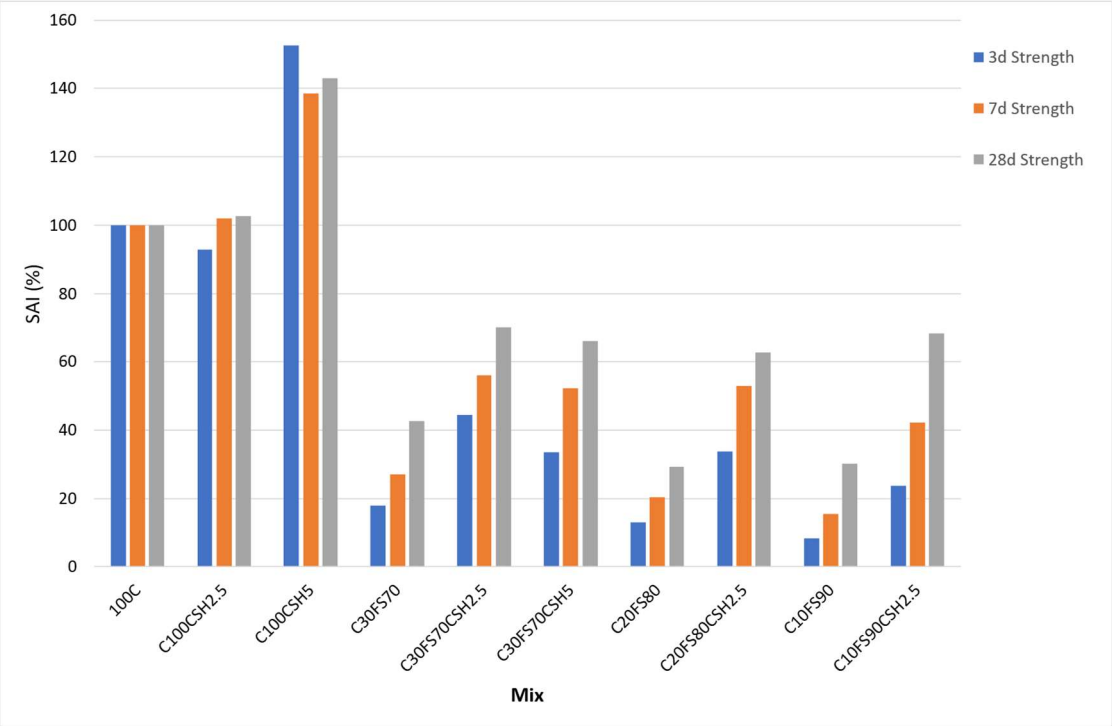

Figure 4.9: SAI of slag + fly ash mixes

Further examining higher replacement levels, Figure 4.9 indicates that for mixes with 40% slag and 40% fly ash (80% total replacement), compressive strength reductions are 87%, 80%, and 71% at 3, 7, and 28 days, respectively. The addition of 2.5% NCSH seeds leads to substantial increases of 160% at both 3 and 7 days, and 115% at 28 days. These results highlight the significant early-age strength gains enabled by the accelerator, which is necessary for structural applications requiring early load-bearing capacity.

For the highest replacement level of 90% (45% slag and 45% fly ash), Figure 4.9 shows a strength reduction of 92%, 84%, and 70% at 3, 7, and 28 days, respectively. However, Figure 4.10 shows that the addition of 2.5% NCSH seeds results in significant increases of 147%, 108%, and 64%, respectively, while 5% NCSH seeds offer improvements of 87%, 94%, and 55% with respect to the same replacement levels without NCSH seed accelerator. These enhancements are consistent with earlier observations and demonstrate the NCSH seed accelerator's ability to enhance both early and late strength, making high-volume fly ash and slag mixes more viable for

construction use. Such improvements have been confirmed by various studies, which consistently highlight the effectiveness of NCSH seed accelerators in enhancing the performance of supplementary cementitious material-based mixes (Rashad, 2014; Li et al., 2017).

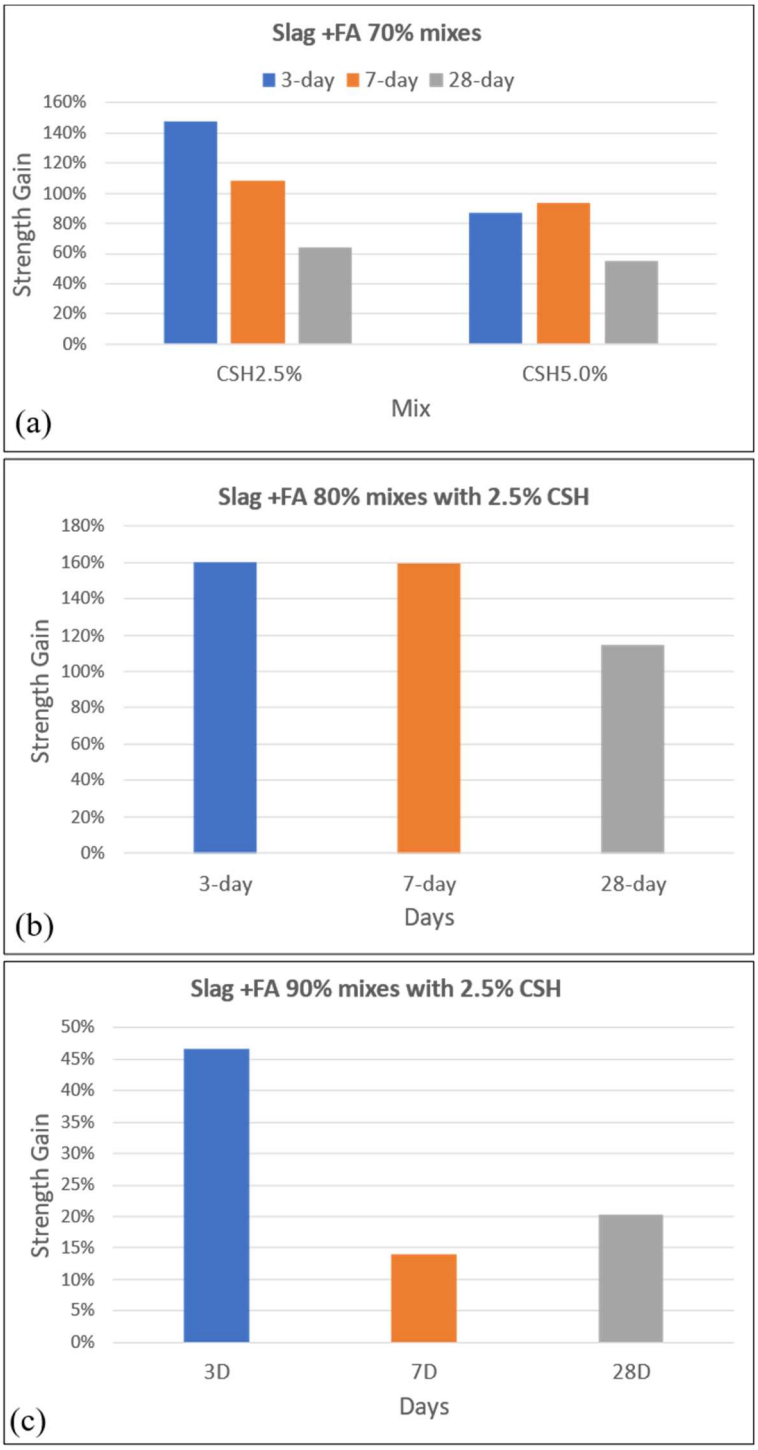

Figure 4.10: Compressive strength gain of slag +fly ash pastes with varying NCSH seed accelerator content with respect to the slag + fly ash pastes without NCSH

The following 8 mixes exhibited highest early age compressive strength values than other mixes and are selected for further analysis to establish the NCSH seed accelerator role on the strength improvement. These samples are tested for Isothermal Calorimetry, SEM, XRD and TGA for further analysis.

1. C100
2. C100CSH5
3. C20S80
4. C20S80CSH7.5
5. C30FA70
6. C30FA70CSH5
7. C20FS80
8. C20FS80CSH2.5

4.4. Isothermal Calorimeter test

The cumulative heat development in cementitious mixes with supplementary cementitious materials and NCSH seed accelerator is necessary for understanding their hydration characteristics and strength development. Figure 4.11 shows that the addition of SCMs significantly reduces the cumulative heat of hydration compared to the control mix with 100% OPC. Among the tested samples, mixes with fly ash exhibited the lowest cumulative heat, followed by those with a combination of fly ash and slag, and then slag mixes. The addition of NCSH seed accelerator induces an increase in cumulative heat, which correlates with the observed early strength improvements in these mixes.

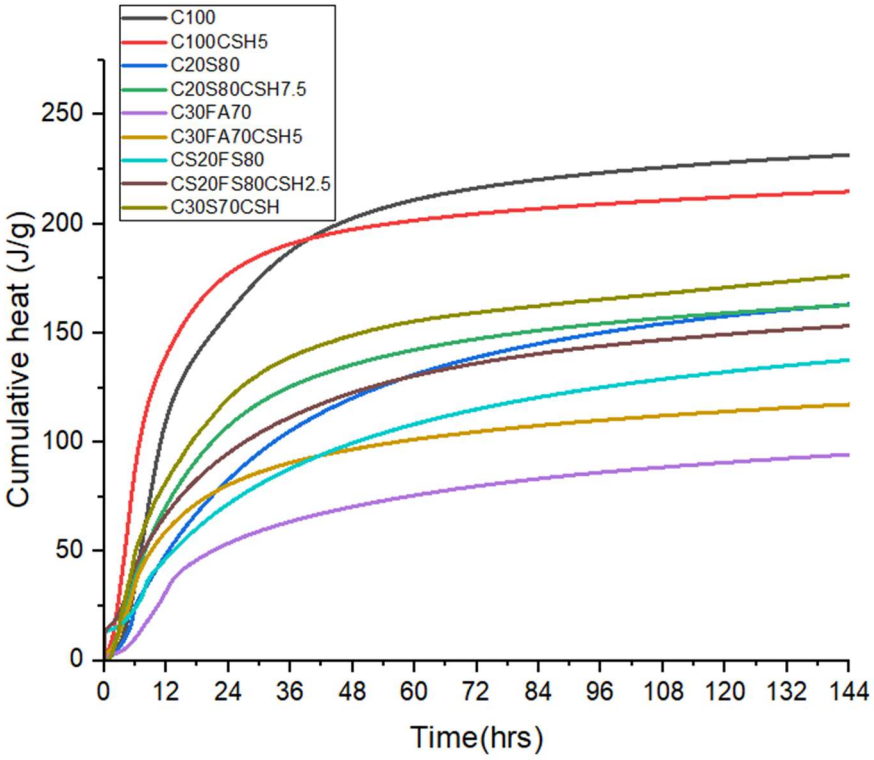

Figure 4.11: Cumulative heat of selected samples

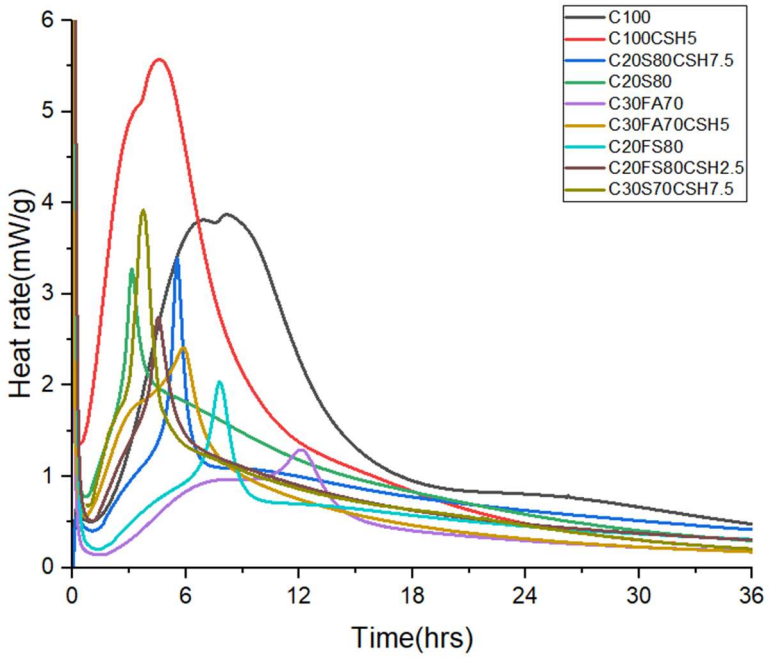

Figure 4.12: Normalized heat flow of selected samples

The heat rate, as depicted in Figure 4.12, further demonstrates the influence of the NCSH seed accelerator on hydration kinetics. The increased heat rate across all mixes after the addition of the NCSH seed accelerator confirms its potential to accelerate the hydration process. This acceleration is particularly beneficial in achieving the required early strength in applications such as pile concreting and mass concreting, where thermal control is critical. The enhanced hydration rate, without a corresponding drastic increase in cumulative heat, suggests that the NCSH seed accelerator can be effectively used to control the thermal profile while ensuring sufficient early strength development. The increase in cumulative heat due to the addition of NCSH seeds is a known consequence of accelerated hydration, which can indeed lead to higher temperatures during curing. Elevated temperatures in the early stages of hydration can increase the risk of thermal shrinkage, potentially leading to cracking, especially in large concrete pours or restrained environments.

The incorporation of NCSH seeds in the mix significantly enhances the heat of hydration, leading to a rapid development of strength and a narrowed dormant period Specifically, the blend with 100% Ordinary Portland Cement (OPC) and 5% NCSH seeds demonstrates a notable increase in heat generation, resulting in faster setting

times and improved early strength. Similar observation was noted by Zhang et al., 2015 & Niu et al., 2017 with lower dosages of NCSH.

This increased workability observed in these mixes compared to the control can be attributed to several factors. The addition of NCSH seeds enhances the packing density of the cement paste, reducing the amount of water required for a given workability level (Khan et al., 2019). The finer particles of NCSH contribute to a greater surface area, promoting better dispersion and hydration of the cement particles, which can lead to a more fluid mixture (Gao et al., 2020).

Furthermore, the increased interfacial area provided by NCSH allows for better bonding between particles, which can also contribute to enhanced workability (Mojir et al., 2020). Thus, the combination of rapid hydration and improved particle interaction results in higher workability while achieving the benefits of accelerated strength development.

While the addition of NCSH seed accelerator increased the cumulative heat of the mixes, hairline cracks were observed in concrete cylinder samples during early stages, the rapid hydration can lead to a higher rate of water consumption, exacerbating evaporation and causing plastic shrinkage cracks.

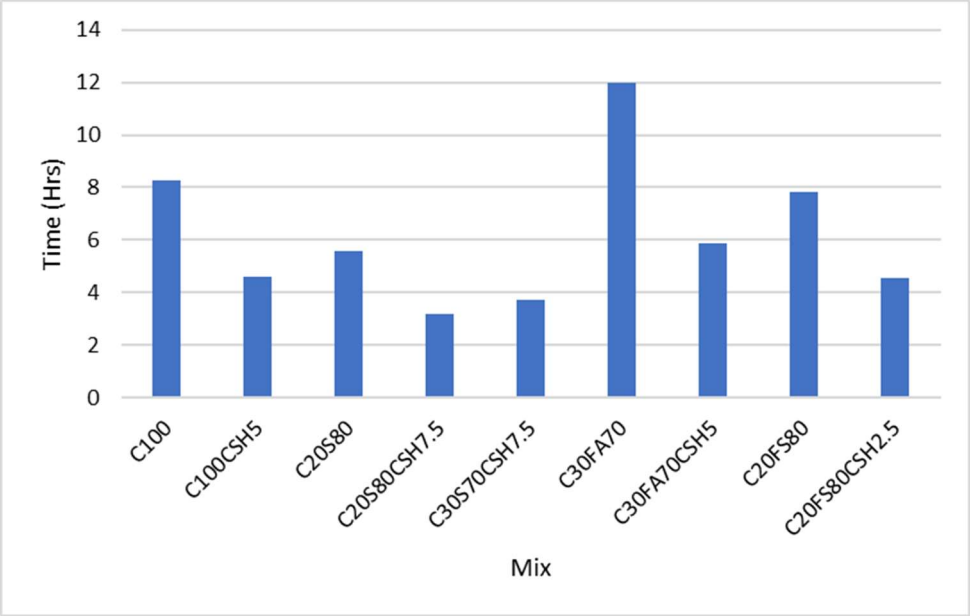

Figure 4.13: Time to achieve primary hydration peak.

Figure 4.13 shows the time to achieve the primary hydration peak for various mixes. The addition of NCSH seeds accelerates the hydration peak by 3.7 hours in the OPC mix, 2.4 hours in the slag 80% replaced mix, 6.1 hours in the fly ash 70% mix, and 3.3 hours in the 80% fly ash and slag mix. This acceleration indicates a faster reaction rate, which is consistent with the increased early strength observed in these mixes. The ability to expedite the hydration process without significantly increasing the cumulative heat is advantageous for maintaining structural integrity and preventing thermal cracking in large concrete pours.

Overall, the behavior of the heat curves in Figures 4.11 and 4.12 confirm the beneficial role of NCSH seed accelerator in enhancing the early strength and hydration kinetics of SCM containing mixes. Accelerated hydration, as shown by the reduced time to peak in Figure 4.13, emphasizes the potential of using NCSH seed accelerator in various concrete applications to achieve optimal strength and durability with controlled thermal development. These findings align with previous research, such as that by Rashad (2014) & Szostak et al., (2020), which highlighted the efficacy of seed accelerators in improving the performance of high-volume SCM mixes.

4.5. Scanning electron microscopy (SEM) and energy dispersive X-ray spectroscopy (EDS) analysis

Figure 4.14 shows the SEM images of microstructure of the 100% OPC mix in 7 day and 28 days. 28-day image shows more denser microstructure than 7-day image confirming the increased compressive strength in 28 days. When comparing the microstructure of control mixes of OPC100% with and without the NCSH seed accelerator, the addition of 5% NCSH seed accelerator results in a noticeably denser microstructure.

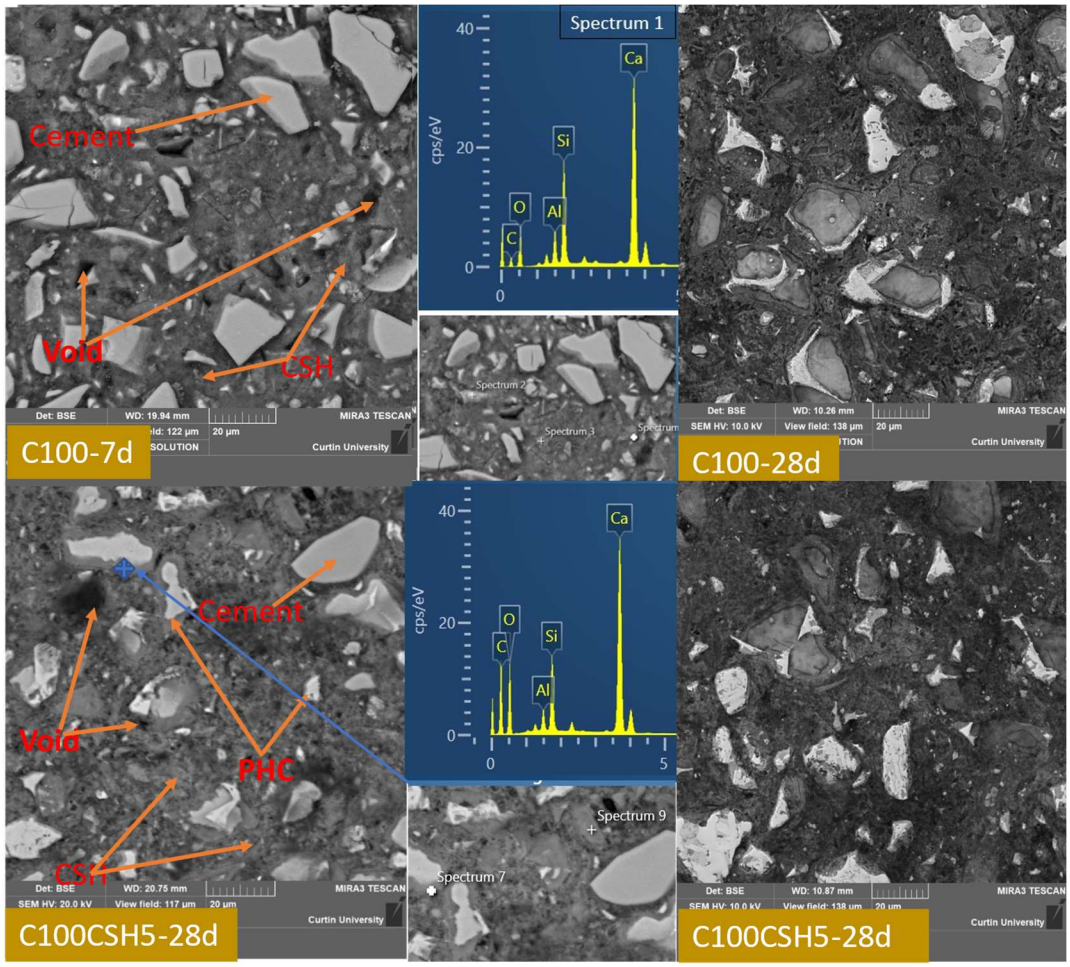

Figure 4.14: SEM image of C100 mix with and without NCSH in 7d and 28d.

The above observation is evident in the EDS map images shown in Figure 4.15 considering Ca, Si & Al in the matrix, which illustrate the microstructure at both 7 days and 28 days. The mix with the NCSH seed accelerator shows a significantly higher density at 7 days, corresponding to a 40% increase in compressive strength compared to the control mix without the accelerator. At 28 days, the SEM/EDS images of the mix with the accelerator reveal an even more densely reacted microstructure, which aligns with a 28% increase in compressive strength over the control mix.

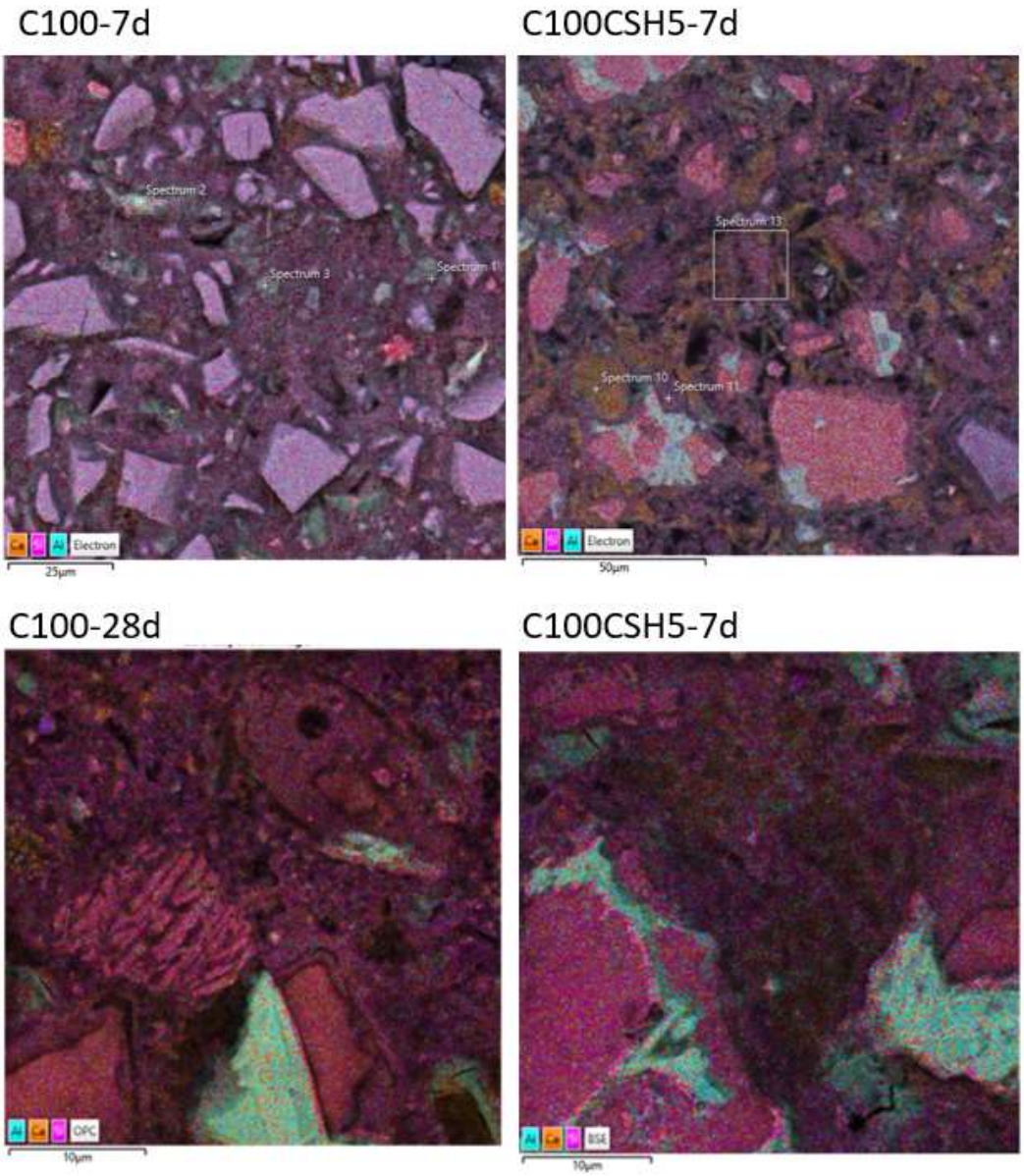

Figure 4.15: EDS map images of C100 mix with and without NCSH in 7d and 28d.

The SEM images presented in Figure 4.16 reveal significant microstructural changes between the 7-day and 28-day samples for the 80% slag mix with and without NCSH seed accelerator. At 7 days, the microstructure shows a higher volume of voids and fewer hydrated particles, indicating the early stages of the hydration process. In contrast, the 28-day samples exhibit a much denser microstructure with significantly fewer voids, confirming substantial strength development over time. This densification is particularly pronounced in the mix with 7.5% NCSH seed accelerator, where the concentration of hydrated particles is markedly higher.

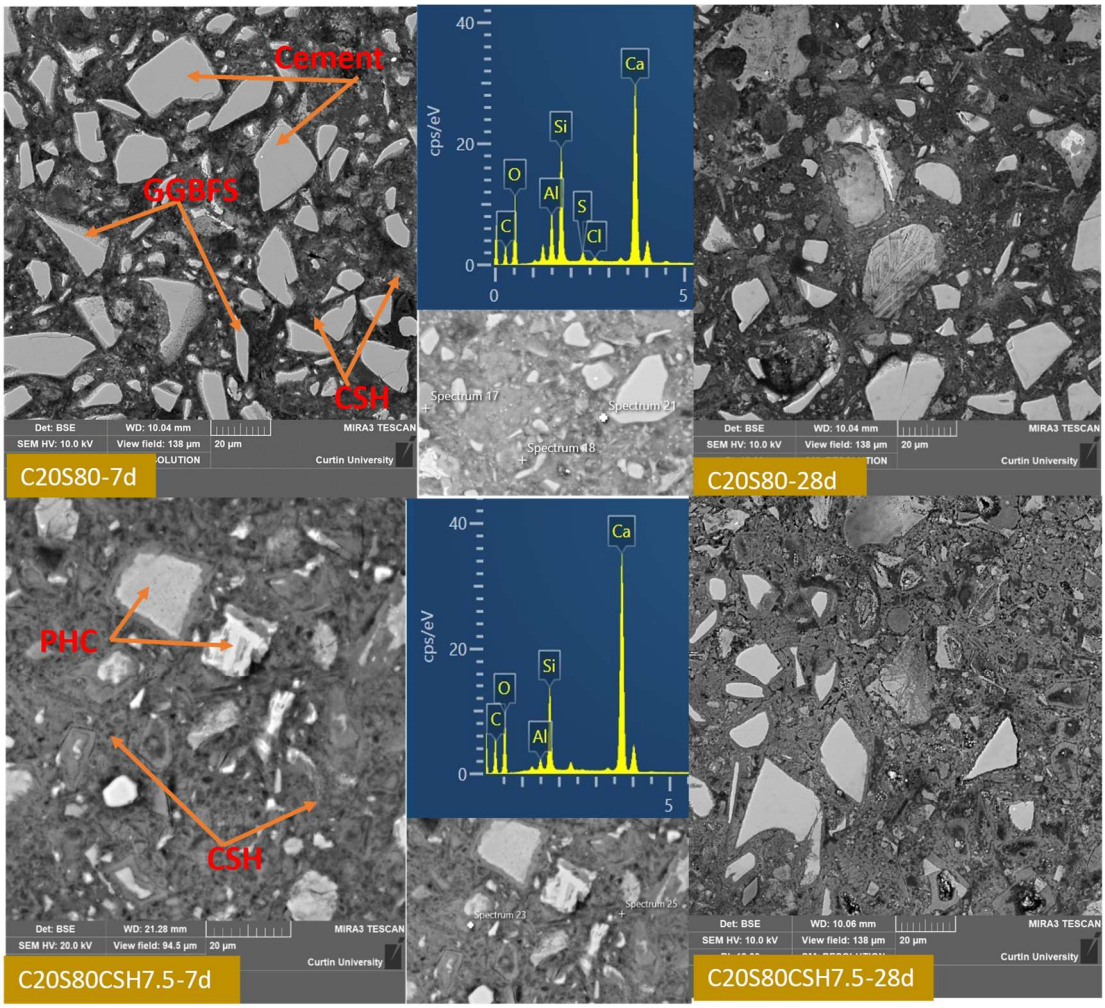

Figure 4.16: SEM image of C20S80 mix with and without NCSH in 7d and 28d.

The comparison between the 7-day and 28-day SEM images highlights the role of NCSH seed accelerator in enhancing hydration. The 7-day image of the 80% slag mix without the accelerator shows prominent slag particles and voids, with the early formation of CSH products. The EDS spectrum and EDS map images support this observation, showing peaks corresponding to calcium (Ca), silicon (Si), and aluminum (Al), indicative of initial hydration. However, at 28 days, the microstructure of the same mix becomes denser, with more uniformly distributed hydration products filling the voids, as evidenced by the reduced number of black spots representing voids.

In the case of the 80% slag mix with 7.5% NCSH seed accelerator, the 7-day SEM image already shows a higher degree of hydration compared to the mix without the accelerator. The presence of partially hydrated cement (PHC) and CSH gel particles is more evident, indicating that the seed accelerator has effectively promoted early

hydration. By 28 days, the microstructure becomes even denser, with a significant reduction in void volume and a higher concentration of CSH gel products.

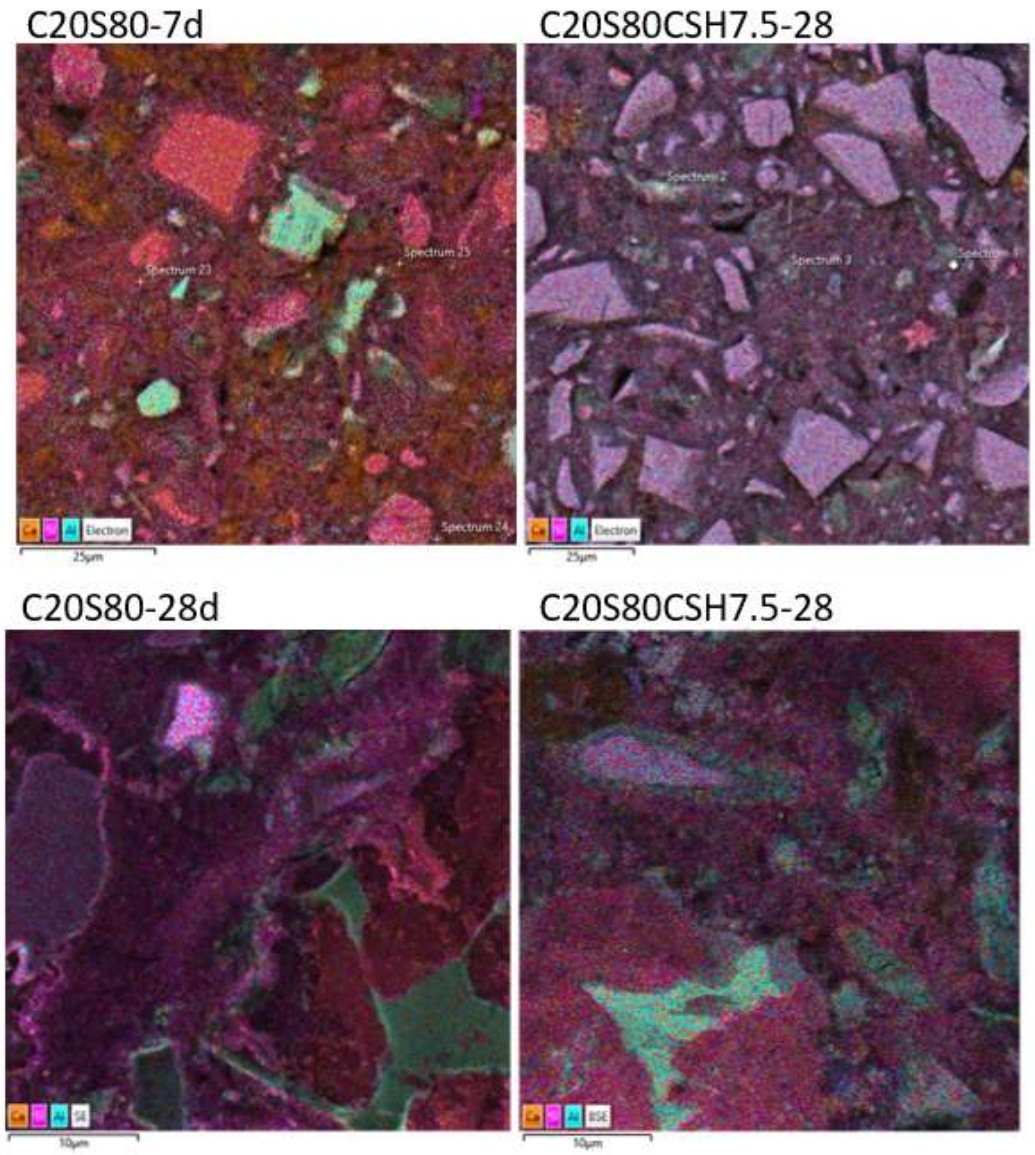

Figure 4.17: EDS map images of C100 mix with and without NCSH in 7d and 28d.

Figure 4.18 presents SEM images of a mix with 70% fly ash replacement, with and without the addition of NCSH seed accelerator, at 7 and 28 days. The 7-day SEM image of the mix without NCSH seed accelerator reveals a significant number of voids and numerous anhydrous fly ash particles, indicating limited early hydration. By 28 days, the SEM image shows that many of these voids have been filled, although numerous unreacted fly ash particles are still visible. This indicates that while hydration progresses over time, the presence of a substantial amount of unreacted fly ash particles suggests a slower reaction rate typical of fly ash mixes.

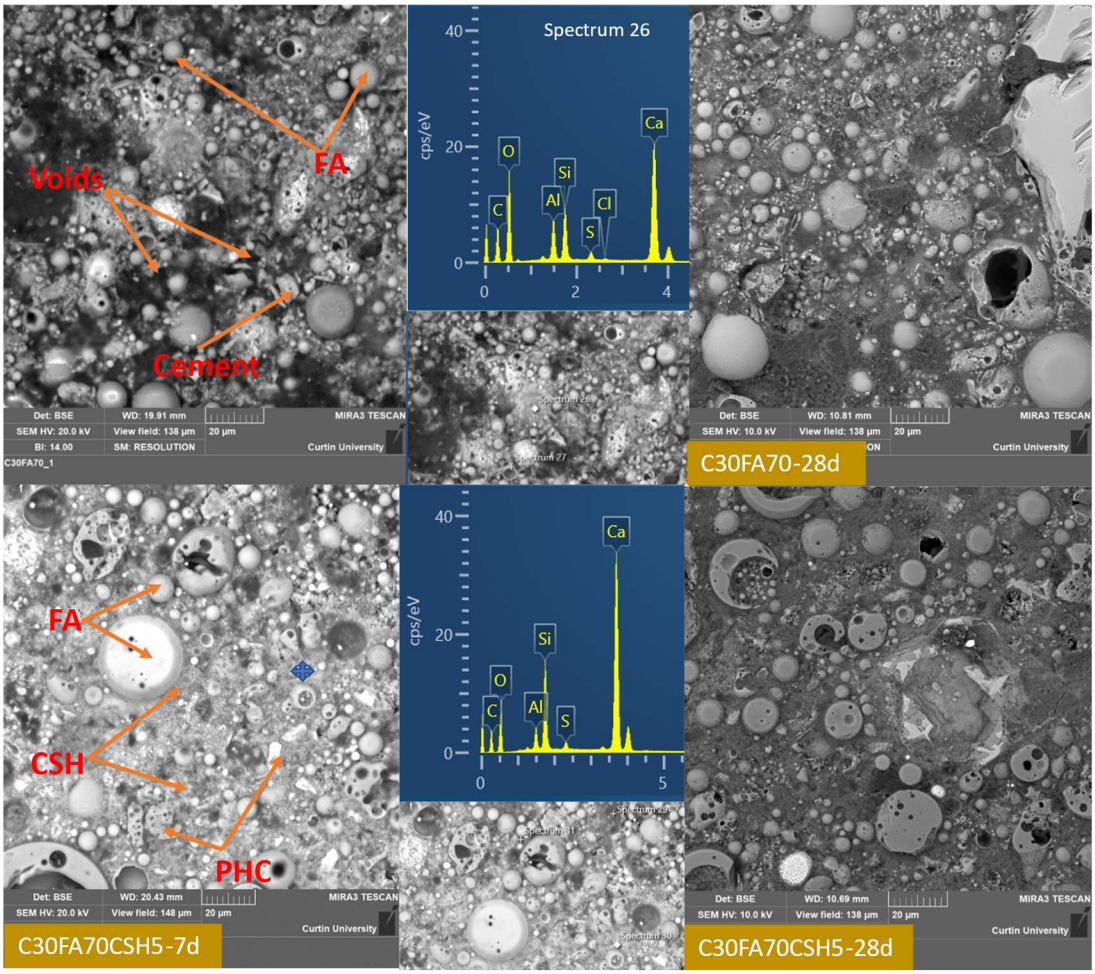

Figure 4.18: SEM image of C30FA70 mix with and without NCSH in 7d and 28d.

In contrast, the mix with the NCSH seed accelerator shows a noticeable increase in the number of hydrated particles at 7 days, though not as prominent as seen in slag-based samples with NCSH. The 28-day SEM image of the mix with NCSH seed accelerator reveals a more densified microstructure compared to the mix without the accelerator. This densification is evidenced by fewer voids and a more uniform distribution of hydration products. This densification is evident with the EDS map images shown in Figure 4.19.

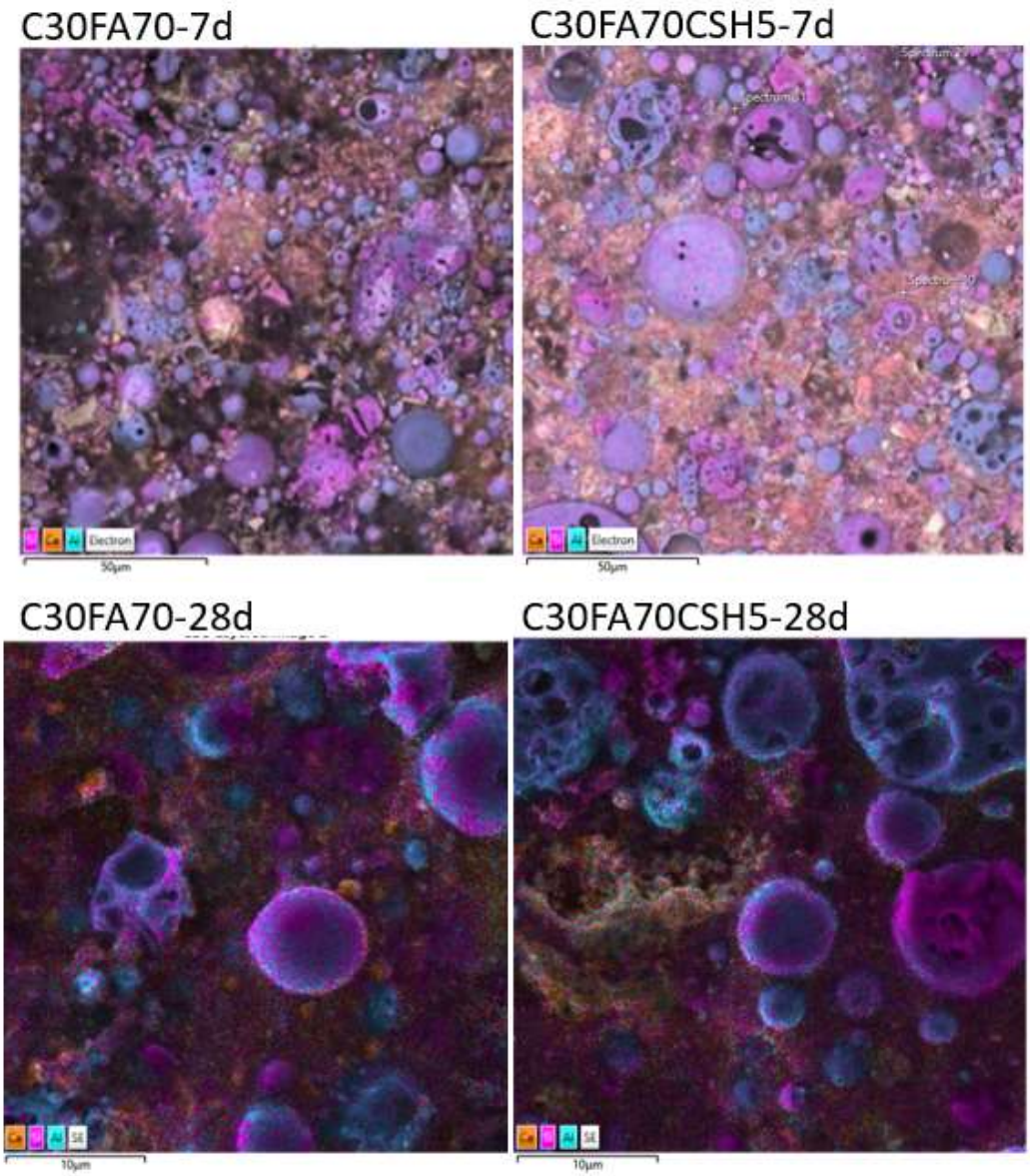

Figure 4.19: EDS map image of C30FA70 mix with and without NCSH in 7d and 28d.

The SEM images in Figure 4.20 illustrate the microstructural evolution of the C20FS80 mix over 7 and 28 days. At 7 days, the microstructure is characterized by numerous voids and a high number of unreacted slag and fly ash particles, indicating limited early hydration. By 28 days, the microstructure shows significant densification, with fewer voids and a reduced number of unreacted particles, demonstrating the progression of hydration over time. The addition of NCSH seed accelerators further enhances this process. At 7 days, the mix with NCSH seeds already exhibits fewer unreacted particles compared to the mix without the accelerator, indicating more advanced early hydration.

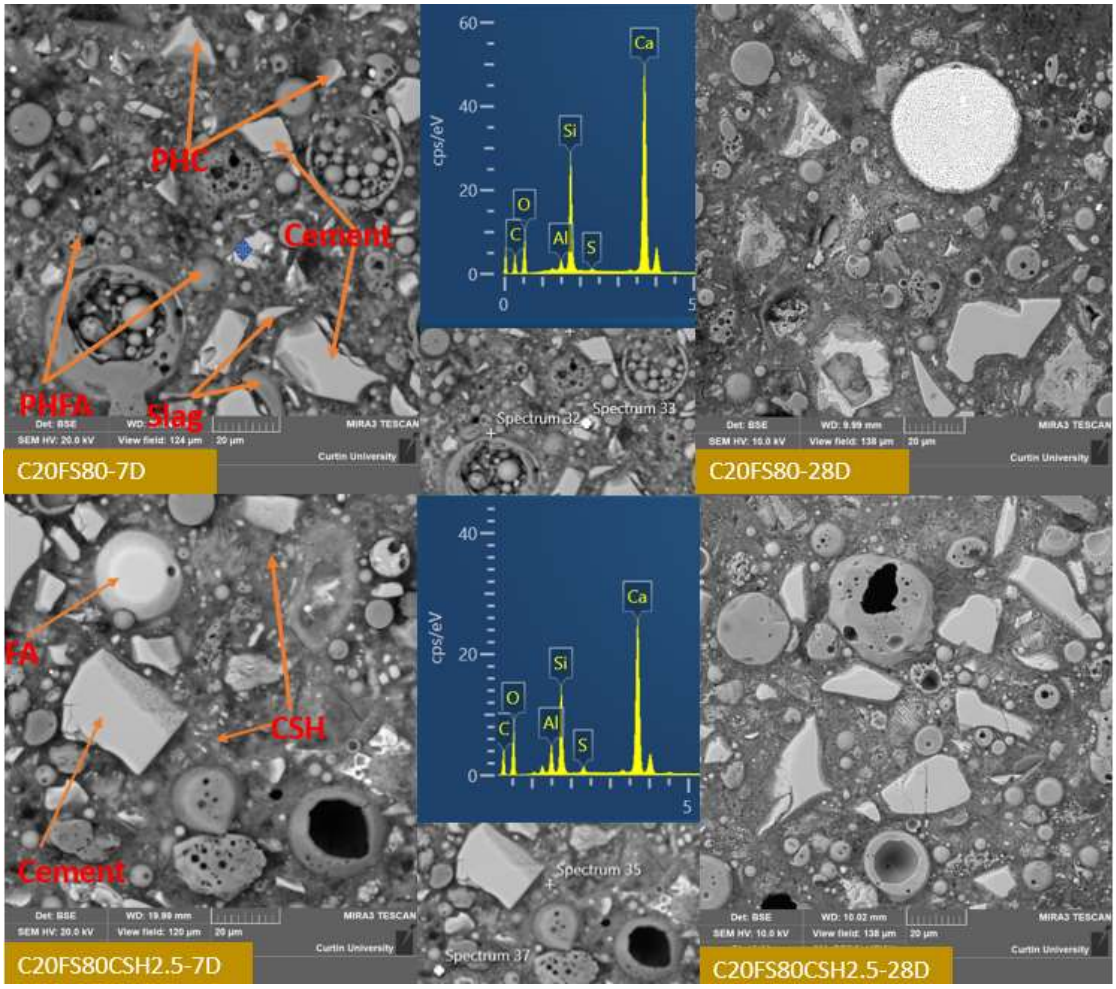

Figure 4.20: SEM image of C20FS80 mix with and without NCSH in 7d and 28d

In the 28-day images, the mix with NCSH seed accelerator displays a denser microstructure with fewer voids and a more uniform distribution of hydration products. This densification is more pronounced compared to the mix without the accelerator, emphasizing the effectiveness of the NCSH seed in promoting hydration and reducing the presence of unreacted FA and slag particles. The EDS spectra verify these observations, showing higher peaks for calcium (Ca) and silicon (Si), which signify the formation of additional CSH and CASH products, contributing to the densified microstructure and improved compressive strength. This densification can be clearly identified by the EDS map data shown in Figure 4.21. The color intensity correlates with the densification of the system with producing more hydration products.

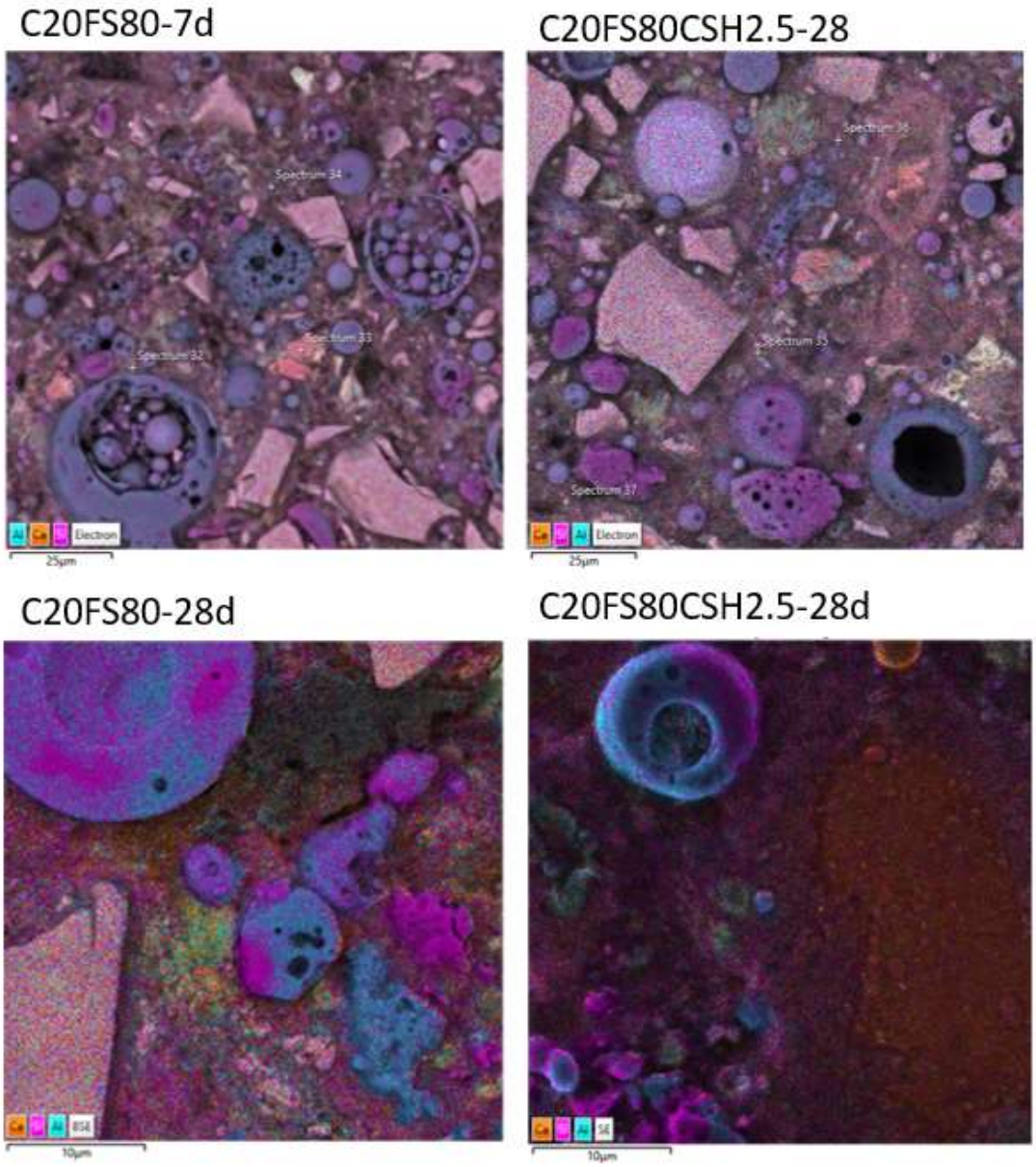

Figure 4.21:EDS map image of C20FS80 mix with and without NCSH in 7d and 28d

The presence of the NCSH seed accelerator promotes the formation of more hydration products, such as Calcium-Silicate-Hydrate (CSH) and Calcium-Aluminate-Silicate-Hydrate (CASH), within the cementitious system. This increased formation of hydration products contributes to the enhanced microstructural density and strength observed in the SEM images. The EDS analysis further supports these findings, showing distinct peaks around the hydration products, which confirm the presence of CSH and CASH phases. The increased peaks of calcium (Ca), silicon (Si), and aluminum (Al) in the EDS spectra indicate a higher degree of hydration and formation of these phases. Also, this is further evident with the EDS map data with the increase of the intensity of the layers.

In conclusion, the SEM, EDS analyses and EDS mapping provide clear evidence of the beneficial effects of adding NCSH seed accelerator to cementitious mixes. The accelerator significantly enhances the formation of hydration products, leading to a denser microstructure and substantial increases in both early and late compressive strengths. These findings suggest that incorporating NCSH seed accelerator can effectively improve the performance of cement-based materials, making them more suitable for various structural applications where early strength development and long-term durability are critical.

4.6. X-Ray Diffraction

Figure 4.19 shows the X-ray diffraction curves of the 100% OPC mixes with and without NCSH seed accelerator in 7d and 28d respectively. CaF_2 was used as the internal standard and does not reflect any properties related to cement hydration. CSH peaks are observed at 2θ angles of 29.4° and 32.8°. The CH peaks are observed at approximately 2θ angles of 18.06° and 34.1°. The highest CH peak appears in the C100-28d mix, indicating a substantial presence of unreacted CH, consistent with the advanced hydration stage in the pure OPC mix. Conversely, the 7-day sample of the same mix shows a less intense CH peak, reflecting the earlier hydration stage.

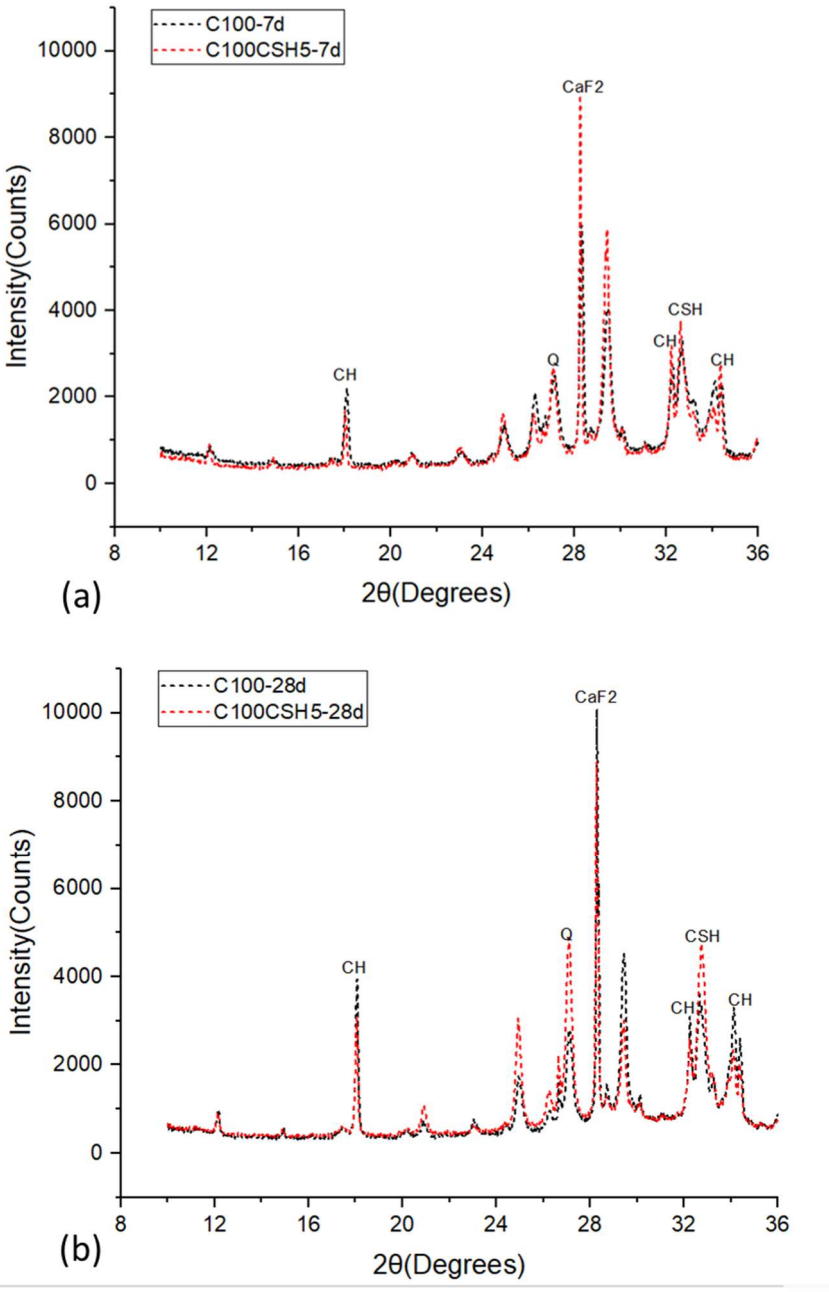

Figure 4.22: XRD curves of C100 mix with and without NCSH in 7d and 28d.

C100 mix with 5% NCSH seeds show an intense CSH peak at 2θ angles of 29.4° in 7 days and in 28 days, an intense CSH peak can be seen at 2θ angle of 32.8° as shown in Figure 4.23 (a) and (b). Confirming that the NCSH seed accelerator has increased the early age strength and late strength by forming more CSH gel in the matrix. This early strength development is evident with the higher initial heat release shown in the isothermal calorimetry results which was discussed previously.

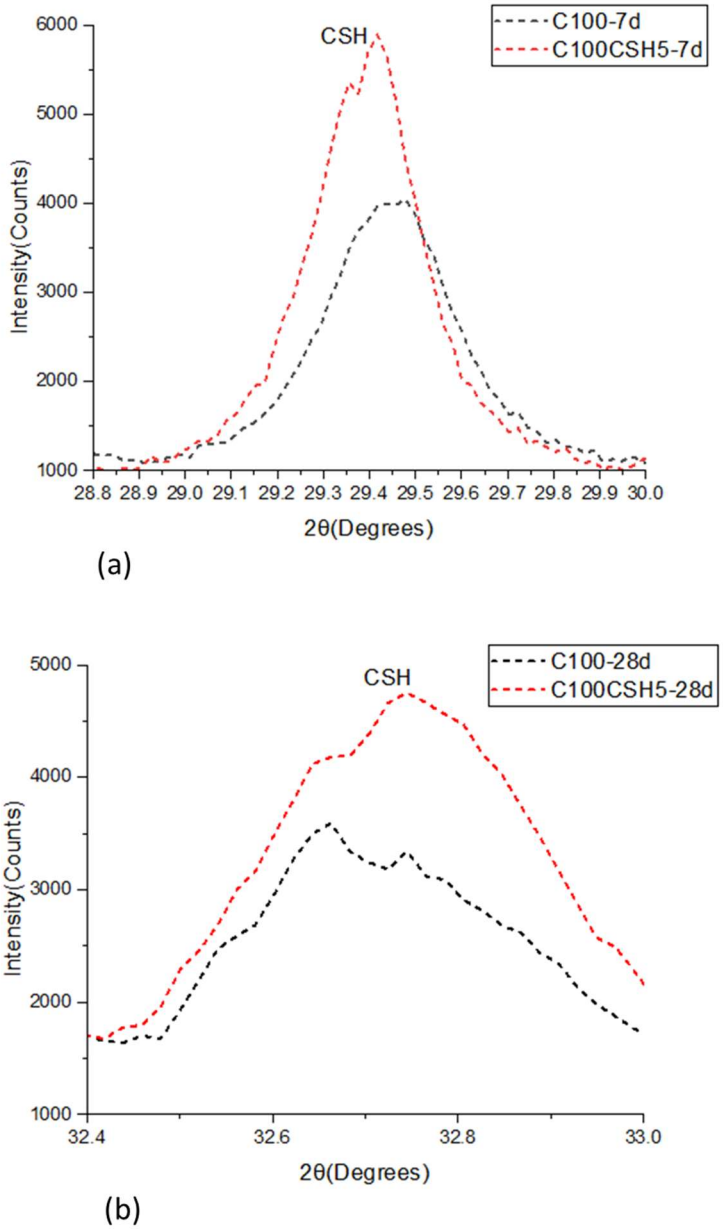

Figure 4.23: CSH peaks of C100 mix with and without NCSH in 7d & 28d.

CSH gel is the primary product of cement hydration and significantly contributes to strength due to its dense, amorphous structure (Taylor, 1997). CH, a by-product of hydration, can enhance early strength but may lead to higher porosity if present in excess (Neville, 2011). Quartz, being inert, serves as a filler that helps reduce porosity in composite materials (Zhang et al., 2016).

As curing age increases, the ratio of CSH to CH typically rises, resulting in lower porosity and enhanced mechanical properties (Bentz & Cohen, 1998). A higher formation of CSH gels at later stages fills voids and enhances the interlocking of particles, improving overall strength. In contrast, excessive CH can create larger pore spaces, weakening the matrix (Feldman & Tazawa, 1997).

Mechanical stretch observations correlate with these chemical transformations; as CSH develops, the material exhibits increased resistance to deformation, indicating enhanced strength and reduced permeability (Bentz, 2000). Thus, controlling the formation of these compounds is crucial for optimizing concrete performance.

4.6.1. X-Ray Diffraction of high-volume slag replaced mixes.

Figure 4.24 illustrates the XRD curves of HVS mixes with and without CSH seeds. The CH peaks are observed at approximately 2θ angles of 18.06° and 34.1°. and CSH peaks at 2θ angles of 29.4° and 32.8°. Lower CH levels in the mix correspond to the most of CH has been transformed in to CSH gel in the matrix.

.

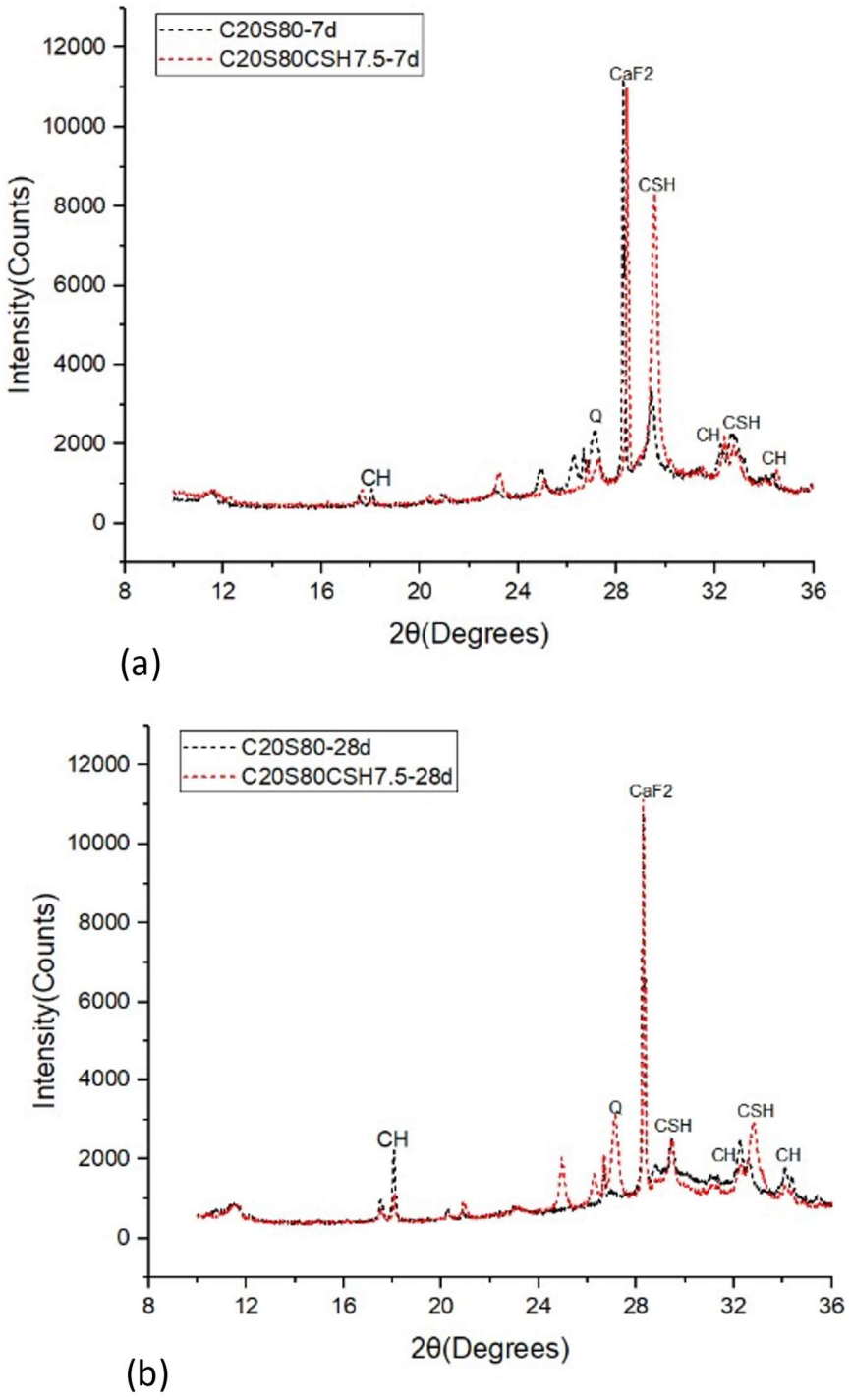

Figure 4.24: XRD curves of high-volume slag mixes with and without NCSH seeds

In the C20S80 mix, the CSH peaks, which are crucial indicators of hydration products, appear at 2θ angles around 29.4° and 32.8°. These peaks are more prominent in the mixes containing NCSH seed accelerators, signifying an increase in the formation of CSH gel. As shown in Figure 4.25, increased formation is also evident in the C20S80CSH7.5-28d mix, where the CSH peaks are more intense than in the C20S80-28d mix without the accelerator.

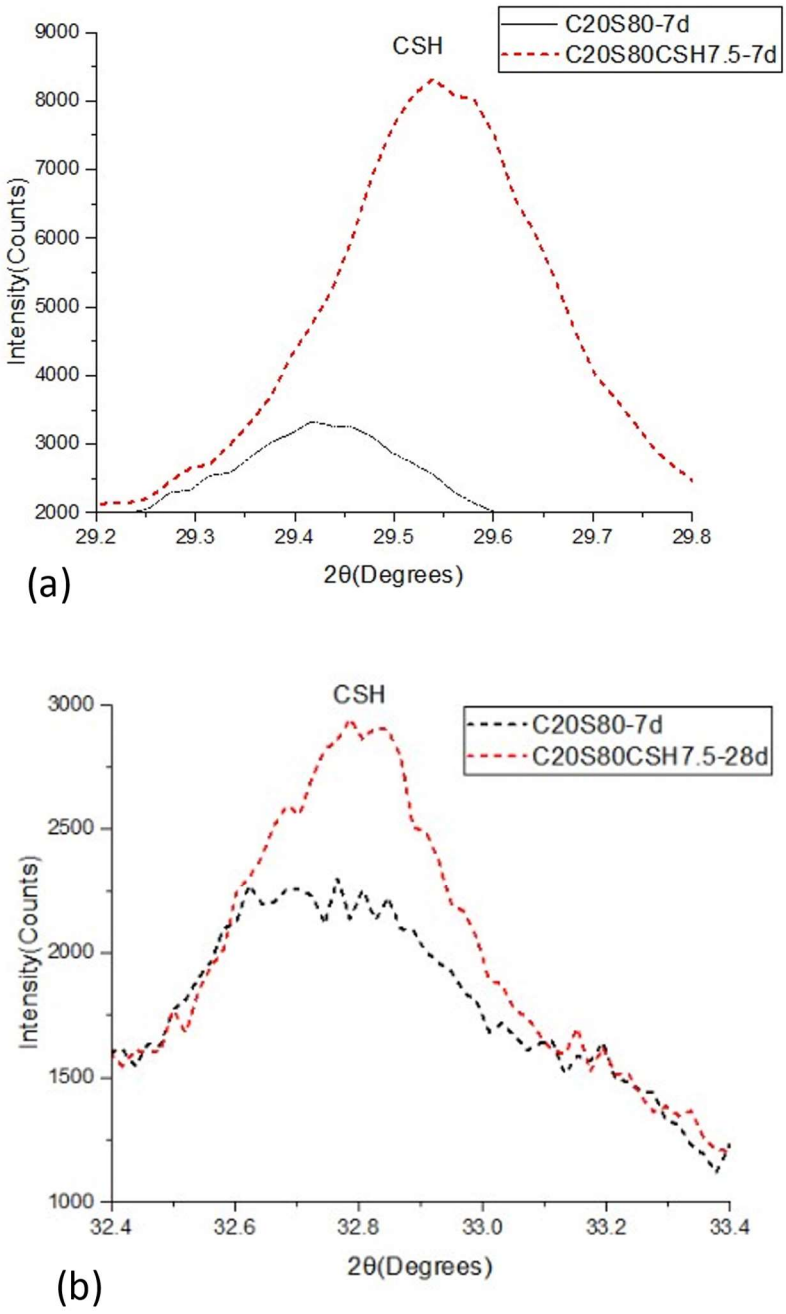

Figure 4.25: CSH peaks of C20S80 mix with and without NCSH in 7d and 28d.

4.6.2. X-Ray Diffraction of Fly ash replaced mixes.

The XRD curves of high-volume fly ash mixes with and without NCSH seeds are shown in figure 4.26. The CH peaks can be seen at 2θ angles of approximately 18.06° and 34.1°. Mixes without NCSH seed accelerator in both at 7 and 28 days, show reduced CH peak intensities compared to their counterparts without NCSH seeds, confirming that the seeds promote further hydration and conversion of CH into CSH gel by accelerating the pozzolanic reaction.

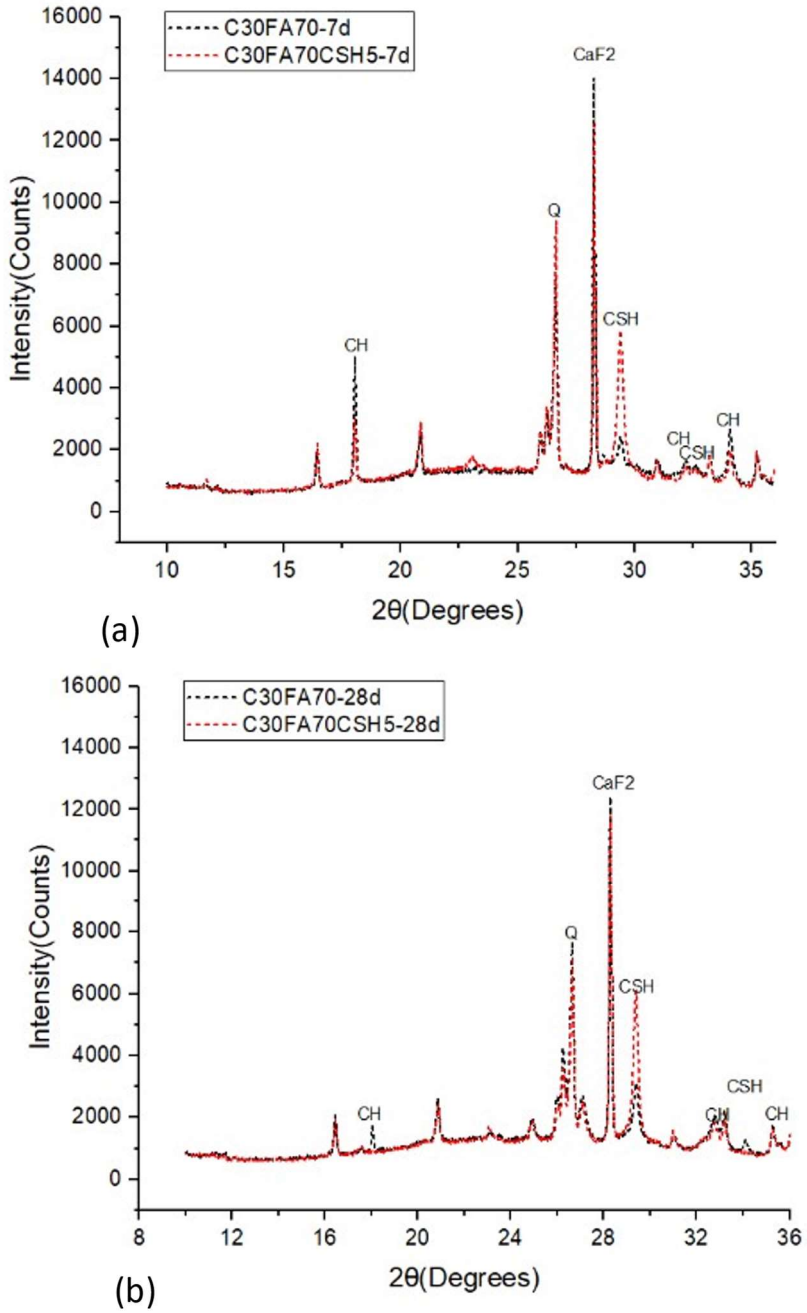

Figure 4.26: XRD curves of high-volume fly ash mixes with and without NCSH seeds

As shown in figure 4.27, the CSH peaks at 2θ angle of 29.4° are more evident in mixes containing NCSH seed accelerators in both 7 day and 28 days, demonstrating the effectiveness of NCSH seeds in promoting hydration product formation. The SiO_2 peaks around 26.6°, prominent in fly ash mixes due to the high silica content of fly ash, are present in both mixes with and without NCSH seeds.

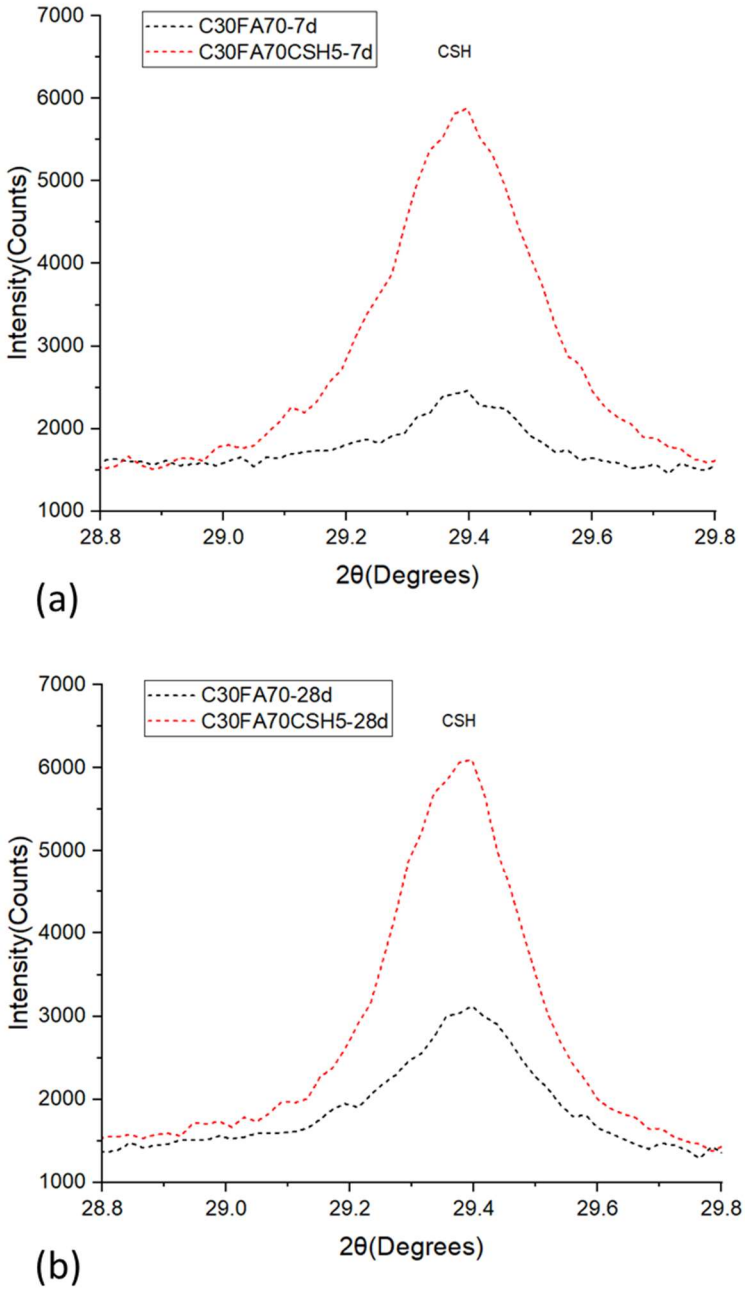

Figure 4.27: CSH peaks of C70FA70 mix with and without NCSH in 7d and 28d.

4.6.3. X-Ray Diffraction of Fly ash+ slag replaced mixes.

4.28 shows the XRD curves of high volume fly ash and slag combination mixes with and without NCSH seed accelerator. The CH peaks can be seen at 2θ angles of approximately 18.06° and 34.1° both mixes, the intensity of CH peaks at both 7 days and 28 days show less intensity compared to the mixes with NCSH seed accelerator confirming enhanced hydration and CH consumption due to pozzolanic reaction.

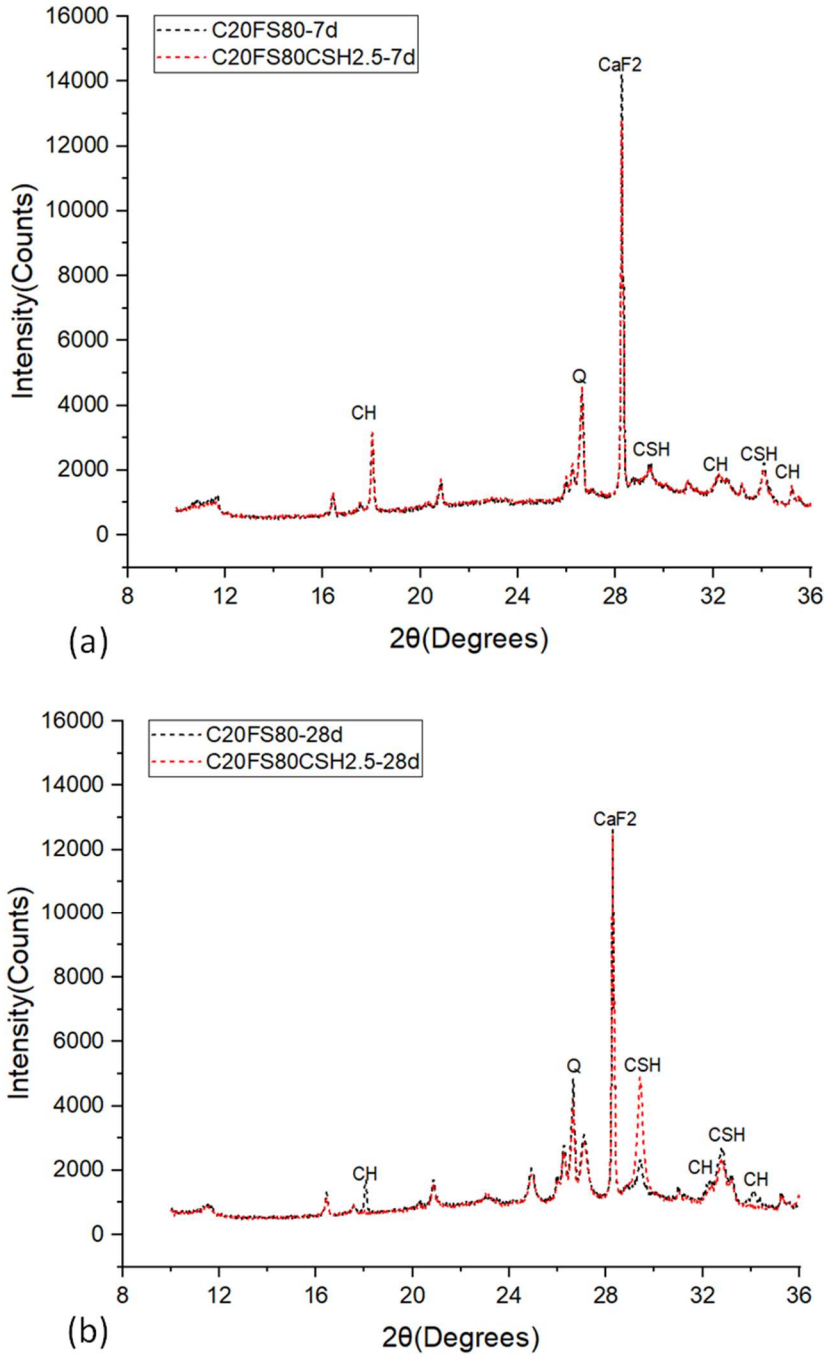

Figure 4.28: XRD curves of high-volume slag + fly ash mixes with and without NCSH seeds

As shown in Figure 4.29, the CSH peaks at 2θ angles of approximately 29.4° and 32.8° are more pronounced in mixes containing CSH seed accelerators, signifying increased formation of CSH gel. The C20FS80CSH2.5 mixes at both 7 and 28 days show increased CSH peak intensities compared to the C20FS80 mixes without CSH seeds, demonstrating the effectiveness of NCSH seeds in promoting the formation of hydration products.

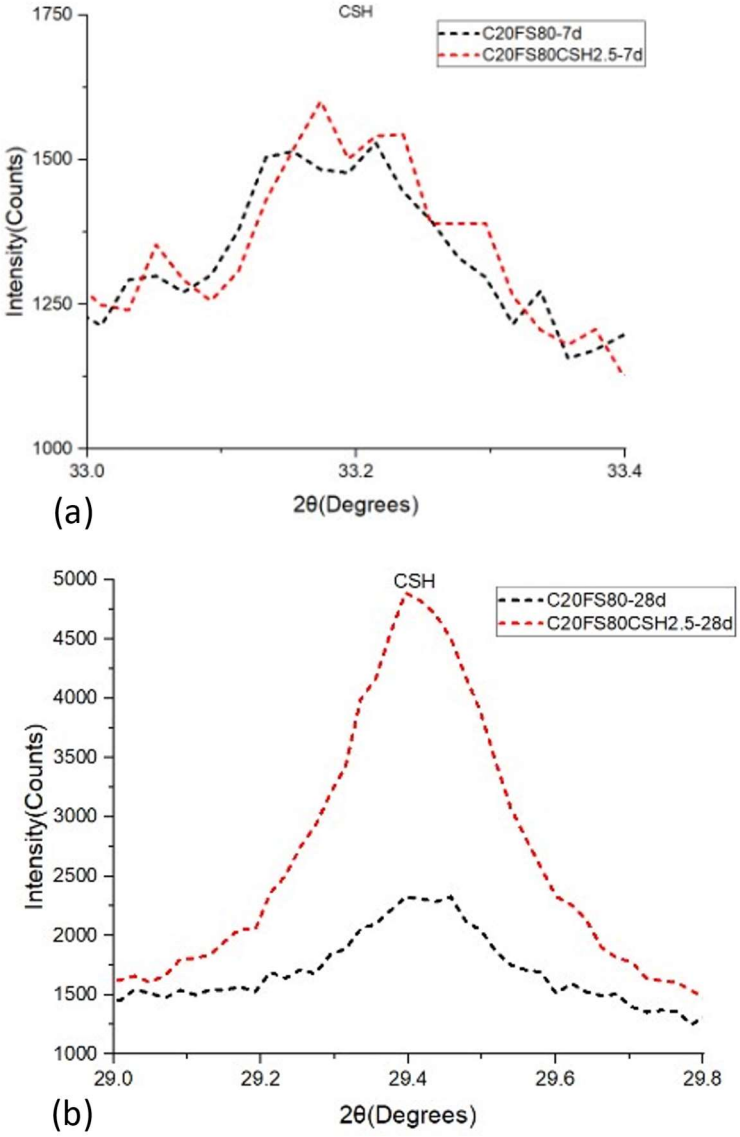

Figure 4.29: CSH peaks of C70FA70 mix with and without NCSH in 7d and 28d.

The addition of NCSH seed accelerators significantly reduces the intensity of CH peaks, indicating the consumption of CH to form additional CSH gel. This reaction is beneficial for the densification of the microstructure and the improvement of compressive strength. The increased intensity of NCSH peaks in mixes with seed accelerators emphasizes their role in enhancing hydration. The presence of these peaks

In both the 7-day and 28-day samples indicates that the NCSH seeds promote both early and continued hydration, leading to a more uniform and robust microstructure. Overall, the XRD analysis confirms that NCSH seed accelerators are effective in improving the hydration and mechanical properties of high-volume fly ash and slag cementitious systems by facilitating the conversion of CH into beneficial CSH gel.

4.7. Thermogravimetric Analysis (TGA) and Differential Scanning Calorimetry (DSC)

Thermogravimetric analysis (TGA) curves and differential scanning calorimetry-(DSC) of selected 8 mixes are shown in Figure 4.22. TGA measures the change of mass of a sample when it is heated in a controlled environment while DSC measures the heat flow in or out of a sample when it is heated in a controlled environment. In this test the samples were heated in a nitrogen gas environment to study the mass change between 20-1000^{o}C. It has been reported that mass loss between 105 ^{o}C and 420 ^{o}C, accounts to the dehydration of CSH, Ettringite (Aft), and CASH. Between 420 ^{o}C and 540^{o}C, mass loss corresponds to the dehydration of calcium hydroxide and decomposition of $CaCO_3$ occurs between 720 ^{o}C - 950 ^{o}C. Shaikh et al, (2014). The amount of CH can also be quantified according to Taylor's formula (Taylor, 1975) shown as follows in equation (2): The calculated Calcium Hydroxide content is shown in Figure 4.23.

$$\boldsymbol{CH}(\%) = \boldsymbol{WL_{CH}}(\%).\frac{\boldsymbol{MW_{CH}}}{\boldsymbol{MW_{H_2O}}} \qquad \textbf{Eq.2}$$

$\boldsymbol{WL_{CH}}$ is the weight loss during the dehydration of CH as percentage of the sample weight (%); $\boldsymbol{MW_{CH}}$ is the molecular weight of CH; $\boldsymbol{MW_{H2O}}$ is the molecular weight of H_2O.

As shown in Figure 4.30, the TGA curve for 100% OPC mix with and without NCSH seed accelerator, indicates a significant weight loss at around 450-550^{o}C, corresponding to the dehydration of CH, this reduction is less in the mix with NCSH seed accelerator showing that more CH has been consumed to produce more CSH gel with the addition of NCSH seed accelerator. The DSC curve confirm the deep dip at 483 ^{o}C in the curve showing the dehydration of CH is an endothermic reaction. The higher strength in the mix with NCSH is evident by these results.

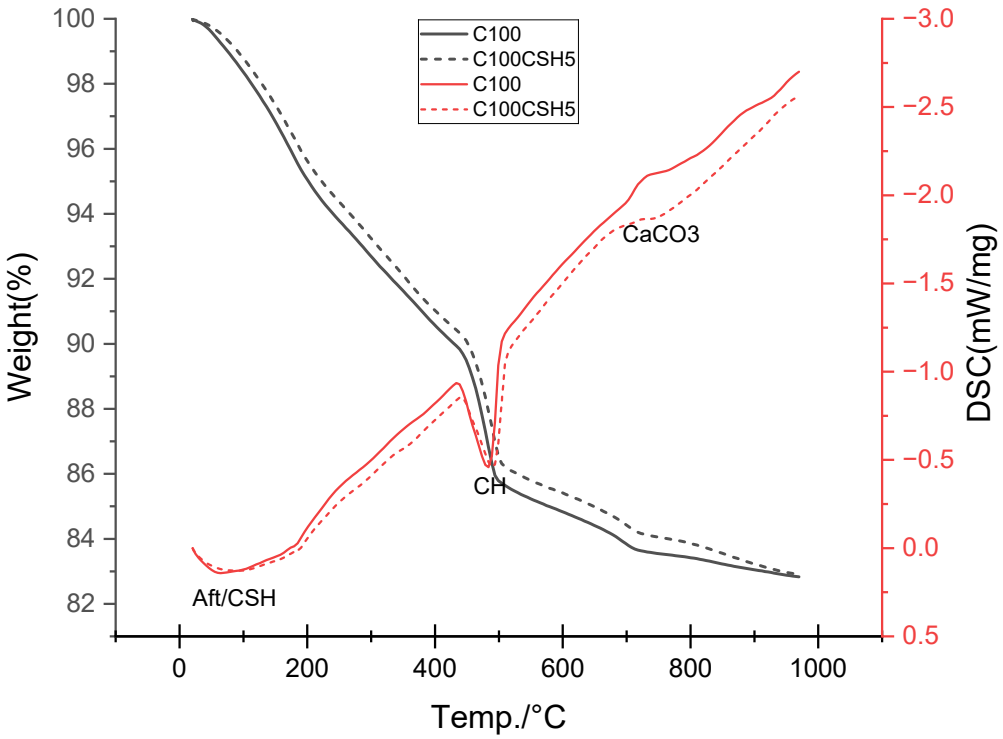

Figure 4.30: TGA and DSC curves of C100 mix with and without NCSH.

Figure 4.31 shows the TGA and DSC curves for the 80% slag replacement mix with and without NCSH. The mix with NCSH seeds shows a lower intense peak than its counterpart, in 467.6 ºC in the DSC curve showing the endothermic reaction of the dehydration of CH. This means more CH has been transformed in to CSH gel.

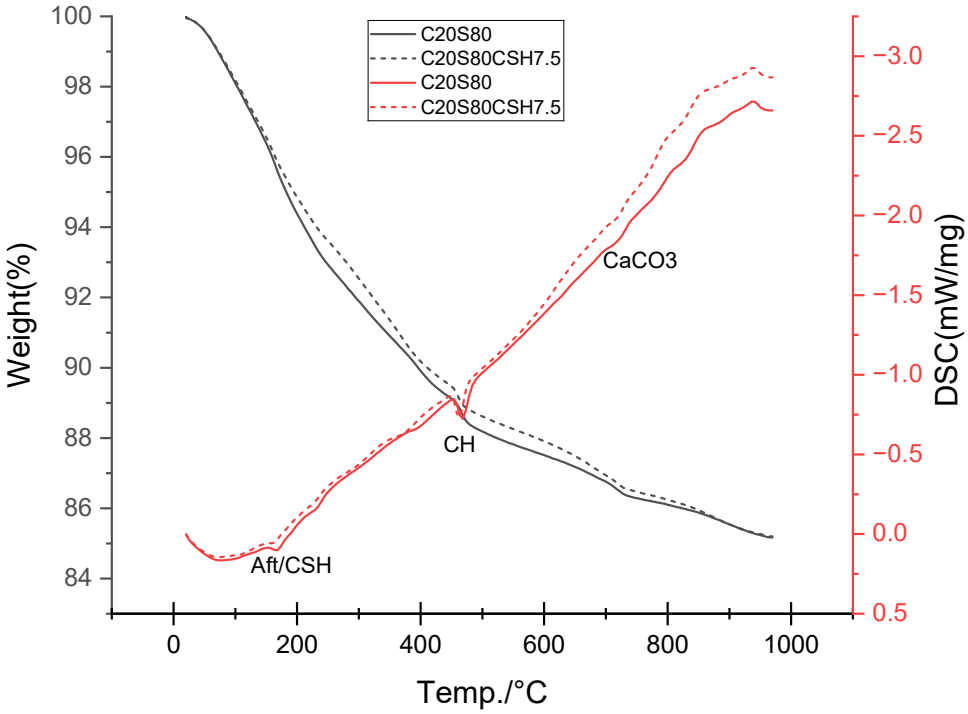

Figure 4.31: TGA and DSC curves of C20S80 mix with and without NCSH.

Figure 4.32 shows the TGA and DSC curves of 70% fly ash replacement mix with and without NCSH seed accelerator. It also shows the similar peaks for Aft/CSH dehydration, CH dehydration, and $CaCO_3$ decomposition at previously discussed temperature ranges. The intensity of the CH peak is less intense in the mix with NCSH seed accelerator in it showing that more CH has consumed to form CSH gel in the matrix and increasing the compressive strength of the mix.

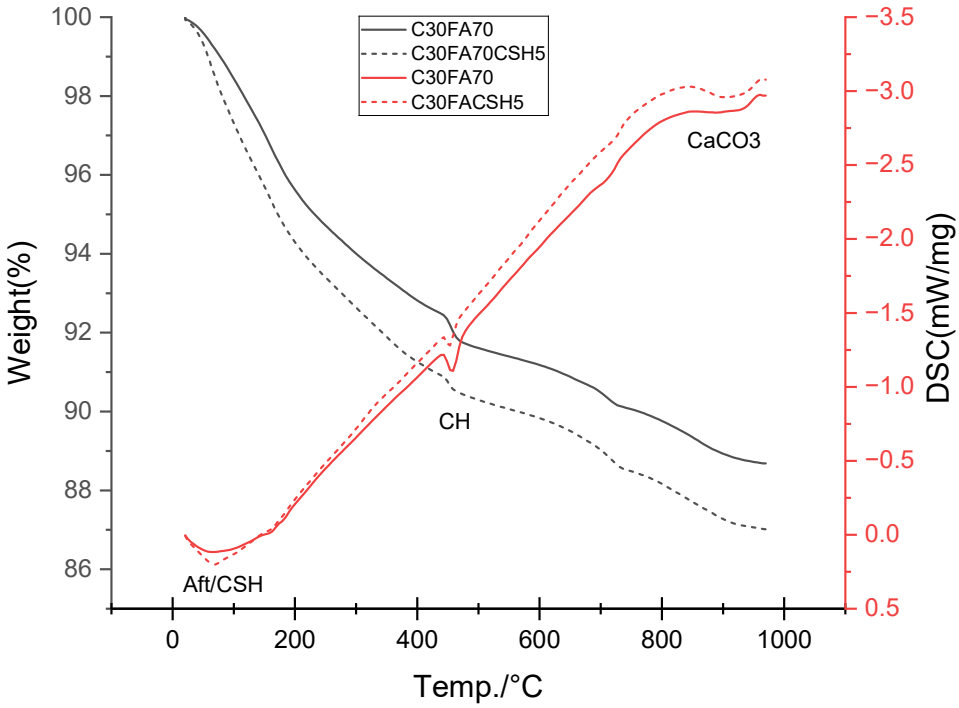

Figure 4.32: TGA and DSC curves of C30FA70 mix with and without NCSH.

Figure 4.33 shows the TGA and DSC curves of 80% fly ash and slag replaced mix with and without seed accelerator, the CH peak of this mix also shows a reduction in the mix with NCSH seeds. Confirming the acceleration of the consumption of CH with the addition of NCSH seed accelerator. Minor DSC peaks of CSH/Aft and $CaCO_3$ also can be seen. The mix with NCSH showed better compressive strength than the mix without NCSH and it can be correlated with the TGA results of the CH decomposition.

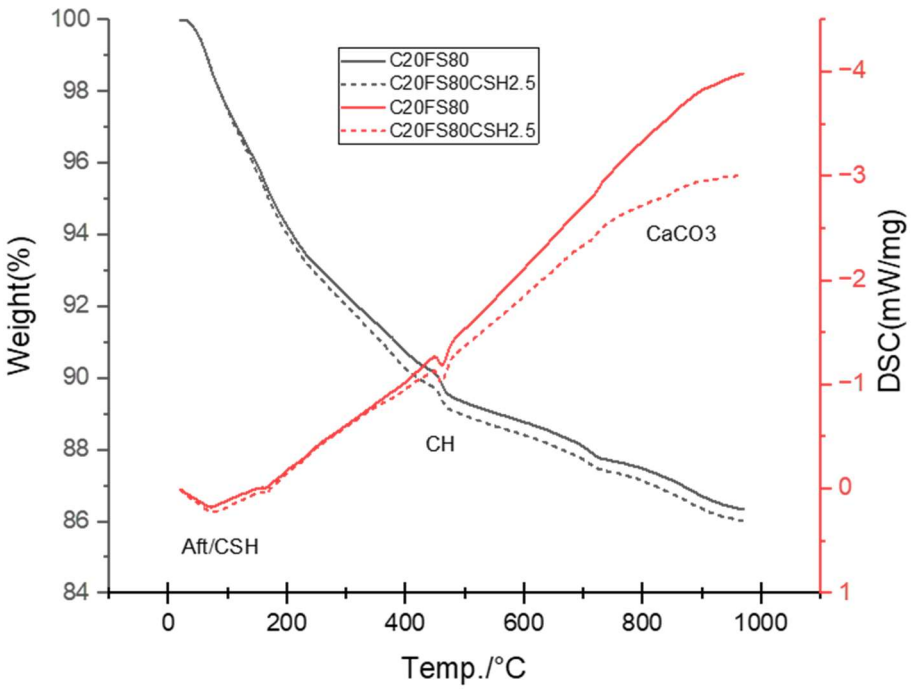

Figure 4.33. TGA and DSC curves of C20FS80 mix with and without NCSH.

The reduction in CH content with the addition of NCSH seed accelerator, as shown in Figure 4.34, is closely linked to both the strength and durability improvements observed in the mixes. The control mix with 100% OPC has the highest CH content (around 18%), indicating that much of the hydration is incomplete, with a significant amount of unreacted CH present. This excess CH is less beneficial for long-term concrete performance, as it can lead to issues like shrinkage and increased porosity.

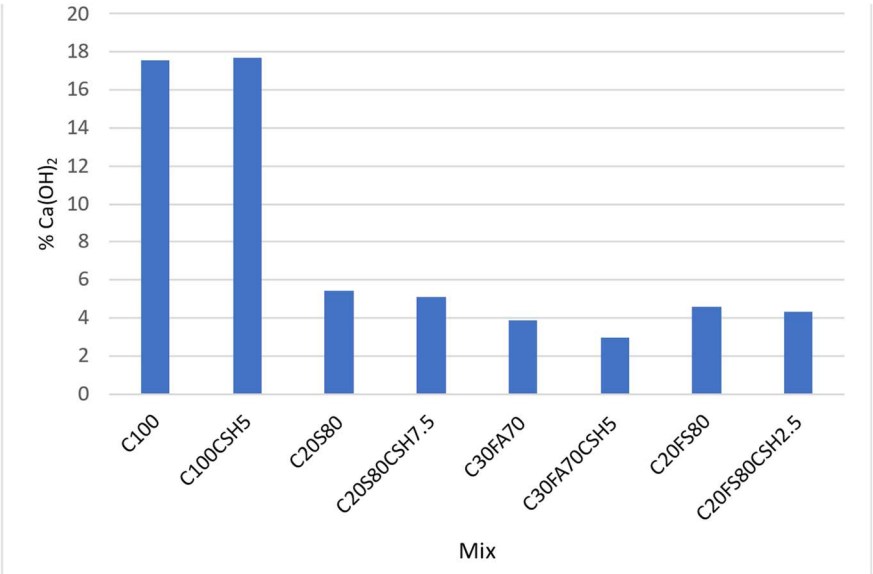

Figure 4.34: Calcium Hydroxide Content

With the addition of NCSH seeds, CH is consumed in the reaction to form CSH gel, which is the primary product responsible for strength development in concrete. This reduction in CH content reflects a more efficient hydration process, leading to stronger bonds between particles and improved overall strength. The CSH gel also enhances durability by reducing the amount of unreacted CH, which can be prone to deleterious reactions over time, such as sulphate attack.

In the high-volume slag and fly ash mixes, the addition of NCSH seeds shows a similar reduction in CH content, with the highest reduction (24%) occurring in the high-volume fly ash mix, followed by a 5.66% reduction in the slag and fly ash combination mix. This suggests that NCSH seeds help accelerate pozzolanic reactions, especially in the fly ash mix, which typically reacts more slowly. As a result, these mixes exhibit better strength and durability due to the increased formation of CSH gel and a reduction in excess CH, improving both long-term stability and performance.

4.8. Concrete Test results

4.8.1. Workability

The workability of concrete is crucial for its placement, compaction, and finishing without segregation. The slump test results, as shown in Figure 4.35, indicate that the control concrete mix with 100% OPC had a slump of approximately 150 mm, suggesting moderate workability. In contrast, the mix with 80% slag replaced with OPC, and incorporating a 7.5% NCSH seed accelerator, exhibited a significantly higher slump of about 220 mm. This increase can be attributed to the enhanced particle packing and lubrication effect from the slag and the NCSH seeds provide a lubricating effect, further improving the mix's flowability.

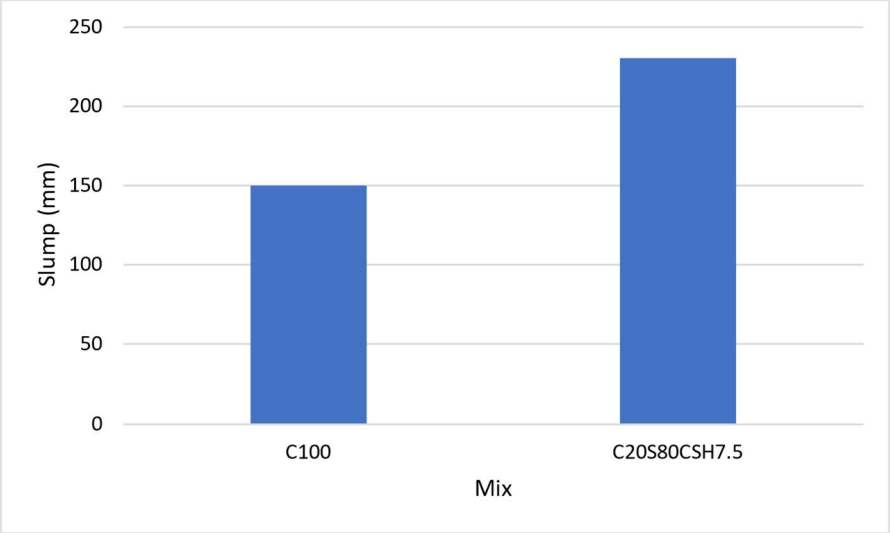

Figure 4.35: Slump of concrete mixes

4.8.2. Mechanical Properties of concrete

Mechanical properties, including compressive strength, tensile strength, and elastic modulus are essential for structural performance. As shown in Figure 4.36 based on table A35 of appendix, the 7-day compressive strength for the control mix with 100% OPC was 40.6 MPa, whereas the mix with 80% partial replacement of OPC with slag including 7.5% NCSH seed accelerator had a slightly higher strength of 43.17 MPa. On 28 days, the strengths were 49.16 MPa and 61.77 MPa, respectively. The inclusion of slag and NCSH accelerator not only maintained early strength but also significantly enhanced long-term compressive strength due to the supplementary cementitious properties of slag and the accelerating effect of NCSH seeds.

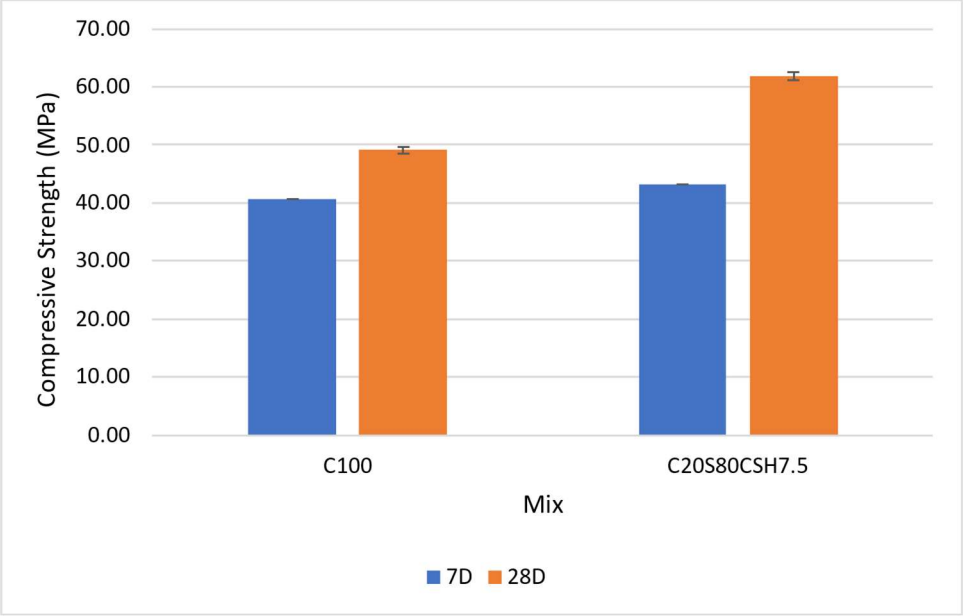

Figure 4.36: Compressive strength of concrete

The split tensile strength at 28 days, illustrated in Figure 4.37 based on table A36 of appendix, also showed improvements with the modified mix. The control mix had a tensile strength of 3.76 MPa, whereas the slag and NCSH modified mix exhibited a strength of 5.33 MPa. This enhancement is likely due to the refined microstructure and increased bond strength between the cement matrix and aggregates provided by the slag and NCSH seeds.

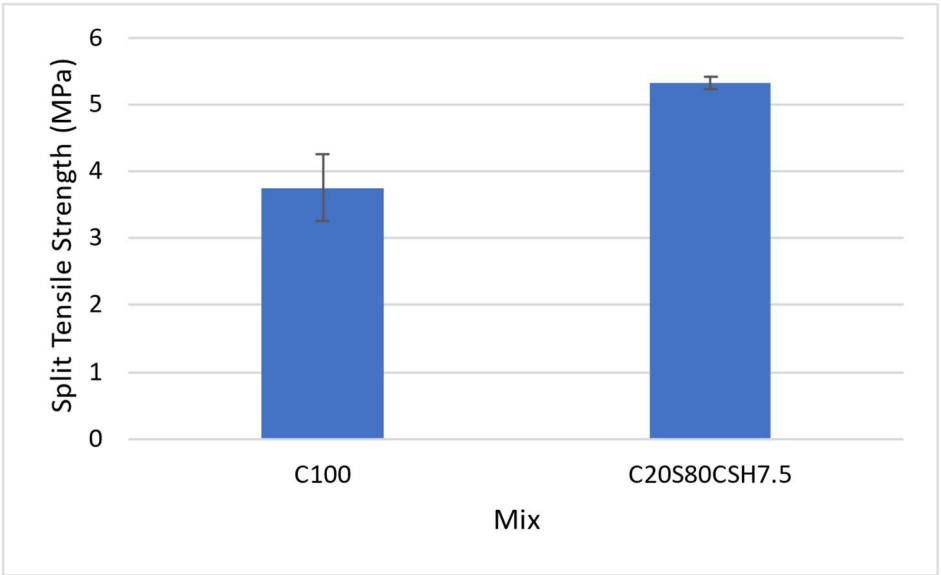

Figure 4.37: Split tensile strength of concrete at 28 days.

The elastic modulus at 28 days, depicted in Figure 4.38 based on table A37 of appendix, was approximately 38 GPa for the control mix, while the 80% slag replaced mix with 7.5% C-S-H had a modulus elasticity of 44 GPa. This increased modulus reflects the stiffer and more resilient nature of the slag modified concrete.

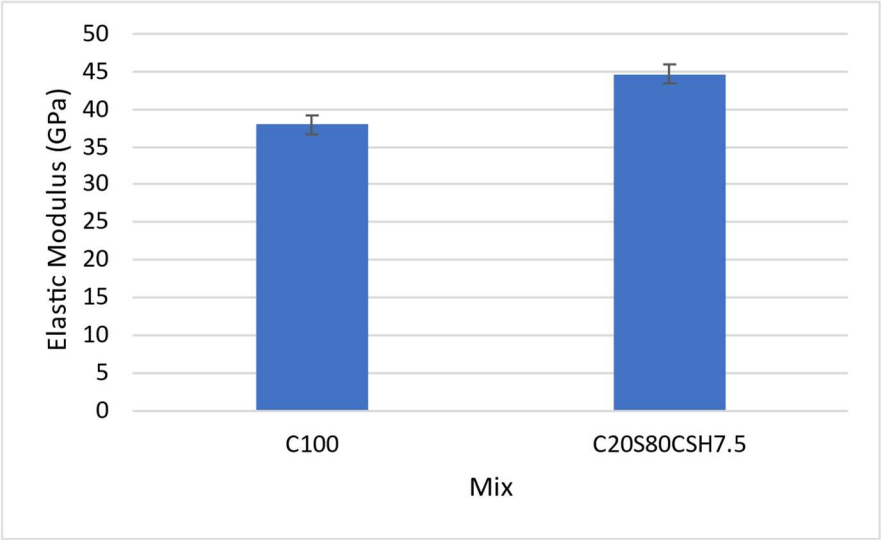

Figure 4.38: Modulus of elasticity of concrete at 28 days

4.8.3. Durability Properties

Durability properties such as permeability, chloride penetration resistance, and volume of permeable voids are critical for the long-term performance of concrete structures. The volume of permeable voids (VPV) and the depth of water permeability indicate the concrete's ability to resist the ingress of harmful agents. As shown in Figure 4.39 based on table A38 of appendix, the VPV for the control mix was 4.5%, and 3.7% for the slag mix with NCSH seed accelerator. The reduction of the pores suggests that mix with NCSH seed accelerator is less permeable and thus more durable.

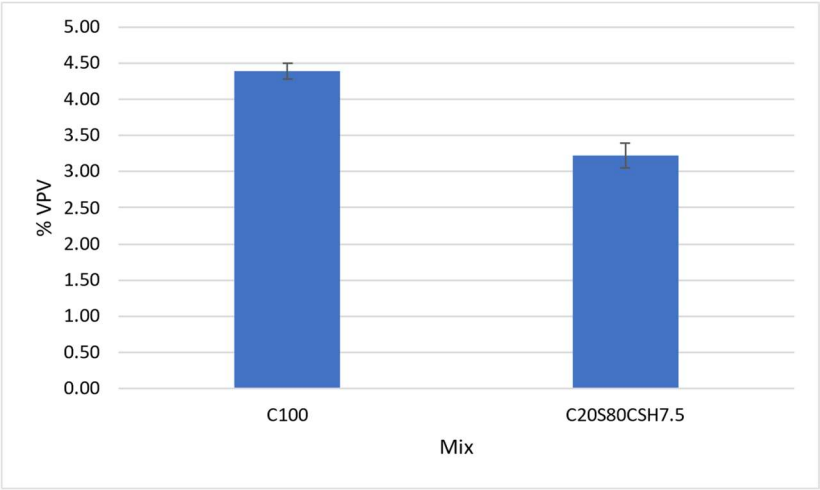

Figure 4.39: Volume of Permeable voids

Water permeability is a critical factor for the durability of concrete exposed to moisture. The control mix had a penetration depth of around 32 mm, whereas the mix with slag and NCSH showed a penetration depth of 25 mm, as illustrated in Figure 4.40 based on table A39 of appendix. The lower water permeability in the modified mix suggests better performance in resisting water ingress, which is essential for the longevity of concrete structures, especially in wet environments.

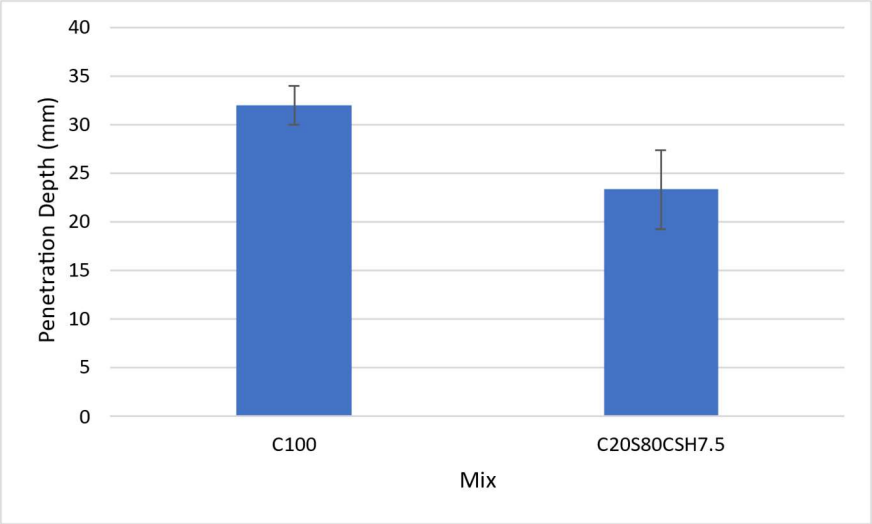

Figure 4.40: Depth of water permeability

The rapid chloride permeability test (RCPT), depicted in Figure 4.41 based on table A40 in appendix, measures concrete's ability to resist chloride ion ingress, which is crucial for structures exposed to de-icing salts or marine environments. The control mix showed a high charge passed around 3243 Coulombs, indicating higher permeability to chlorides. In contrast, the slag modified mix showed a significantly lower charge passed around 393 Coulombs, demonstrating enhanced resistance to chloride penetration. This improvement is attributed to the denser microstructure and reduced pore connectivity provided by the slag and NCSH seeds.

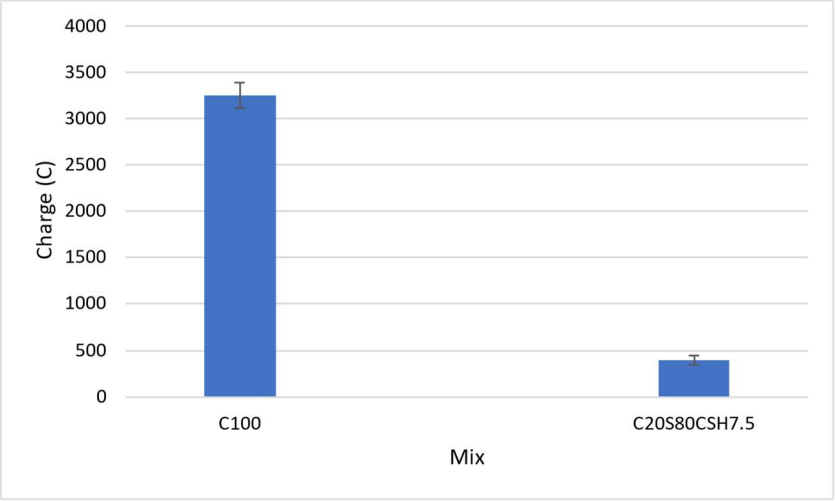

Figure 4.41: RCPT Test results

4.9. CO_2 Emissions of HVFA and HVS Concrete with NCSH seed accelerator

Figure 4.42 shows the calculated CO_2 emissions per ton of binder for the mixes used in this research, based on the published emission data of 930kg/tonne for OPC, 52kg/tonne for slag and 4kg/tonne for fly ash (King, D.,2012). Since there was no published data available for the CO_2 footprint of NCSH seed accelerator, it was assumed as same as emission value of OPC. The data highlights the substantial reduction in CO_2 emissions achieved by replacing OPC with high-volume fly ash and slag, which have much lower carbon footprints. HVFA and HVS mixes show a huge decrease in emissions compared to the 100% OPC mix, reflecting the environmental benefits of using these supplementary cementitious materials.

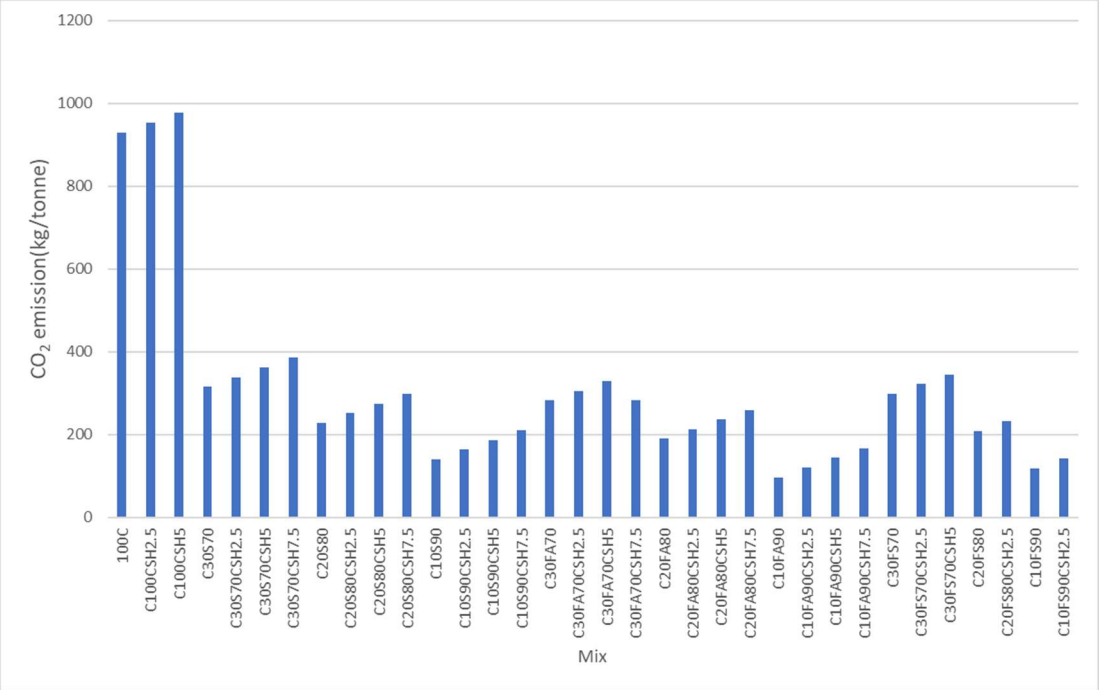

Figure 4.42: CO_2 emission analysis of high-volume slag and fly ash mixes.

Incorporating NCSH seed accelerators into the high-volume slag and fly ash mixes results in a slight increase in CO_2 emissions, but it enhances the mechanical and durability performance and allows the use of a higher amount of SCM, which was not possible to use much higher amount due to a significant reduction of mechanical properties compared to 100% OPC. This considerable amount of SCM, along with NCSH seed accelerator, could dramatically reduce CO_2 emissions, which satisfy the sustainability requirements.

Overall, utilizing high volumes of fly ash and slag in concrete mixes, supplemented by NCSH seed accelerators, presents an effective strategy for sustainable construction. This approach not only significantly reduces CO_2 emissions but also leverages industrial byproducts, supporting a circular economy. The combined use of these materials achieves a balance between environmental sustainability and enhanced concrete performance, contributing to more eco-friendly construction practices.

4.10. Cost comparison of HVFA and HVS Concrete with NCSH seed accelerator

Figure 4.43 shows the total cost per cubic meter ($/m³) for concrete with binder mixes used in this research, based on the cost of Master X-Seed 1500 as $2697.4/tonne (Zhou et al., 2021) and the cost of other raw materials from Shobeiri et al. (2023) as shown in Table 4.1. A detailed comparative analysis reveals insights into the cost implications of using these supplementary cementitious materials.

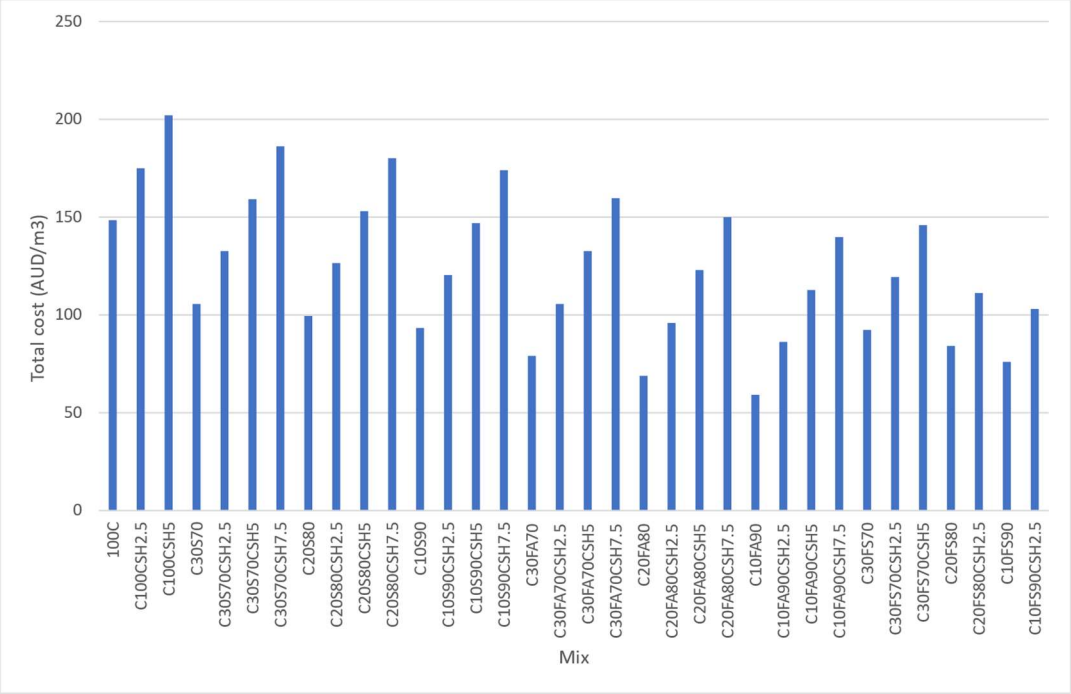

Figure 4.43: Total cost of production on $1m^3$ of concrete

HVFA concretes, exhibit significantly lower costs compared to the control mix with 100% OPC. This cost reduction is primarily due to the lower price of fly ash compared to OPC. The incorporation of NCSH seed accelerators in these mixes slightly increases the total cost per cubic meter. Despite this increase, the overall cost remains lower than that of the control mix with same NCSH seed accelerator dosage. The NCSH seed

accelerator improve the performance and early strength of the concrete, making the additional cost justifiable in many construction applications.

Table 4.1: Cost of raw materials used in cost calculation.

Material	Cost AUD/kg	Reference
Cement	0.293	Shobeiri et al. (2023)
Fly Ash	0.045	
Slag	0.14	
Coarse Aggregate	0.019	
Fine Aggregate	0.012	
Water	0.002	
Master X-Seed 1500	2.6974	Zhou et al. (2021)

HVS concretes, also demonstrate cost benefits compared to the 100% OPC mix. The cost saving is due to the lower price of slag relative to OPC. When NCSH seed accelerators are added to these mixes, there is a noticeable but moderate increase in cost. However, like fly ash mixes, the total cost remains competitive. The inclusion of NCSH accelerators in slag mixes enhances the early strength and durability of the concrete, providing a balance between cost and performance as well as significant reductions in CO_2 footprint.

HVFA concretes tend to be slightly more economical than HVS concretes but less performing with respect to strength. The addition of NCSH seed accelerators increases the cost in both types of mixes, but the increase is marginal compared to the overall cost savings from replacing a significant portion of OPC with either fly ash or slag. Therefore, the choice between fly ash and slag may depend on other factors such as availability, specific performance requirements, and environmental considerations. Both approaches provide cost-effective solutions for sustainable construction, with the added benefit of improved concrete properties when NCSH seed accelerators are used.

CHAPTER 5: CONCLUSIONS AND RECOMMENDATIONS

This research was conducted to evaluate the effectiveness of NCSH seed in enhancing the early age compressive strength of HVFA, HVS and HVS-FA binder and develop low carbon binder for sustainable construction. To achieve this aim, the effect of various NCSH seed contents on early age compressive strength of HVFA, HVS, and HVS-FA blended binders were studied in the first part. In the second part, optimum blended binder mixes were selected based on the 3-day compressive strength improvement. Investigation of the microstructural development of these selected blended binders were carried out with SEM, EDS, XRD, and TGA. To understand the reaction kinetics of selected mixes, isothermal calorimetry test was performed. In the third part, the mechanical and durability properties of concrete containing the best performing blended binder containing nano NCSH seeds are evaluated and benchmarked its performance with control OPC concrete. Compressive strength, split tensile strength and modulus of elasticity were measured to study the mechanical properties. Durability properties such as volume of permeable voids, water penetration depth and rapid chloride permeability test was evaluated. Finally, an analysis of the cost and the CO_2 emission of the concrete mixes with all the binders studied in first part was carried out.

5.1. Main research findings

The following research findings can be summarised as the main achievements of this study on the effectiveness of NCSH seed in HVFA, HVS and HVS-FA binder.

5.1.1. Effect of NCSH seed on HVFA, HVS and HVS-FA binder pastes.

1. Compressive strength in HVS paste improved significantly with NCSH seeds: 3-day strength increased by 82-167%, 55-195%, and 47-141% for 70%, 80%, and 90% slag replacements, respectively. The best results came from 80% slag and 7.5% NCSH, achieving an 88% SAI.
2. In HVFA pastes, the addition of NCSH seeds boosted compressive strength: increases were 54-118%, 91-154%, and 37-84% for 70%, 80%, and 90% fly ash replacements. Lower NCSH levels improved strength, but overall SAI remained low due to fly ash's limited pozzolanic reactivity.

3. HVS-FA mixes with 2.5-7.5% C-S-H seed accelerator showed strength gains of 147%, 160%, and 47% at 70%, 80%, and 90% slag and fly ash replacement levels, respectively.
4. NCSH seeds enhance concrete workability due to their water-reducing properties, improving flowability by optimizing particle packing. However, excessive amounts can lead to bleeding, requiring careful dosage.
5. The reduction of CH content in hydrated pastes with NCSH seeds confirms strength development, as much CH reacts to form additional hydration products.
6. Isothermal calorimetry revealed decreased cumulative heat and hydration peaks in mixes with partial replacements of slag and fly ash. NCSH seeds slightly increased cumulative heat.
7. NCSH seeds accelerated the time to reach the primary hydration peak compared to mixes without the seeds in HVS, HVFA, and HVS-FA binders.
8. SEM images showed densified microstructures and fewer pores in mixes with NCSH seeds. EDS spectra indicated higher Ca, Si, and Al peaks, confirming CSH and CASH gel formation.
9. XRD patterns revealed reduced CH peaks and increased CSH peaks in mixes with NCSH seeds, aligning with the improved compressive strength.
10. Thermogravimetric analysis showed reduced CH in mixes with NCSH seeds, supporting XRD data and indicating greater CSH gel formation.

5.1.2. Effect of NCSH seed on high-volume slag concrete.

1. The concrete mix with HVS and NCSH seed accelerator offers improved workability compared to the control mix.
2. Compressive strength, tensile strength, and modulus of elasticity are higher in the mix containing 80% slag and 7.5% NCSH than in the control OPC concrete.
3. HVS concrete with 80% slag and 7.5% NCSH shows reduced permeable voids, water penetration depth, and chloride penetration.
4. HVS, HVFA, and HVS-FA mixes significantly lower CO_2 emissions compared to 100% OPC, with the 80% slag and 7.5% NCSH mix reducing emissions by 68%.

5. While the NCSH seed accelerator slightly increases costs, HVS, HVFA, and HVS-FA mixes remain economical due to improved performance and reduced carbon footprint.

1.2. Recommendations for further study

1. The compressive strength and other mechanical properties in 56, 90 and 365 days needs to be measured to evaluate the effectiveness of NCSH seed accelerator in long term strength development of the mix.
2. Long term durability properties should be measured to make confidence of using the NCSH seed accelerator with HVS, HVFA and HVS-FA blended binders in concrete.
3. Effect of the NCSH seed accelerator with different w/b ratios should be evaluated and optimization of the NCSH seed content can be studied to develop an economical mix.
4. Early and later age porosity of the mixes can be studied to evaluate the microstructural change in terms of quantified pore filling.
5. More durability parameters such as sorptivity, corrosion resistance, sulphate resistance, alkali silica reaction (ASR) should be studied to validate the findings of this study and long-term implications should be verified.
6. Feasibility of using seed accelerator with novel supplementary materials such as mine waste residue (e.g.: lithium slag, copper heap leach residue) can be studied.

REFERENCES

Alzaza, A., Ohenoja, K., & Illikainen, M. (2022). Improved strength development and frost resistance of Portland cement ground-granulated blast furnace slag binary binder cured at 0 C with the addition of calcium silicate hydrate seeds. *Journal of Building Engineering*, *48*, 103904.

Alzaza, A., Ohenoja, K., Langås, I., Arntsen, B., Poikelispää, M., & Illikainen, M. (2022). Low-temperature (− 10° C) curing of Portland cement paste–synergetic effects of chloride-free antifreeze admixture, C–S–H seeds, and room-temperature pre-curing. *Cement and Concrete Composites*, *125*, 104319.

Alzaza, A., Ohenoja, K., Shaikh, F. U. A., & Illikainen, M. (2022). Mechanical and durability properties of C–S–H-seeded cement mortar cured at fluctuating low temperatures with granulated blast furnace slag as fine aggregates. *Journal of Building Engineering*, *57*, 104879.

American Society for Testing and Materials. (2012). *ASTM C109: Standard test method for compressive strength of hydraulic cement mortars (using 50 mm cube specimens)*. ASTM International.

American Society for Testing and Materials. (2012). *ASTM C143: Standard test method for slump of hydraulic-cement concrete*. ASTM International.

American Society for Testing and Materials. (2012). *ASTM C39: Standard test method for compressive strength of cylindrical concrete specimens*. ASTM International.

American Society for Testing and Materials. (2012). *ASTM C496: Standard test method for splitting tensile strength of cylindrical concrete specimens*. ASTM International.

American Society for Testing and Materials. (2021). *ASTM C642: Standard test method for density, absorption, and voids in hardened concrete*. ASTM International.

American Society for Testing and Materials. (2022). *ASTM C1202: Standard test method for electrical indication of concrete's ability to resist chloride ion penetration*. ASTM International.

American Society for Testing and Materials. (2022). *ASTM C469: Standard test method for static modulus of elasticity and Poisson's ratio of concrete in compression*. ASTM International.

American Society for Testing and Materials. (2023). *ASTM C230: Standard specification for flow table for use in tests of hydraulic cement*. ASTM International.

Amran, M., Makul, N., Fediuk, R., Lee, Y. H., Vatin, N. I., Lee, Y. Y., & Mohammed, K. (2022). Global carbon recoverability experiences from the cement industry. *Case Studies in Construction Materials*, *17*, e01439.

Bai, Y., Zhang, Z., & Wei, Z. (2017). The role of chemical composition and morphology of fly ash in the hydration of cement-based materials. Construction and Building Materials, 139, 354-363.

BASF,2015 Master X-Seed Solutions for energy efficient concrete https://assets.construction-chemicals.mbcc-group.com/en-mne/master%20xseed%20solutions%20for%20energy%20efficient%20concrete.pdf (Accessed date:20 August 2023)

Bentz, D. P. (2000). Microstructure development in cementitious materials. Cement and Concrete Research, 30(10), 1585-1595.

Bentz, D. P., & Cohen, M. D. (1998). Modeling the effects of pore structure on the properties of cement paste. Cement and Concrete Research, 28(4), 573-584.

Bishnu Kant Shukla, Aakash Gupta, Sachin Gowda, Yuvraj Srivastav, Constructing a greener future: A comprehensive review on the sustainable use of fly ash in the construction industry and beyond, *Materials Today: Proceedings*, Volume 93, Part 3, 2023, Pages 257-264

Chia, K. S., Zain, M. F. M., & Gan, S. (2020). The effects of nano-silica on the microstructure and properties of fly ash concrete. Materials Today: Proceedings, 28, 110-115.

Cuesta, A., Morales-Cantero, A., De la Torre, A. G., & Aranda, M. A. (2023). Recent advances in CSH nucleation seeding for improving cement performances. *Materials*, *16*(4), 1462.

European Committee for Standardization. (2009). BS EN 12390-8: Testing hardened concrete - Part 8: Depth of penetration of water under pressure.

Faisal Hussain, Inderpreet Kaur, Amir Hussain, Reviewing the influence of GGBFS on concrete properties, *Materials Today: Proceedings*,Volume 32, Part 4, 2020, Pages 997-1004

Feldman, R. F., & Tazawa, E. (1997). Concrete Science and Technology. RILEM Publications.

Gao, Y., Zhang, W., & Hu, Z. (2020). Effects of nano-silica and nano-C-S-H on the properties of cement paste. Construction and Building Materials, 234, 117307.

Golewski, G. L., & Szostak, B. (2021). Application of the CSH phase nucleating agents to improve the performance of sustainable concrete composites containing fly ash for use in the precast concrete industry. *Materials*, *14*(21), 6514.

Hannesson, G., Kuder, K., Shogren, R., & Lehman, D. (2012). The influence of high volume of fly ash and slag on the compressive strength of self-consolidating concrete. *Construction and Building Materials*, *30*, 161-168.

Hosan, A., & Shaikh, F. U. A. (2021). Compressive strength development and durability properties of high volume slag and slag-fly ash blended concretes containing nano-CaCO3. *Journal of Materials Research and Technology*, *10*, 1310-1322.

Huang, Y., Bird, R. N., & Heidrich, O. (2007). A review of the use of recycled solid waste materials in asphalt pavements. *Resources, conservation and recycling*, *52*(1), 58-73.

Ibáñez-Gosálvez, J., Real-Herraiz, T., & Ortega, J. M. (2021). Microstructure, durability and mechanical properties of mortars prepared using ternary binders with addition of slag, fly ash and limestone. Applied Sciences, 11(14), 6388.

Juenger, M. C., Snellings, R., & Bernal, S. A. (2019). Supplementary cementitious materials: New sources, characterization, and performance insights. *Cement and Concrete Research*, *122*, 257-273.

Khan, M. I., Poon, C. S., & Wong, H. S. (2019). Influence of nano-C-S-H on the workability and strength of cement pastes. Materials Science and Engineering: A, 748, 176-185.

Land, G., & Stephan, D. (2012). The influence of nano-silica on the hydration of ordinary Portland cement. Journal of materials science, 47, 1011-1017.

Land, G., & Stephan, D. (2015). The Synthesis of CSH Seeds Methods. *Variables and their Impact on the Ability to accelerate Cement Hydration, ICCC*.

Land, G., & Stephan, D. (2018). The effect of synthesis conditions on the efficiency of CSH seeds to accelerate cement hydration. *Cement and Concrete Composites*, *87*, 73-78.

Lehne, J., & Preston, F. (2018). Making concrete change. *Innovation in Low-carbon Cement and Concrete*. https://www.chathamhouse.org/2018/06/making-concrete-change-innovation-low-carbon-cement-and-concrete (Accessed date : 21 June 2023)

Mehta, P. K. (2002). Greening of the concrete industry for sustainable development. *Concrete international*, *24*(7), 23-28.

Mo, L., Zhang, F., Deng, M., Jin, F., Al-Tabbaa, A., & Wang, A. (2017). Accelerated carbonation and performance of concrete made with steel slag as binding materials and aggregates. *Cement and Concrete Composites*, *83*, 138-145.

Mojir, S., Aghaei, A., & Fadaei, S. (2020). Effect of nano-C-S-H on the mechanical properties of cement paste. Journal of Materials in Civil Engineering, 32(2), 04020258.

Neville, A. M. (2011). Properties of Concrete (5th ed.). Pearson.

Niu, Y., Zhang, Z., & Zhou, C. (2017). The influence of nano-C-S-H on the hydration of ordinary Portland cement. Cement and Concrete Composites, 79, 93-102.

Roychand, R., De Silva, S., Law, D., & Setunge, S. (2016). High volume fly ash cement composite modified with nano silica, hydrated lime and set accelerator. *Materials and Structures*, *49*, 1997-2008.

Roychand, R., De Silva, S., Setunge, S., & Law, D. (2020). A quantitative study on the effect of nano SiO_2, nano $Al2O_3$ and nano $CaCO_3$ on the physicochemical properties of very high volume fly ash cement composite. *European Journal of Environmental and Civil Engineering*, *24*(6), 724-739.

Schneider, M., Romer, M., Tschudin, M., & Bolio, H. (2011). Sustainable cement production—present and future. *Cement and concrete research*, *41*(7), 642-650..

Scrivener, K. L., John, V. M., & Gartner, E. M. (2018). Eco-efficient cements: Potential economically viable solutions for a low-CO_2 cement-based materials industry. *Cement and concrete Research*, *114*, 2-26.Fennell, P.S., Davis, S.J. and Mohammed, A., 2021. Decarbonizing cement production. *Joule*, *5*(6), pp.1305-1311.

Shaikh, F. U. A., & Hosan, A. (2019). Effect of nano alumina on compressive strength and microstructure of high volume slag and slag-fly ash blended pastes. *Frontiers in Materials*, *6*, 90.

Shaikh, F. U. A., Supit, S. W. M., & Sarker, P. K. (2014). A study on the effect of nano silica on compressive strength of high volume fly ash mortars and concretes. *Materials & Design*, *60*, 433-442.

Shaikh, F. U., & Hosan, A. N. W. A. R. (2019). High volume slag and slag-fly ash blended cement pastes containing nano silica. In *Materials Science Forum* Vol. 967, pp. 205-213

Shaikh, F. U., & Supit, S. W. (2014). Mechanical and durability properties of high volume fly ash (HVFA) concrete containing calcium carbonate (CaCO3) nanoparticles. *Construction and building materials*, *70*, 309-321.

Shaikh, F. U., Supit, S. W., & Barbhuiya, S. (2017). Microstructure and nanoscaled characterization of HVFA cement paste containing nano-SiO_2 and nano-$CaCO_3$. *Journal of Materials in Civil Engineering*, *29*(8), 04017063.

Shi, C., Krivenko, P. V., & Roy, D. M. (2006). *Alkali-activated cements and concretes*. CRC Press.

Shobeiri, V., Bennett, B., Xie, T., & Visintin, P. (2023). Mix design optimization of concrete containing fly ash and slag for global warming potential and cost reduction. *Case Studies in Construction Materials*, *18*, e01832.

Snellings, R., Suraneni, P., & Skibsted, J. (2023). Future and emerging supplementary cementitious materials. *Cement and concrete Research*, *171*, 107199.

Standard, A. (1998). Supplementary cementitious materials for use with portland and blended cement. *AS3582*, *1*.

Supit, S. W., & Shaikh, F. U. (2014). Effect of nano-$CaCO_3$ on compressive strength development of high volume fly ash mortars and concretes. *Journal of Advanced Concrete Technology*, *12*(6), 178-186.

Supit, S. W., Shaikh, F. U., & Sarker, P. K. (2014). Effect of ultrafine fly ash on mechanical properties of high volume fly ash mortar. *Construction and building materials*, *51*, 278-286.

Szostak, B., & Golewski, G. L. (2020). Improvement of strength parameters of cement matrix with the addition of siliceous fly ash by using nanometric CSH seeds. *Energies*, *13*(24), 6734.

Taylor, H. F. W. (1997). Cement Chemistry (2nd ed.). Thomas Telford.

Technical note 78, Cement Concrete and Aggregates Australia, Jan 2018 https://www.ccaa.com.au/common/Uploaded%20files/CCAA/Publications/Tech%20Notes/TECH_NOTE_78_-_Ground_Slag.pdf (Access date : 03 September 2022)

Velandia, D. F., Lynsdale, C. J., Provis, J. L., Ramirez, F., & Gomez, A. C. (2016). Evaluation of activated high volume fly ash systems using Na_2SO_4, lime and quicklime in mortars with high loss on ignition fly ashes. *Construction and Building Materials*, *128*, 248-255.

Worrell, E., Price, L., Martin, N., Hendriks, C., & Meida, L. O. (2001). Carbon dioxide emissions from the global cement industry. *Annual review of energy and the environment*, *26*(1), 303-329.

Xu, G., Tian, Q., Miao, J., & Liu, J. (2017). Early-age hydration and mechanical properties of high volume slag and fly ash concrete at different curing temperatures. *Construction and Building Materials*, *149*, 367-377.

Yang, J., Yang, M., He, X., Ma, M., Fan, M., Su, Y., & Tan, H. (2021). Green reaction-type nucleation seed accelerator prepared from coal fly ash ground in water environment. *Construction and Building Materials*, *306*, 124840.

Yao, Y., Zhang, Y., & Li, J. (2021). Hydration kinetics and microstructure of blended cement incorporating nanosilica and ground granulated blast furnace slag. Cement and Concrete Composites, 123, 104152.

Zhang, M. H., Islam, M. A., & Zeng, Z. (2016). Effect of quartz on the microstructure and mechanical properties of cement paste. Construction and Building Materials, 102, 484-493.

Zhang, Y., Liu, C., & Yang, J. (2015). Influence of nanosilica and nano-C-S-H on the hydration process of cement. Journal of Materials Science, 50(12), 3989-3998.

Zhang, Y., Wang, S., & Feng, D. (2020). The pozzolanic activity of slag in cement-based materials: A review. Construction and Building Materials, 249, 118850.

Zhou, Z., Sofi, M., Liu, J., Li, S., Zhong, A., & Mendis, P. (2021). Nano-CSH modified high volume fly ash concrete: Early-age properties and environmental impact analysis. *Journal of Cleaner Production*, *286*, 124924.

APPENDIX

Test Results Analysis

Table A1: Compressive strength of C100 paste at different age.

Days	Load.KN	Compressive strength, MPa	Average Compressive strength, MPa	Standard Deviation
3	113.55	45.42	49.18	3.34
	129.53	51.81		
	125.80	50.32		
7	133.58	53.43	50.41	3.55
	116.25	46.50		
	128.28	51.31		
28	156.53	62.61	62.57	5.07
	143.70	57.48		
	169.05	67.62		

Table A2: Compressive strength of C100CSH2.5 paste at different age.

Days	Load.KN	Compressive strength, MPa	Average Compressive strength, MPa	Standard Deviation
3	109.13	43.65	45.63	1.00
	133.88	53.55		
	99.20	39.68		
7	133.575	48.91	51.42	2.19
	116.25	52.45		
	128.275	52.91		
28	156.525	88.10	64.18	20.86
	143.7	49.81		
	169.05	54.63		

Table A3: Compressive strength of C100CSH5 paste at different age.

Days	Load.KN	Compressive strength, MPa	Average Compressive strength, MPa	Standard Deviation
3	194.48	77.79	75.03	2.46
	182.70	73.08		
	185.53	74.21		
7	205.30	82.12	69.87	11.06
	167.20	66.88		
	151.55	60.62		
28	194.45	77.78	89.53	10.17
	238.10	95.24		
	238.90	95.56		

Table A4: Compressive strength of C30S70 paste at different age.

Days	Load.KN	Compressive strength, MPa	Average Compressive strength, MPa	Standard Deviation
3	35.43	14.17	15.47	1.38
	38.33	15.33		
	42.28	16.91		
7	63.48	25.39	27.78	2.36
	69.65	27.86		
	75.25	30.1		
28	107.33	42.93	41.34	1.38
	101.43	40.57		
	101.28	40.51		

Table A5: Compressive strength of C30S70CSH2.5 paste at different age.

Days	Load.KN	Compressive strength, MPa	Average Compressive strength, MPa	Standard Deviation
3	86.15	34.46	28.15	5.2
	57.20	22.88		
	67.78	27.11		
7	124.30	49.72	44.94	15.26
	69.65	27.86		
	143.10	57.24		
28	93.55	37.42	51.63	18.85
	111.13	44.45		
	182.55	73.02		

Table A6: Compressive strength of C30S70CSH5 paste at different age.

Days	Load.KN	Compressive strength, MPa	Average Compressive strength, MPa	Standard Deviation
3	118.00	47.2	37.91	6.2
	96.00	38.4		
	70.33	28.13		
7	122.23	48.89	49.55	4.68
	113.08	45.23		
	136.30	54.52		
28	157.90	63.16	62.27	0.77
	154.55	61.82		
	154.55	61.82		

Table A7: Compressive strength of C30S70CSH7.5 paste at different age.

Days	Load.KN	Compressive strength, MPa	Average Compressive strength, MPa	Standard Deviation
3	80.28	32.11	36.62	4.63
	103.40	41.36		
	91.00	36.4		
7	117.60	47.04	52.03	6.86
	149.63	59.85		
	123.00	49.2		
28	156.43	62.57	63.96	1.87
	158.08	63.23		
	165.23	66.09		

Table A9: Compressive strength of C20S80 paste at different age.

Days	Load.KN	Compressive strength, MPa	Average Compressive strength, MPa	Standard Deviation
3	35.43	14.77	14.24	0.47
	38.33	14.1		
	42.28	13.86		
7	63.48	26.07	26.11	0.48
	69.65	26.61		
	75.25	25.66		
28	107.33	31.6	34.16	2.27
	101.43	34.97		
	101.28	35.91		

Table A10: Compressive strength of C20S80CSH2.5 paste at different age.

Days	Load.KN	Compressive strength, MPa	Average Compressive strength, MPa	Standard Deviation
3	45.60	18.24	23.27	0.27
	64.00	25.6		
	64.95	25.98		
7	100.33	40.13	39.65	1.42
	95.13	38.05		
	101.90	40.76		
28	110.55	44.22	49.02	9.11
	108.28	43.31		
	148.80	59.52		

Table A11: Compressive strength of C20S80CSH5 paste at different age.

Days	Load.KN	Compressive strength, MPa	Average Compressive strength, MPa	Standard Deviation
3	98.33	39.33	36.51	4.38
	96.83	38.73		
	78.65	31.46		
7	95.38	38.15	39.7	9.77
	125.40	50.16		
	77.00	30.8		
28	146.15	58.46	42.42	14.55
	75.15	30.06		
	96.83	38.73		

Table A12: Compressive strength of C20S80CSH7.5paste at different age.

Days	Load.KN	Compressive strength, MPa	Average Compressive strength, MPa	Standard Deviation
3	94.75	37.9	43.28	4.79
	117.75	47.1		
	112.10	44.84		
7	137.00	54.8	50.44	5.75
	131.50	52.6		
	109.80	43.92		
28	145.10	58.04	62.24	3.83
	157.93	63.17		
	163.80	65.52		

Table A13: Compressive strength of C10S90 paste at different age.

Days	Load.KN	Compressive strength, MPa	Average Compressive strength, MPa	Standard Deviation
3	27.68	11.07	11.96	1.62
	34.58	13.83		
	27.45	10.98		
7	53.20	21.28	22.03	2.64
	49.63	19.85		
	62.40	24.96		
28	72.88	29.15	28.96	0.67
	70.53	28.21		
	73.78	29.51		

Table A14: Compressive strength of C10S90CSH2.5 paste at different age.

Days	Load.KN	Compressive strength, MPa	Average Compressive strength, MPa	Standard Deviation
3	49.03	19.61	17.54	0.64
	46.78	18.71		
	35.75	14.3		
7	64.23	25.69	25.11	0.61
	61.18	24.47		
	62.90	25.16		
28	78.88	31.55	32.54	5.2
	95.43	38.17		
	69.78	27.91		

Table A15: Compressive strength of C10S90CSH5 paste at different age.

Days	Load.KN	Compressive strength, MPa	Average Compressive strength, MPa	Standard Deviation
3	73.93	29.57	28.81	0.69
	71.63	28.65		
	70.55	28.22		
7	63.95	25.58	27.71	3.35
	78.93	31.57		
	64.93	25.97		
28	91.60	36.64	31.66	7.87
	56.48	22.59		
	89.38	35.75		

Table A16: Compressive strength of C10S90CSH7.5 paste at different age.

Days	Load.KN	Compressive strength, MPa	Average Compressive strength, MPa	Standard Deviation
3	73.25	29.3	27.18	0.44
	71.70	28.68		
	58.88	23.55		
7	101.35	40.54	34.88	5.55
	73.60	29.44		
	86.68	34.67		
28	122.25	48.9	46.54	2.3
	110.78	44.31		
	116.00	46.4		

Table A17: Compressive strength of C30FA70 paste at different age.

Days	Load.KN	Compressive strength, MPa	Average Compressive strength, MPa	Standard Deviation
3	9.10	3.64	5.03	1.51
	14.43	5.77		
	14.20	5.68		
7	19.68	7.87	7.28	0.6
	16.70	6.68		
	18.23	7.29		
28	37.93	15.17	18.72	4.94
	41.58	16.63		
	60.90	24.36		

Table A18: Compressive strength of C30FA70CSH2.5 paste at different age.

Days	Load.KN	Compressive strength, MPa	Average Compressive strength, MPa	Standard Deviation
3	19.78	7.91	7.75	0.16
	19.20	7.68		
	19.18	7.67		
7	22.78	9.11	9.89	1.56
	29.23	11.69		
	22.18	8.87		
28	49.90	19.96	19.68	2.92
	56.15	22.46		
	41.58	16.63		

Table A19: Compressive strength of C30FA70CSH5 paste at different age.

Days	Load.KN	Compressive strength, MPa	Average Compressive strength, MPa	Standard Deviation
3	26.40	10.56	10.96	0.81
	29.25	11.7		
	26.55	10.62		
7	36.23	14.49	12.77	1.5
	29.25	11.7		
	30.33	12.13		
28	54.45	21.78	22.63	1.05
	55.75	22.3		
	59.50	23.8		

Table A20: Compressive strength of C30FA70CSH7.5 paste at different age.

Days	Load.KN	Compressive strength, MPa	Average Compressive strength, MPa	Standard Deviation
3	19.75	7.9	8.41	1.07
	23.53	9.41		
	19.80	7.92		
7	26.13	10.45	12.06	1.41
	32.70	13.08		
	31.65	12.66		
28	63.43	25.37	25.92	1.87
	57.05	22.82		
	66.18	26.47		

Table A21: Compressive strength of C20FA80 paste at different age.

Days	Load.KN	Compressive strength, MPa	Average Compressive strength, MPa	Standard Deviation
3	7.23	2.89	3.46	0.69
	4.78	1.91		
	13.98	5.59		
7	13.83	5.53	4.74	0.69
	10.73	4.29		
	11.00	4.4		
28	32.55	13.02	11.74	2.75
	18.83	7.53		
	26.13	10.45		

Table A22: Compressive strength of C20FA80CSH2.5 paste at different age.

Days	Load.KN	Compressive strength, MPa	Average Compressive strength, MPa	Standard Deviation
3	11.70	4.68	5.62	0.51
	13.50	5.4		
	16.93	6.77		
7	19.78	7.91	7.75	0.14
	19.20	7.68		
	19.18	7.67		
28	33.58	13.43	12.31	2.56
	40.73	16.29		
	27.98	11.19		

Table A23: Compressive strength of C20FA80CSH5 paste at different age.

Days	Load.KN	Compressive strength, MPa	Average Compressive strength, MPa	Standard Deviation
3	12.20	4.88	4.13	0.3
	13.25	5.3		
	5.53	2.21		
7	21.40	8.56	8.59	0.26
	22.18	8.87		
	20.88	8.35		
28	42.18	16.87	15.82	1.17
	41.78	16.71		
	36.90	14.76		

Table A24: Compressive strength of C10FA90 paste at different age.

Days	Load.KN	Compressive strength, MPa	Average Compressive strength, MPa	Standard Deviation
3	3.53	1.41	1.38	0.08
	3.80	1.52		
	3.05	1.22		
7	7.00	2.8	2.54	0.51
	7.18	2.87		
	4.88	1.95		
28	20.28	8.11	8.14	0.12
	20.85	8.34		
	20.43	8.17		

Table A25: Compressive strength of C10FA90CSH2.5 paste at different age.

Days	Load.KN	Compressive strength, MPa	Average Compressive strength, MPa	Standard Deviation
3	5.53	2.21	1.89	0.54
	3.60	1.44		
	5.05	2.02		
7	8.08	3.23	3.37	0.21
	8.18	3.27		
	9.03	3.61		
28	23.78	9.51	9.4	0.27
	22.45	8.98		
	23.20	9.28		

Table A26: Compressive strength of C10FA90CSH5 paste at different age.

Days	Load.KN	Compressive strength, MPa	Average Compressive strength, MPa	Standard Deviation
3	4.95	1.98	1.98	0.06
	5.15	2.06		
	4.73	1.89		
7	14.98	5.99	4.92	0.95
	11.55	4.62		
	10.40	4.16		
28	32.43	12.97	12.48	6.02
	5.20	2.08		
	29.95	11.98		

Table A27: Compressive strength of C10FA90CSH7.5 paste at different age.

Days	Load.KN	Compressive strength, MPa	Average Compressive strength, MPa	Standard Deviation
3	6.55	2.62	2.54	0.42
	5.08	2.03		
	7.43	2.97		
7	12.53	5.01	5.41	0.5
	14.93	5.97		
	13.15	5.26		
28	62.30	24.92	23.29	1.88
	62.20	24.88		
	54.13	21.65		

Table A28: Compressive strength of C30FS70 paste at different age.

Days	Load.KN	Compressive strength, MPa	Average Compressive strength, MPa	Standard Deviation
3	20.08	8.03	8.83	0.25
	20.98	8.39		
	25.15	10.06		
7	35.28	14.11	13.59	2.12
	38.53	15.41		
	28.15	11.26		
28	73.63	29.45	26.67	7.89
	34.68	13.87		
	59.70	23.88		

Table A29: Compressive strength of C30FS70CSH2.5 paste at different age.

Days	Load.KN	Compressive strength, MPa	Average Compressive strength, MPa	Standard Deviation
3	57.05	22.82	21.82	0.52
	55.23	22.09		
	51.35	20.54		
7	82.35	32.94	28.27	6.45
	77.38	30.95		
	52.28	20.91		
28	108.18	43.27	43.85	3.49
	124.53	49.81		
	111.05	44.42		

Table A30: Compressive strength of C30FS70CSH5 paste at different age.

Days	Load.KN	Compressive strength, MPa	Average Compressive strength, MPa	Standard Deviation
3	45.88	18.35	16.5	1.9
	39.15	15.66		
	38.75	15.5		
7	94.10	37.64	26.32	9.87
	54.45	21.78		
	48.85	19.54		
28	116.95	46.78	41.36	6.81
	85.53	34.21		
	89.85	35.94		

Table A31: Compressive strength of C20FS80 paste at different age.

Days	Load.KN	Compressive strength, MPa	Average Compressive strength, MPa	Standard Deviation
3	14.75	5.9	6.39	0.92
	18.00	7.2		
	15.18	6.07		
7	27.95	11.18	10.30	0.81
	25.28	10.11		
	24.00	9.6		
28	28.20	11.28	18.28	7.52
	57.65	23.06		
	63.18	25.27		

Table A32: Compressive strength of C20FS80CSH2.5 paste at different age.

Days	Load.KN	Compressive strength,MPa	Average Compressive strength, MPa	Standard Deviation
3	42.40	16.96	16.61	0.42
	40.90	16.36		
	41.30	16.52		
7	64.25	25.7	26.74	1.08
	66.63	26.65		
	69.65	27.86		
28	100.93	40.37	39.23	1.14
	97.95	39.18		
	95.23	38.09		

Table A33: Compressive strength of C10FS90 paste at different age.

Days	Load.KN	Compressive strength, MPa	Average Compressive strength, MPa	Standard Deviation
3	10.93	4.37	4.06	0.45
	9.35	3.74		
	10.80	4.32		
7	19.90	7.96	7.84	0.44
	18.40	7.36		
	20.53	8.21		
28	48.33	19.33	18.85	1.01
	43.28	17.31		
	45.90	18.36		

Table A34: Compressive strength of C10FS90CSH2.5 paste at different age.

Days	Load.KN	Compressive strength,MPa	Average Compressive strength, MPa	Standard Deviation
3	29.20	11.68	11.67	0.02
	29.13	11.65		
	26.48	10.59		
7	56.65	22.66	21.24	2.16
	46.88	18.75		
	55.75	22.3		
28	73.50	29.4	42.79	13.53
	98.50	39.4		
	140.43	56.17		

Table A35: Compressive strength of C100 % C20S80CSH7.5 concrete mixes at different age.

Days	Mix	Load.KN	Compressive strength, MPa	Average Compressive strength, MPa	Standard Deviation
7	C100	318.9	40.60	40.60	
	C20S80CSH7.5	339.1	43.17	43.17	
28	C100	381.3	48.54	49.16	0.61
		390.8	49.75		
		386.3	49.18		
	C20S80CSH7.5	480.9	61.23	61.77	0.65
		490.8	62.49		
		483.7	61.58		

Table A36: Tensile Strength of C100 % C20S80CSH7.5 concrete mixes

Mix	Load, kN	Tensile Strength, MPa	Average, MPa	SD
C100-1	226.7	3.21	3.76	0.49
C100-2	278.9	3.94		
C100-3	232.4	4.14		
C20S80CSH7.5-1	370.5	5.24	5.33	0.09
C20S80CSH7.5-2	382.1	5.41		
C20S80CSH7.5-3	378.3	5.35		

Table A37: Modulus of elasticity of C100 % C20S80CSH7.5 concrete mixes

Mix	Modulus of Elasticity (GPa)	Average (GPa)	SD
C100-1	37.93	37.93	1.20
C100-2	39.13		
C100-3	36.74		
C20S80CSH7.5-1	43.27	44.65	1.29
C20S80CSH7.5-2	44.86		
C20S80CSH7.5-3	45.82		

Table A38: Volume of Permeable Voids Calculation

Sample	A	B	C	D	g1	g2	VPV	Average	SD
C100-1	936.00	962.30	963.50	563.70	2406.95	2514.10	4.26	0.11	4.39
C100-2	938.00	966.70	967.10	568.40	2424.63	2537.88	4.46		
C100-3	941.00	968.10	969.40	570.30	2425.71	2538.44	4.44		
C20S80CSH7.5-1	944.00	962.50	963.70	565.70	2418.34	2495.37	3.09	0.17	3.23
C20S80CSH7.5-2	941.00	962.10	962.10	564.30	2418.55	2498.01	3.18		
C20S80CSH7.5-3	939.00	961.10	961.50	562.10	2406.36	2491.38	3.41		

A- Oven dry weight (g)
B- Weight after immersion in water (g)
C- Weight after boiling (g)
D- Weight under water (g)

Table A39: Depth of water permeability

Mix	Permeability depth(mm)	Average(mm)	SD
C100-1	34	32	2.0
C100-2	30		
C100-3	32		
C20S80CSH7.5-1	24	23	4.0
C20S80CSH7.5-2	19		
C20S80CSH7.5-3	27		

Table A40: RCPT test results

Mix	Charges Passed (Coulomb)	Average (Coulomb)	SD
OPC-1	3392	3243	136
OPC-2	3213		
OPC-3	3124		
C20S80CSH7.5-1	351	393	45
C20S80CSH7.5-2	441		
C20S80CSH7.5-3	387		